2.7.4.2. Differential Thermal Expansion

Differential thermal expansion resulting from the fire transient has minimal consequence to the Model 2000 Transport Package. All stresses are classified ASME Section III Subsection NB as secondary displacement-limited stresses. Heat conditions that bound both NCT and HAC are presented in Section 2.6.7, which evaluates the thermal expansion of the Model 2000 cask by applying a temperature differential 300°F from the outside surface to the inside surface of the cask. Thermal expansion of the closure bolts are evaluated using the temperatures associated with the HAC fire in Section 2.12.4.

2.7.4.3. Stress Calculations

In accordance with the requirements of 10 CFR 71.73(c)(4), the Model 2000 Transport Package is structurally evaluated when subjected to the design pressure of 30 psia. The design pressure is applied in combination with the mechanical loads defined in Section 2.7.1. To obtain stress results, a uniform internal pressure of 30 psia is applied to the ANSYS finite element in combination with the mechanical loading conditions of Section 2.7.1.

2.7.4.4. Comparison with Allowable Stresses

The combined HAC pressure and mechanical stresses are presented in Table 2.7.4-1, which documents the primary membrane (P_m), primary membrane and plus primary bending (P_m+P_b) stresses in accordance with the criteria presented in Regulatory Guide 7.6. As Table 2.7.4-1 shows, the margins of safety are positive when the allowable is compared to the stress intensity for each category. Therefore, the requirement of 10 CFR 71.73(c)(4) is satisfied.

Table 2.7.4-1. Summary of HAC Stress Results

Case	Component	Stress Component	Stress Combination	Stress Intensity	Allowable	Margin of Safety
End Drop	Cask body	P_m	10140	20000	48000	+3.7
		$P_m + P_b$	25830	20000	72000	+1.8
	Cask Lid	P_m	19830	20000	48000	+1.4
		$P_m + P_b$	40720	20000	72000	+0.8
Side Drop	Cask body	P_m	8455	19300	46320	+4.5
		$P_m + P_b$	28200	19300	69480	+1.5
	Cask Lid	P_m	17590	19300	46320	+1.6
		$P_m + P_b$	31350	19300	69480	+1.2

2.7.5. Immersion - Fissile Material

The Model 2000 Transport Package is not licensed for the transport of fissile material. See Chapter 1 for further discussion.

2.7.6. Immersion - All Packages

According to the requirements of 10 CFR 71.73(c)(6), a package must be subjected to water pressure equivalent to immersion under a head of water of at least 15 meters (50 feet) for a period of 8 hours, which is equivalent to 21.7 psig. The cask closure including the lid and bolts are designed to survive puncture loads, which exceed the load experienced during immersion (Sections 2.12.1 and 2.12.4). From ASME Section III-NB, A-2221, when subjected to 21.7 psig the 1.0-inch thick outer shell of the cask with a mean radius of 18.75 inches, produces a primary membrane stress intensity 418 psi that is much less than the material yield strength. Therefore, the Model 2000 Transport Package satisfies all of the immersion requirements for a package that is used for the international shipment of radioactive materials.

2.7.7. Deep Water Immersion Test (for Type B Packages Containing More than 10^5 A_2)

The contents specified in this application is less than 10^5 A_2. Therefore, this is not applicable for the Model 2000 Transport Package with HPI and material basket.

2.7.8. Summary of Damage

The analytical results reported in Sections 2.7.1 through 2.7.7 indicate that the damage incurred by the Model 2000 Transport Package during the hypothetical accident is minimal, and such damage does not diminish the cask ability to maintain the containment boundary. A 30-foot side drop followed by the 40-inch pin puncture accident may damage the overpack and inflict local damage on the outer shell of the cask. However, the shielding remains intact and satisfies the accident shielding criteria. Additionally, the HPI and material baskets maintain structural integrity during all postulated HAC events, which supports the criticality analysis assumptions. Based on the analyses of Sections 2.7.1 through 2.7.7, the Model 2000 Transport Package fulfills the structural and shielding requirements of 10 CFR 71.73 for all of the hypothetical accident conditions.

2.8 Accident Conditions for Air Transport of Plutonium

This section does not apply for the Model 2000 Transport Package with HPI and material basket.

2.9 Accident Conditions for Fissile Material Packages for Air Transport

This section does not apply for the Model 2000 Transport Package with HPI and material basket.

2.10 Special Form

Special form capsules specifically designed for carrying isotope source materials are permitted in the Model 2000 Transport Package. Each special form capsule shall show compliance with the requirements of 10 CFR 71.75 when subjected to the applicable test conditions of 10 CFR 71.77 and independently certified. Special form capsules are not a requirement of this application, because containment is provided by the cask.

2.11 Fuel Rods

This section does not apply for the Model 2000 Transport Package, because containment is provided by the cask.

2.12 Appendix

2.12.1. LS-DYNA Evaluation of the Model 2000 Transport Package

This section summarizes the results of impact evaluation of the Model 2000 Transport Package during NCT of 10 CFR 71.71 and HAC of 10 CFR 71.73 (Reference 2-1) and supplements the test data documented in Section 2.12.5. The primary purpose of this section is to report accelerations for the HPI cask contents and provide realistic damage predictions for the thermal evaluation presented in Chapter 3.

2.12.1.1. Introduction

The NCT and HAC impact analyses presented in this section evaluate the performance of the Model 2000 Transport Package using LS-DYNA Version 971 finite element code (Reference 2-20). Benchmarks of the analysis methodology are first performed using 3-drop orientations to compare with the actual drop tests of a quarter-scale model (see Section 2.12.5). The benchmark results are presented in detail in Section 2.12.1.11.1 through Section 2.12.1.11.3 as Drop Cases 1 through 3, respectively. The benchmark performed confirmed that the LS-DYNA program and dynamic analysis methodology are conservative and bounding.

The accident conditions are conservatively simulated using material properties corresponding to temperatures ranging from -40°F to 300°F for stainless steel and 400°F for aluminum honeycomb. Also considered are variations of the payload weight that is up to 10% of the maximum weight. The overpack toroidal shell thickness is also varied between two thicknesses of 0.50 inches and 0.76 inches. The overall variations include the following configurations,

1. NCT and HAC (2 variations of initial velocities)
2. Hot and cold temperature conditions. (2 variations of material properties)
3. Payload weight of ±10% of the maximum weight. (3 variations of payload weights)
4. Two different toroidal shell thicknesses of 0.50 inches and 0.76 inches. (2 variations of shell thicknesses)
5. Four-drop orientations including two end drops, side drop, and C.G. over corner drops. (4 variations of drop geometries)

There are 96 (=2×2×3×2×4) possible drop configurations. Evaluating the bounding cases reduces the total number of drop configurations. This simplification resulted in performing nine (9) bounding drop configurations. The bounding drop configurations are designated as Drop Cases 4 through 12. The summary of results for the 9 bounding drop cases is presented in Table 2.12.1-1. The worst-case HAC accelerations occur during the cold/thick/light side drop and the hot/thin/heavy bottom end drop. For the bottom end drop, the acceleration trend showed that the accelerations dropped until the honeycomb temperature was increased to 400°F and the honeycomb fully compresses. Because the average temperature of the honeycomb is less than 350°F, the honeycomb has sufficient capacity to protect the package during hot conditions.

Two shallow angle drop simulations are also performed. The drop configurations include nominal payload at ambient temperature with thick toroidal shell thickness (t=0.76 inches) to compare with the side-drop test performed for the benchmarking test. The results for the two shallow angle drop cases are presented in Table 2.12.1-1. The two shallow angles are 5° and 10° slapdown drops that are designated as Drop Case 13 and 14. The results of shallow angle drops for the 0° (Drop Case 2, side drop), 5° (Drop Case 13) and 10° (Drop Case 14) conclude that the side drop bounds the shallow angle cases with an acceleration of 157 g.

Besides the 30-foot drop configurations, two HAC drop configurations (side drop and end drop) are selected to perform the code-required pin puncture test, where the cask is dropped 30 feet and then followed by a drop height of 40 inches onto a rigid pin 6 inches in diameter. The maximum strain in the cask outer shell is 31% and limited to the puncture location. No gross deformations of the cask are predicted and the structural integrity of the containment boundary is maintained. Additionally, results for the combined 30-foot impact and pin puncture are used as input for the HAC thermal evaluation.

Table 2.12.1-1. Summary of Drop Cases and Results

Case No.	Description	Drop Angle degree	Drop Height (ft)	Shell thickness	Applicable Boundary Condition						Acceleration Results (g)
					Temperature			Payload			
					Amb	Hot	Cold	Normal	Heavy	light	
1	Benchmark HAC End Drop	90	30	Thick	X			X			130.0
2	Benchmark HAC Side Drop	0	30	Thick	X			X			157.0
3	Benchmark HAC Corner Drop	68 (=90-22)	30	Thick	X			X			73.8
4	NCT, Cold, End Drop	90	1	Thick			X			X	15.5
5	NCT, Cold, Side Drop	0	1	Thick			X			X	55.1
6	NCT, Cold, Corner Drop	68 (=90-22)	1	Thick			X			X	14.6
7	HAC, Cold, End Drop	90	30	Thick			X			X	129.8
8	HAC, Hot, End Drop	90	30	Thin		X			X		157.5
9	HAC, Cold, Side Drop	0	30	Thick			X			X	161.9
10	HAC, Hot, Side Drop	0	30	Thin		X			X		110.7
11	HAC, Cold, Corner Drop	68 (=90-22)	30	Thick			X			X	80.3
12	HAC, Hot, Corner Drop,	68 (=90-22)	30	Thin		X			X		52.8
13	HAC, Ambient, Slap down	5	30	Thick	X			X			114.4
14	HAC, Ambient, Slap down	10	30	Thick	X			X			118.0
15	HAC, Hot, End Drop + Puncture	90	30 ft + 40 in.	Thin		X			X		Same as Case No. 8
16	HAC, Hot, Side Drop + Puncture	0	30 ft + 40 in	Thin		X			X		Same as Case No. 10

Multiple LS-DYNA dynamic finite element analyses are performed to determine the structural response of the Model 2000 cask during the impacts onto unyielding surface following NCT and HAC accident events. For each drop case the acceleration of the payload and inner containment enclosure is calculated. Three full 3D half-symmetry models are used to account for the asymmetry of the cask configuration. The three finite element models consist of the same node numbers, elements, material properties and control cards. The only differences are the nodal geometry and the direction of initial velocity. A representative finite element solid model is shown in Figure 2.12.1-1.

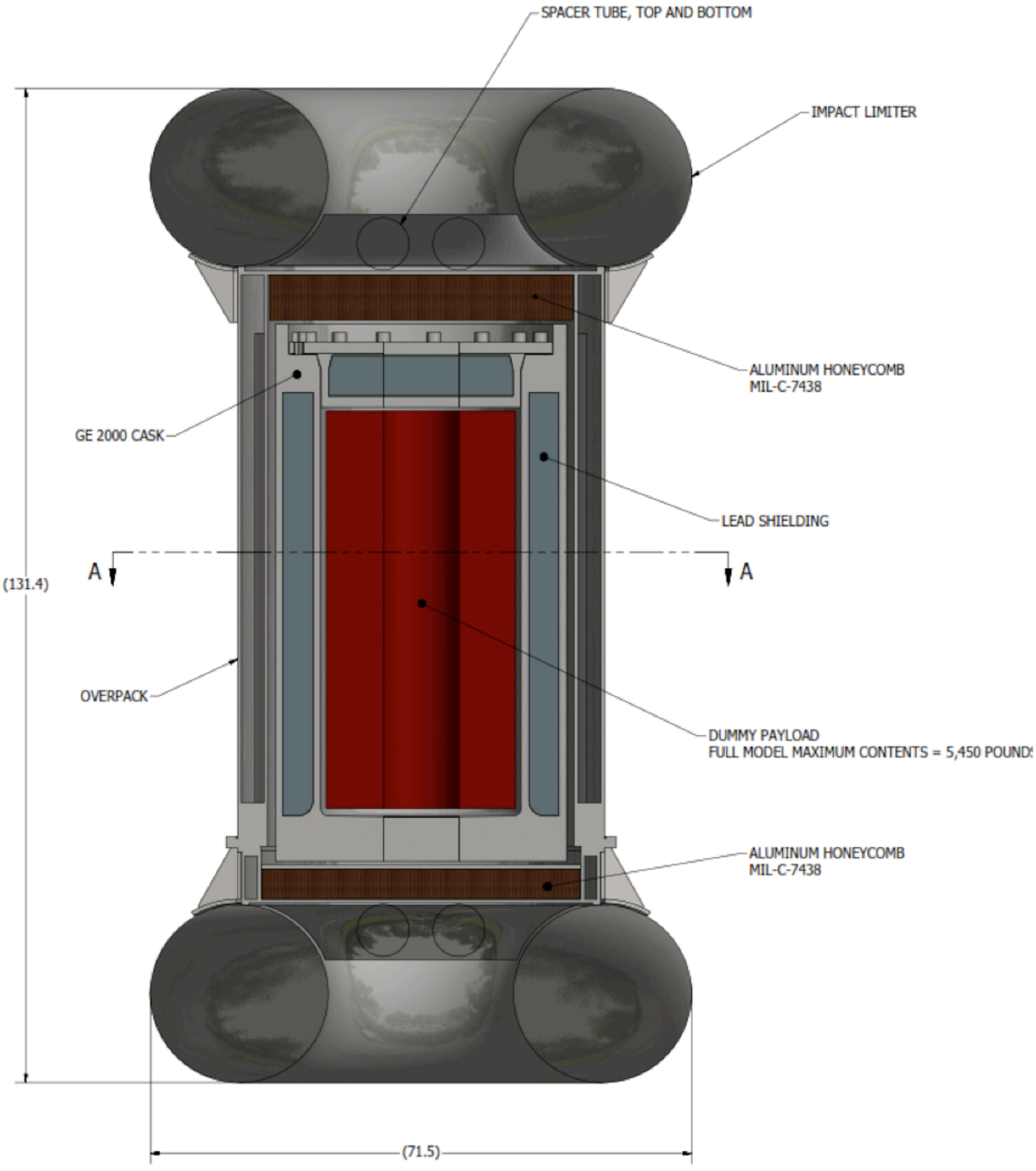

Figure 2.12.1-1. Model 2000 Solid Model

The three drop orientations are shown in Figure 2.12.1-2.

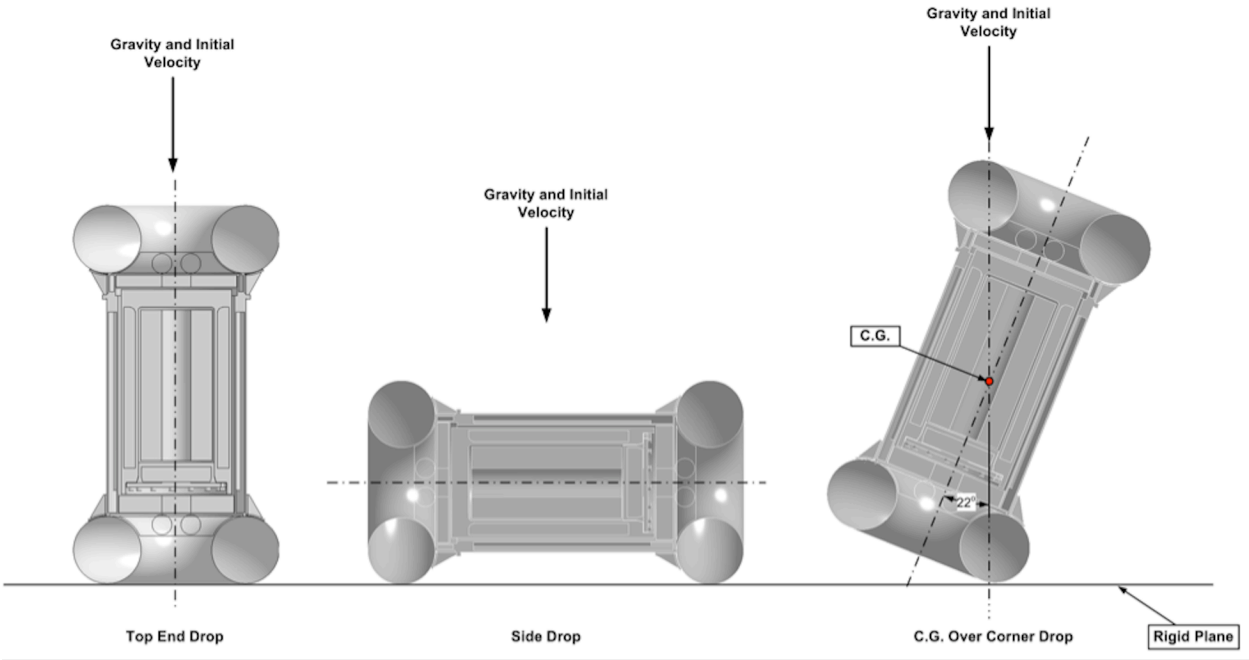

Figure 2.12.1-2. Drop Orientations

2.12.1.2. Benchmarking Runs

The selection of the drop cases is described in this section. Section 2.12.1.12.1 contains the benchmark results. Benchmarks of the analysis methodology are performed using the 3-drop orientations shown in Figure 2.12.1-2 to compare with the actual drop tests performed on a quarter-scale model. The benchmark runs are designated as Drop Cases 1 through 3. The actual drop tests were performed under at ambient temperature. The nominal payload weight is 5,450 pounds. The thickness in the toroidal shell is 0.76 inches. The drop height is 30 feet. The parameters of the benchmarking runs are listed in Table 2.12.1-2.

Table 2.12.1-2. Benchmark Runs and the Drop Parameters

Case No.	Description	Drop Angle degree	Drop Height, (ft)	Toroid Thickness (in)	Applicable Boundary Condition					
					Temperature			Payload		
					Amb.	Hot	Cold	Normal	Heavy	light
1	End Drop	90	30	0.76	X	—	—	X	—	—
2	Side Drop	0	30	0.76	X	—	—	X	—	—
3	C.G. Over Corner Drop	22	30	0.76	X	—	—	X	—	—

2.12.1.3. Normal Condition of Transport

The purpose of the drop simulation is to determine the peak acceleration of the payload and contents during the drop. The bounding acceleration occurs when the toroidal shell is thick so a stiffer response will result. At cold temperature, the material properties have greater elasticity and

yield strength, therefore results in a stiffer response. Finally, a lighter payload will result in lower total cask weight, which in turn causes greater acceleration during impact. The bounding three drops are simulated with thick toroidal shell, reduced-weight payload, and material properties at cold temperature. The drop cases are designated as Drop Case 4 through Drop Case 6, as listed in Table 2.12.1-3.

Table 2.12.1-3. Normal Condition of Transport Runs and the Drop Parameters

Case No.	Description	Drop Angle degree	Drop Height, (ft)	Shell Thickness (in)	Applicable Boundary Condition					
					Temperature			Payload		
					Amb.	Hot	Cold	Normal	Heavy	light
4	NCT Cold, End Drop	90	1.0	0.76	—	—	X	—	—	X
5	NCT Cold, Side Drop	0	1.0	0.76	—	—	X	—	—	X
6	NCT Cold, Corner Drop	68 (=90-22)	1.0	0.76	—	—	X	—	—	X

2.12.1.4. Hypothetical Accident Condition

The purpose of the drop simulation is to determine the peak acceleration of the payload and/or the maximum damage during the drop.

The bounding acceleration occurs when the toroidal shell is thick so a stiffer response will result. At cold temperatures, the material properties have greater elasticity and yield strength, which results in a stiffer response. Finally, a lighter payload will result in lowered total cask weight, which in turn causes greater acceleration during impact. The three drops with bounding accelerations are simulated with thick toroidal shell, reduced payload, and material properties at cold temperature. For the end drop, the maximum force on the closure lid bolts occurs when the container lid is oriented towards to the rigid plane. The drop cases are designated as Drop Cases 7, 9, and 11 for the end drop, side drop and C.G. over corner drop, respectively.

The maximum damage of the cask occurs when the toroidal shell is thin and has less structural strength. At warmer temperature, comparing with the material strength at ambient temperature, the material has lower elasticity and yield strength therefore resulted in greater damage to the cask. The heavier payload will also result in greater deformation of the toroidal shell. The drop cases with the bounding damage are designated as Drop Cases 8, 10, and 12 for the end drop, side drop and C.G. over corner drop, respectively. The six bounding drop cases for the HAC are listed in Table 2.12.1-4.

Table 2.12.1-4. Hypothetical Accident Condition of Transport Runs and the Drop Parameters

Case No.	Description	Drop Angle degree	Drop Height, (ft)	Shell Thickness (in)	Applicable Boundary Condition					
					Temperature			Payload		
					Amb.	Hot	Cold	Normal	Heavy	light
7	HAC, Cold, End Drop	90	30.0	0.76	—	—	X	—	—	X
8	HAC, Hot, End Drop	90	30.0	0.50	—	X	—	—	X	—
9	HAC, Cold, Side Drop	0	30.0	0.76	—	—	X	—	—	X
10	HAC, Hot, Side Drop	0	30.0	0.5	—	X	—	—	X	—
11	HAC, Cold, Corner Drop	68 (=90-22)	30.0	0.76	—	—	X	—	—	X
12	HAC, Hot, Corner Drop	68 (=90-22)	30.0	0.50	—	X	—	—	X	—

2.12.1.5. Shallow Angle Drops

Two shallow angle drops (5° and 10° from horizontal) with the drop configuration shown in Figure 2.12.1.5-1 are performed to compare the acceleration with the result of the side drop benchmark run. With the same material parameters as the benchmark run, the shallow angle drop parameters consist of the nominal payload weight, material properties at ambient temperature, and thick toroidal shell thickness. The drop cases are designated as Drop Cases 13 and 14 as listed in Table 2.12.1-5.

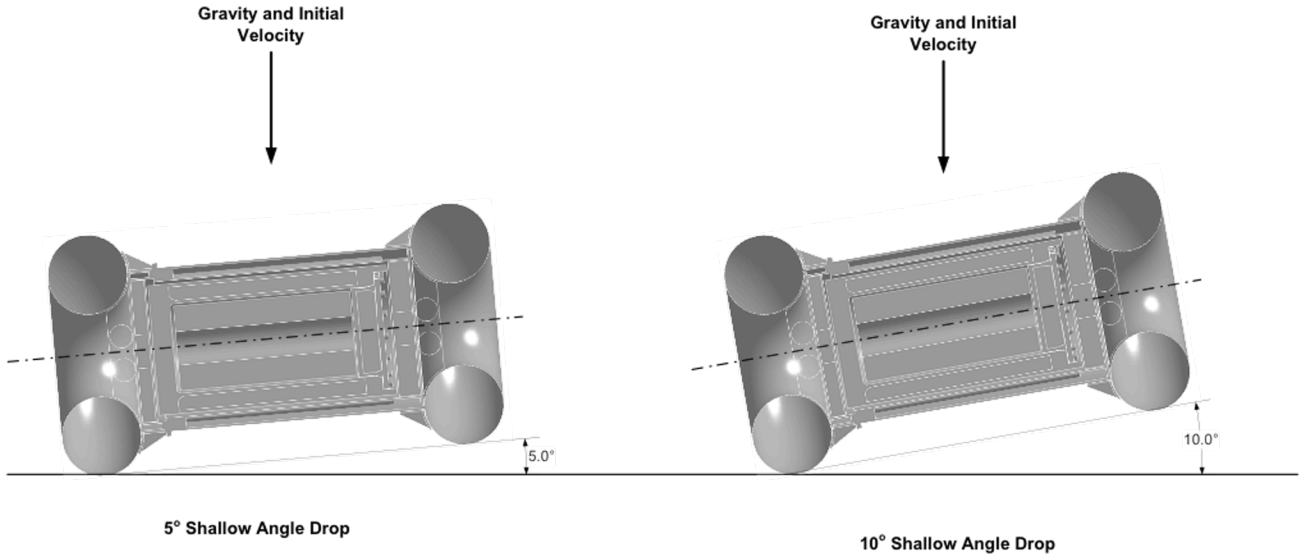

Figure 2.12.1.5-1. Shallow Angle Drops

Table 2.12.1-5. Shallow Angle Drop Runs and the Drop Parameters

Case No.	Description	Drop Angle degree	Drop Height, (ft)	Shell Thickness (in)	Applicable Boundary Condition					
					Temperature			Payload		
					Amb.	Hot	Cold	Normal	Heavy	light
13	HAC, Ambient, Slap Down	5	30.0	0.76	X	—	—	X	—	—
14	HAC, Ambient, Slap Down	10	30.0	0.76	X	—	—	X	—	—

2.12.1.6. Pin Puncture

10 CFR 71.73 requires that a free drop of the specimen through a distance of 1 meter (40 inches) in a position for which maximum damage is expected, onto the upper end of a solid, vertical, cylindrical, mild steel bar mounted on an essentially unyielding, horizontal surface. The bar must be 15 cm (6 inches) in diameter, with the top horizontal and its edge rounded to a radius of not more than 6 mm (0.25 inches), and of a length as to cause maximum damage to the package, but not less than 20 cm (8 inches) long. The long axis of the bar must be vertical.

To simulate the sequential drops, a rigid plane and a rigid pin 6 inches in diameter and 8 inches long are created, for the end drop and side drop respectively. During the pin puncture, the model is allowed to pass through the rigid plane; therefore, the puncture is independent of the pin length. Two-drop configurations are selected, that will be subjected to maximum damage. The drop configurations selected for the pin puncture drop are listed in Table 2.12.1-6. The drop cases are designated as Drop Cases 15 and 16 as listed in Table 2.12.1-6.

Table 2.12.1-6. HAC Drop Cases with Pin Puncture

Case No.	Description	Drop Angle degree	Drop Height (ft)	Pin Puncture Height in)	Shell Thickness (in)	Applicable Boundary Condition					
						Temperature			Payload		
						Amb.	Hot	Cold	Normal	Heavy	light
15	HAC, Hot, End Drop + Pin Puncture	90	30.0	40	0.50	—	X	—	—	X	—
16	HAC, Hot, Side Drop + Pin Puncture	0	30.0	40	0.50	—	X	—	—	X	—

2.12.1.7. Material Properties

2.12.1.7.1. 304 Stainless Steel

This material is used in the cask inner shell, over pack outer shell, gussets, and toroidal shell (impact limiter). The mechanical properties of the 304 SS at three different temperatures of interest in this calculation are tabulated in Table 2.12.1-7.

Table 2.12.1-7. Mechanical Properties of SS304 at Temperature of Interest

Temperature	-40°F	70°F	300°F
Ultimate Tensile Strength, ksi	75.0	75.0	66.2
Yield Strength, ksi	30.0	30.0	22.4
Modulus of Elasticity, E (10^6 psi)	28.8	28.3	27.0
Poisson's Ratio	0.31	0.31	0.31
Density, lb/in^3	0.29	0.29	0.29

The stress strain curves for SS304, taken from References 2-7 and 2-21, and are presented in Tables 2.12.1-8 through 2.12.1-10. The graphical representations of the stress strain curves of the SS304 are displayed in Figures 2.12.1.7-1 through 2.12.1.7-3.

Table 2.12.1-8. Stress Strain Curve of SS304 at -40°F

Strain	Stress, psi
0.0020	27,000
0.0034	30,000
0.0074	34,868
0.0182	39,736
0.0395	44,604
0.0625	49,472
0.0816	54,340
0.0998	59,208
0.1189	64,076
0.1398	68,944
0.1624	73,812
0.1870	78,680
0.2134	83,548
0.2418	88,416
0.2722	93,284
0.3045	98,152
0.3389	103,020
0.3753	107,888
0.4137	112,755
0.4542	117,623
0.5542	117,623
0.6542	117,623
0.7542	117,623

Table 2.12.1-9. Stress Strain Curve of SS304 at Ambient Temperature

Strain	Stress, psi
0.0020	27,000
0.0035	30,000
0.0075	34,868
0.0183	39,736
0.0396	44,604
0.0626	49,472
0.0817	54,340
0.0999	59,208
0.1191	64,076
0.1399	68,944
0.1626	73,812
0.1871	78,680
0.2136	83,548
0.2420	88,416
0.2723	93,284
0.3047	98,152
0.3391	103,020
0.3755	107,888
0.4139	112,755
0.4544	117,623
0.5544	117,623
0.6544	117,623
0.7544	117,623

Table 2.12.1-10. Stress Strain Curve of SS304 at 300°F

Strain	Stress, psi
0.0022	22,500
0.0033	25,000
0.0076	29,477
0.0198	33,953
0.0431	38,430
0.0659	42,906
0.0849	47,383
0.1036	51,859
0.1236	56,336
0.1454	60,812
0.1691	65,289
0.1947	69,765
0.2223	74,242
0.2518	78,719
0.2832	83,195
0.3167	87,672
0.3522	92,148
0.3896	96,625
0.4291	101,101
0.4707	105,578
0.5707	105,578
0.6707	105,578

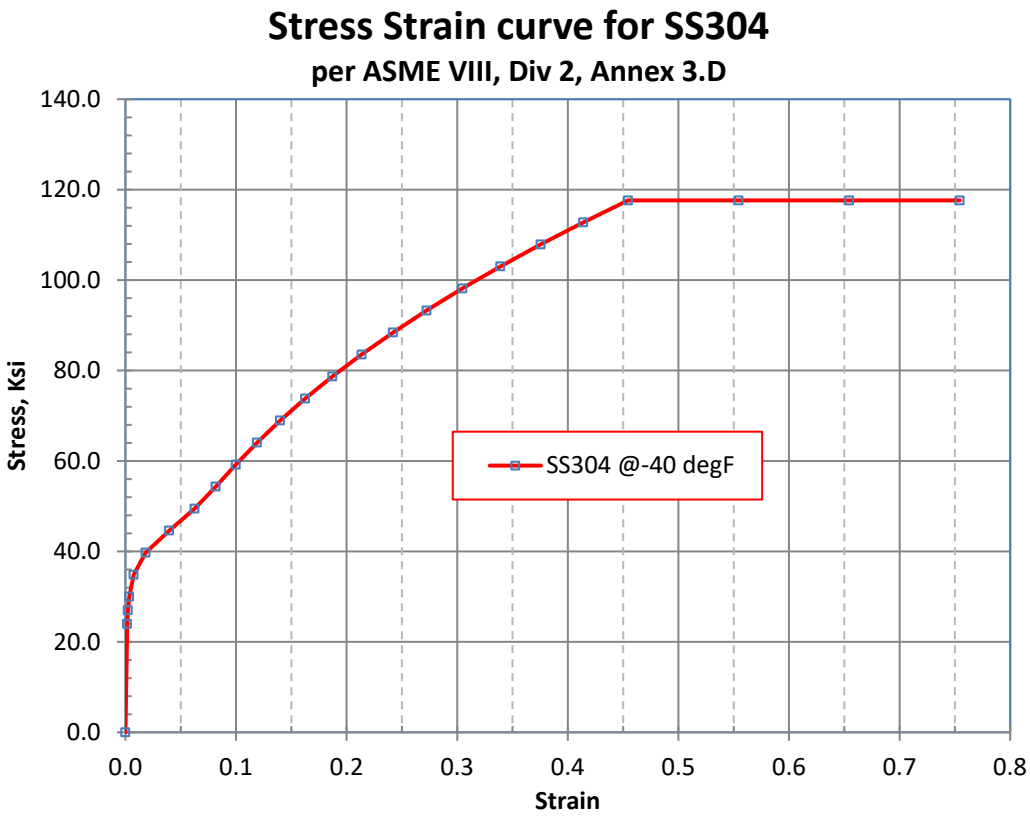

Figure 2.12.1.7-1. Stress-Strain Curve of SS304 at -40°F

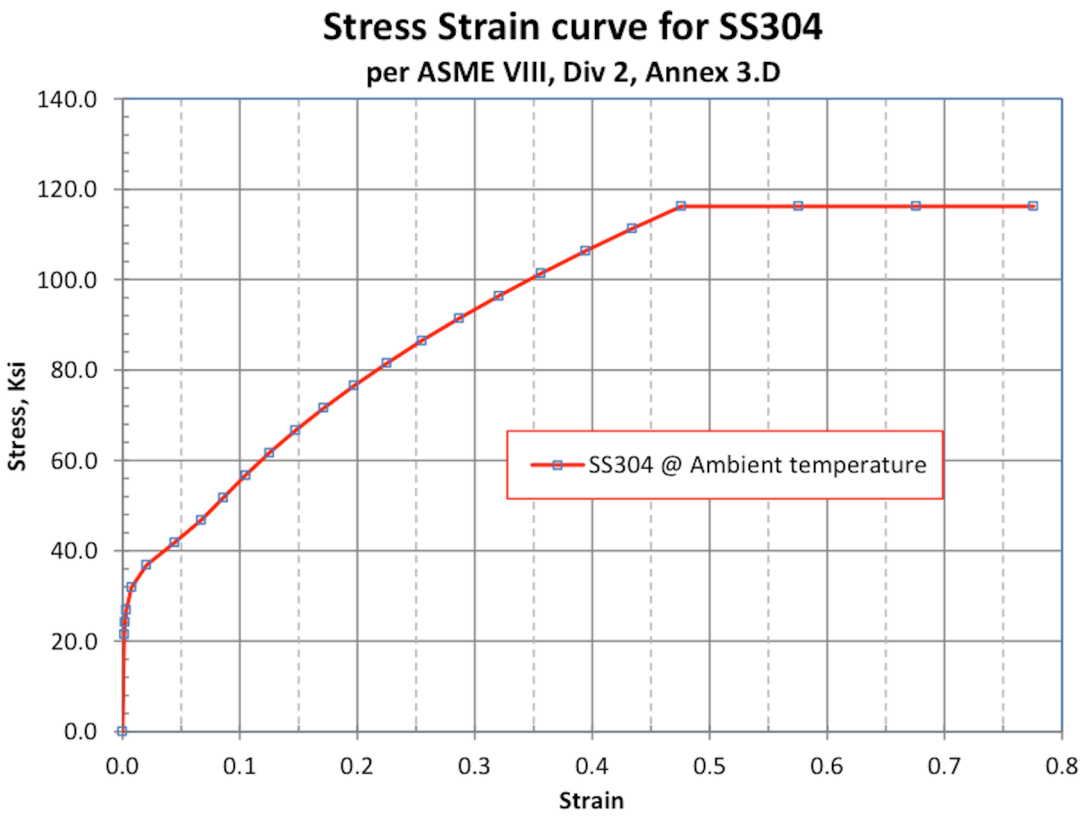

Figure 2.12.1.7-2. Stress-Strain Curve of SS304 at Ambient Temperature

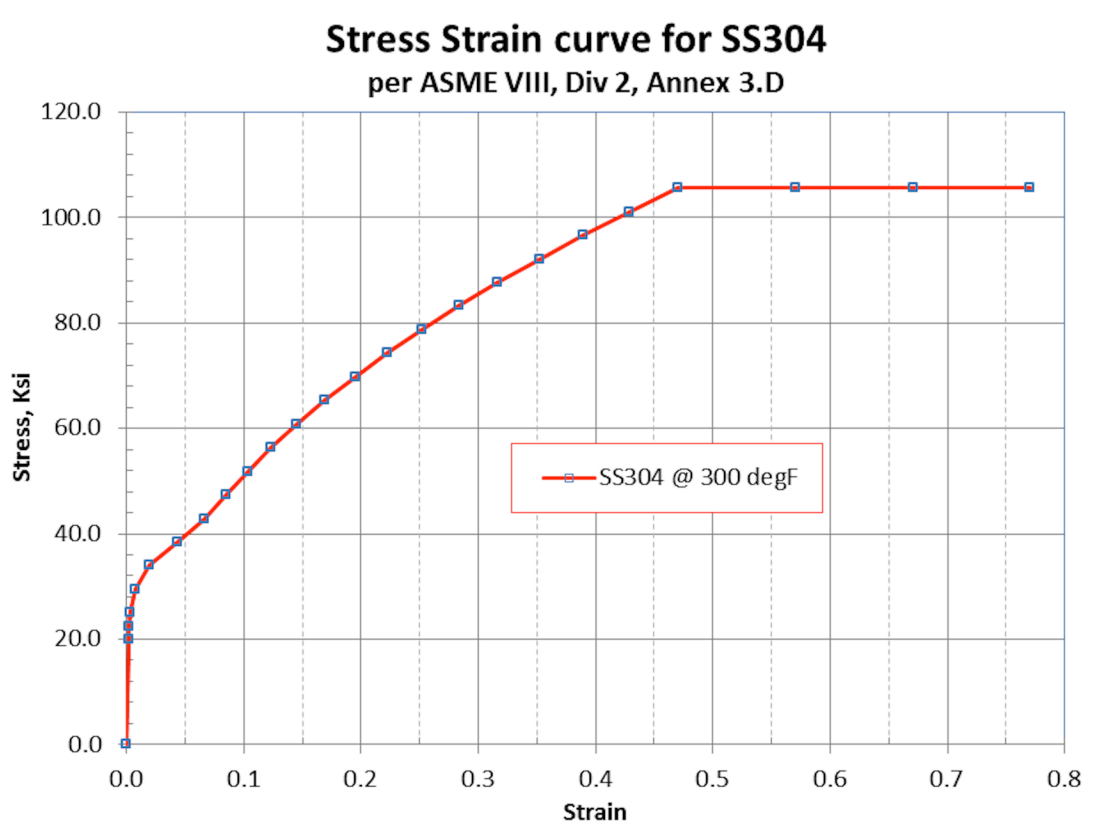

Figure 2.12.1.7-3. Stress-Strain Curve of SS304 at 300°F

2.12.1.7.2. Lead

Chemical lead is used in the cask as shielding material. The mechanical property of the chemical lead is presented in Table 2.12.1-11.

Table 2.12.1-11. Lead Temperature Dependent Properties

Temperature, (°F)	Modulus of Elasticity, $\times 10^6$ (psi)	Density (lb_m/in^3)	Yield Strength, (psi)
-40	2.58	0.41	795
75	2.41	0.41	620
100	2.38	0.41	580
150	2.30	0.41	550
300	2.04	0.41	390

2.12.1.7.3. Strain-Rate Sensitive Material Properties of SS304

The factors that elevate true stress-strain curves for SS304 at various strain rates and temperatures were generated by Reference 2-22 (pp. 84-87) and reproduced in Table 2.12.1-12.

Table 2.12.1-12. Strain-Rate Factors that elevated the Stress-Strain Curves of SS304

Strain Rate (in/in/sec)	-20°F	70°F	300°F	600°F
5	1.333	1.235	1.166	1.043
10	1.361	1.278	1.210	1.094
22	1.428	1.381	1.316	1.217
25	1.445	1.407	1.342	1.247

The data from the above table are used to generate the strain-rate multiplication factors for the current analyses at temperatures of -40°F, ambient temperature and 300°F.

2.12.1.7.4. Honeycomb Material Property

The crush strength of the honeycomb material is 750 psi. The material property at temperature of -20°F is assigned a value of 10% greater to account for the increase of rigidity due to cold temperature. Based on the HPI thermal analyses presented in Section 3, the temperature of the honeycomb material is bounded by 400°F. For the crush strength of honeycomb material at 400°F, a reduction of the crush strength of 40% is conservatively assigned. This is based on the thermal tests from Reference 2-23, p. 9. The temperature test result is presented in Figure 2.12.1.7-4.

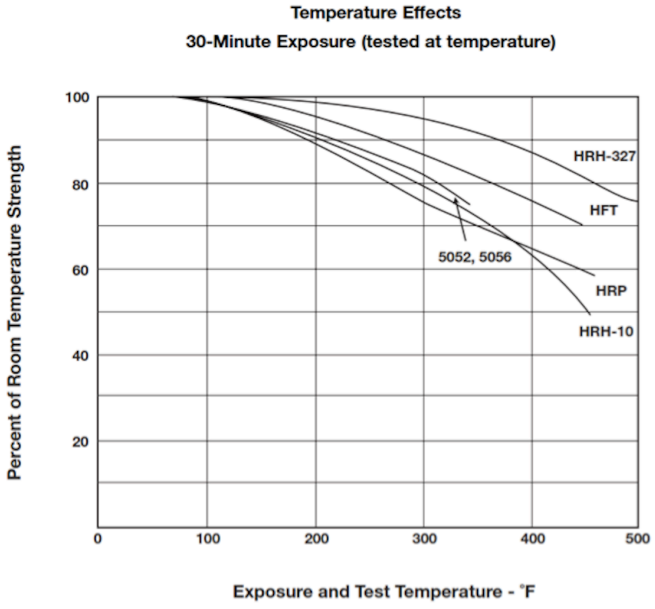

Figure 2.12.1.7-4. Temperature Effect of Honeycomb Material

2.12.1.7.5. Temperature Range for Material Properties

The component temperature range and justification for the applied temperature is discussed in Table 2.12.1-13.

Table 2.12.1-13. Component Temperature Range and Justification

Component, Material	Predicted Temperature Range	Applied Temperature	Justification for Use of Non-Bounding Peak Temperature
Overpack Toroids, 304 SS	-20 to 110-250	-20 to 300	Bounding. Provides primary impact protection
Cask Shell, 304 SS	-20 to 300-460	-20 to 300	Cask does not provide primary impact protection. Temperature range selected to best represent the performance of the cask during impact.
Cask Shielding, Lead	-20 to 330-450	-20 to 300	Lead does not provide primary impact protection. Therefore, temperature range considered acceptable for analyses.
Overpack Cover and Base, 304 SS	-20 to 170-370	-20 to 300	Overpack cover not included in model. The base does not provide primary impact protection. Therefore, range considered acceptable for analyses.
Overpack Honeycomb, Aluminum	-20 to 200-360	-20 to 400	40% compressive strength reduction bounds temperature of 400F. 10% compressive strength increase bounds temperature of -20F.

2.12.1.8. LS-DYNA Model Description

2.12.1.8.1. Finite Element Model

In accordance with the Model 2000 licensing drawings, an LS-DYNA finite element model was generated to evaluate the structural performance of the cask when loaded with the maximum content weight. The model includes the overpack and the Model 2000 cask body with lead shield and lid. The contents of the cask are modeled as a rigid body.

The 3D (half-symmetry) solid model of the Model 2000 cask and overpack was generated using Autodesk Inventor, which was imported into ANSYS Workbench Design Modeler (Reference 2-16). The finite element mesh was generated using the ANSYS Workbench Mechanical interface. The completed FEA model was then saved as a text input file to perform the analyses. Figure 2.12.1.8-1 shows the finite element model.

The finite element model is comprised of 3D brick elements (fully integrated selective-reduced solid) that represent the main body of cask components. Contact between components is modeled as surfaces using contact pairs. Boundary conditions such as symmetry are applied to the symmetry plane of the model. The final model includes 790,526 elements and 1,355,593 nodes.

[[

]]

Figure 2.12.1.8-1. Model 2000 Overpack and Cask Finite Element Model

2.12.1.8.2. Pin Puncture Analysis Methodology

The accident sequence presented in 10 CFR 71.73 requires that the cask, after a 30-foot drop, be dropped onto 6-inch diameter pin. To simulate the sequential drops, a rigid plane and a rigid pin with a 6-inch diameter and 8-inch length are created as shown in Figures 2.12.1.8-2 and 2.12.1.8-3 for the end drop and side drop, respectively.

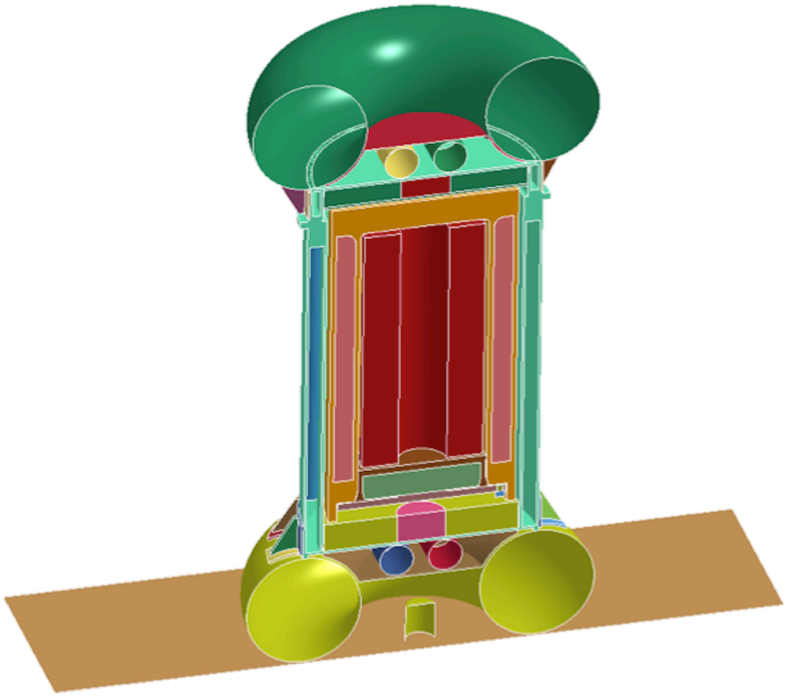

Figure 2.12.1.8-2. Rigid Plane and Pin Model for the End Drop Configuration

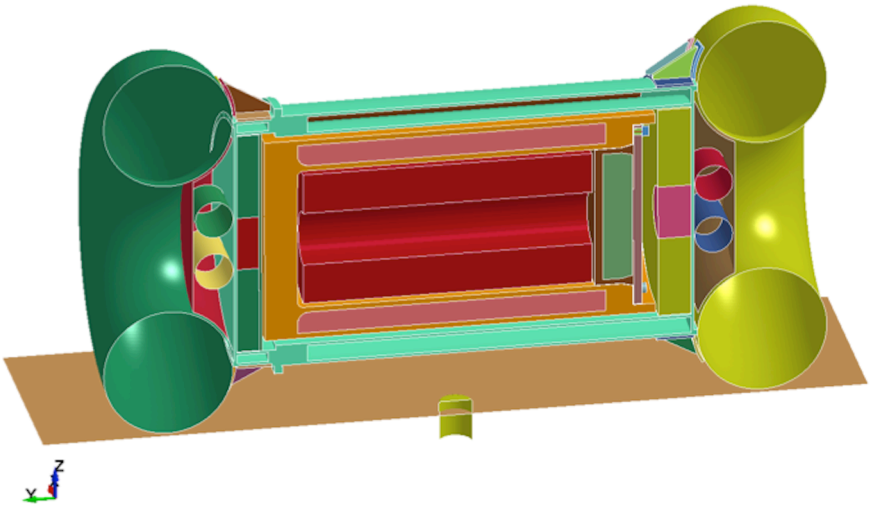

Figure 2.12.1.8-3. Rigid Plane and Pin Model for the Side Drop Configuration

The dynamic simulation for this 30-foot drop onto an unyielding surface followed by a 40-inch drop onto a pin is performed using a two steps drop sequence. For the first sequence, the impact velocity of the 30-foot drop is 527.5 in/sec. For the second sequence, the initial velocity for a 40-inch drop is 175.8 in/sec.

During the first drop sequence at the beginning of the 30-foot drop accident, the cask travels in the downward direction with an initial velocity of 703.3 in/sec (=527.5+175.8). The rigid plane and the pin travel at an initial velocity of 175.8 in/sec and the contact interface is activated between the cask and the rigid plane while the contact interface between the cask and the pin is not activated. Therefore, the relative velocity between the cask and the rigid plane is 527.5 in/sec, which is equivalent to a drop height of 30 feet. During this sequence, the distance between the cask the pin is reduced as time progresses. The kinetic energy of the cask dissipates to zero at time = 35 milliseconds. This is the time at which the puncture impact starts.

At the beginning of the second sequence, the distance between the pin and the cask is reduced to a minimum gap but not touching. At this point, the absolute velocity of the cask and pin is 175.8 in/sec. At this time, the contact interface between the pin and the cask is activated while the contact interface between the rigid plane and the cask is deactivated, which allows the damaged impact limiters to pass through the rigid plane. Additionally, the velocity of the pin is set to zero, which results in relative velocity between the cask and the pin of 175.8 in/sec. Figure 2.12.1.8-4 shows the cumulative damage following the 30-foot top end drop and 40-inch pin puncture.

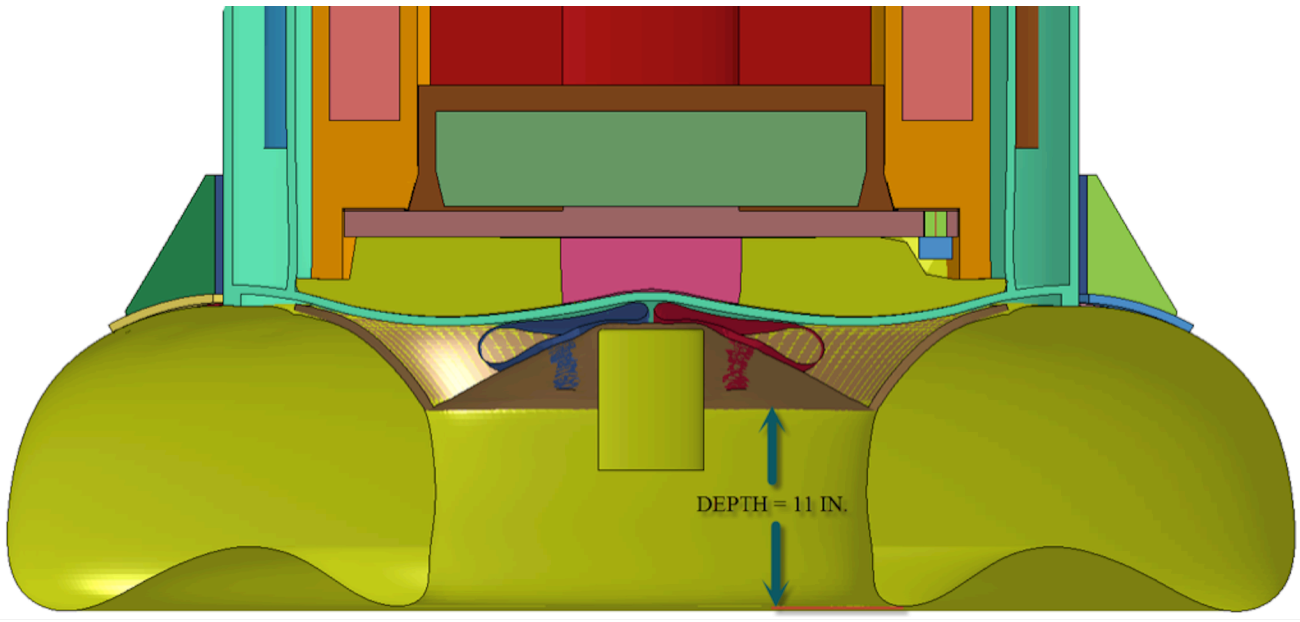

Figure 2.12.1.8-4. Deformed Geometry of the Overpack after a 30 foot End Drop

Figure 2.12.1.8-5 shows the cumulative damage for the side drop and pin puncture sequence. For the side drop, the depth of the unexposed cavity below the toroidal shell is less than 2.3 inches (taken from the result of Drop Case 10). Therefore, the modeled pin length of 8 inches is sufficient to sustain maximum damage.

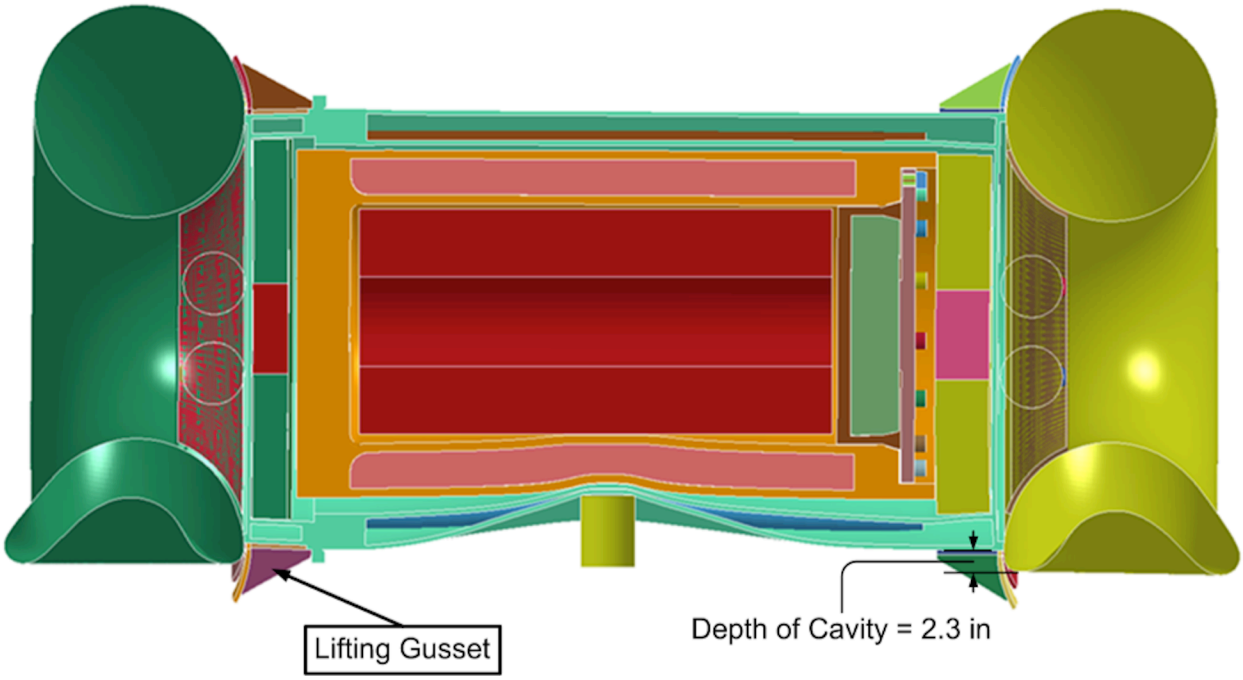

Figure 2.12.1.8-5. Deformed Geometry of the Overpack after a 30 foot Side Drop

2.12.1.9. Weight

The Model 2000 Transport Package components consist of the closure lid, cask body and overpack. The dimensions used in the calculations are taken from the Model 2000 Transport Package fabrication drawings. The total weight of the Model 2000 Transport Package empty is calculated to be 28,100 lb. From the finite element model, the center of gravity is located 1.5 inches below the centerline of the overpack, 64.25 inches from the bottom line. Table 2.1-3 presents the breakdown of the components weights used for the dynamic analyses.

2.12.1.9.1. Material Model

The LS-DYNA material models used in the analyses are described below:

- The stainless steel shells are modeled using *MAT_PIECEWISE_LINEAR_PLASTICITY.
- The honeycomb impact limiters are modeled using *MAT_CRUSHABLE_FOAM.
- The payload is modeled as *MAT_RIGID.
- The closure lid bolts of the inner shell are modeled as *MAT_ELASTIC.

2.12.1.9.2. Contact Interfaces

The control card *CONTACT_TIED_SURFACE_TO_SURFACE is used to fasten the welded components. For the components within the cask and the overpack, the control card *CONTACT_AUTOMATIC_SINGLE_SURFACE is used to provide global contact control. The honeycomb material has significant stiffness difference between the adjacent part, therefore the control card *CONTACT_AUTOMATIC_SURFACE_TO_SURFACE is used to control and prevent penetration between parts.

2.12.1.10. Boundary Conditions

2.12.1.10.1. Symmetry Plane

The half-symmetry finite element model utilizes symmetry boundary conditions that are applied to the cut plane of the half-model in the Z-direction.

2.12.1.10.2. Initial Velocity

The drop height, H, is converted to kinetic energy using the formula below.

$$V = \sqrt{2 \times g \times H}$$

where

V = the initial velocity at the threshold of impact, in/s

g = gravity constant = 386.4 in/s².

H = drop height, in

Therefore, the drop height of H=30 ft is converted to initial velocity, V360-in, as

$$V_{360\text{-in}} = \sqrt{2 \times g \times 360} = 527.45 \text{ in/s}$$

And the drop height of H=40-in is converted to initial velocity, V40-in, as

$$V_{40\text{-in}} = \sqrt{2 \times g \times 40} = 175.8 \text{ in/s}$$

2.12.1.10.3. Gravity

The gravity of 386.4 in/s is applied to all components in the global Z-direction with an initial ramp up period of 0.05 seconds.

2.12.1.11. Dynamic Analysis Results HAC 30-foot Drops

The results of the impact analyses of the Model 2000 cask model in the forms of acceleration of the payload and plastic strain of the toroid shell are presented in Sections 2.12.1.11.1 through 2.12.1.11.14. Further, each section contains four plots, which include a plot for the deformed overpack shape, the cask acceleration time history, energy time histories and interface sliding energy time history (Figures 2.12.1.11-1 through 2.12.1.11-58). Section 2.12.1.11.15 presents the results of the 30-foot drop followed by pin puncture drop. The significance of the accelerations and energy time histories (kinetic energy, internal energy, hourglass energy, and sliding energy) of the simulations are described below.

Accelerations – Accelerations are extracted from the LS-DYNA MATSUM file. Using the MATSUM data allows for the reporting of the maximum acceleration in any part and at any point in the model.

Kinetic Energy - The kinetic energy time history is used to confirm that the kinetic energy of the cask assembly is completely dissipated during the impact and the acceleration has peaked. For a normal and completed drop impact scenario, the kinetic energy must be decreasing to a minimum value as close to zero as possible and starts to increase (due to gravity loading). At the moment of minimum kinetic energy, the primary impact event is over.

Internal Energy - The internal energy plot is a measure of how much of the kinetic energy is converted into strain energy, either elastic or inelastic. Most likely, the internal energy is a measure of inelastic strain energy corresponding to the permanent deformation of the energy absorber material. The accumulated internal energy is a measure of how well the impact limiter is working as designed. Internal energy that is significantly smaller than the initial kinetic energy is an indication that the impact limiter is not dissipating the impact energy.

Hourglass Energy - The hourglass energy and the sliding energy are numerical terms that are produced by the mathematic solver but not derived from kinetic energy. The hourglass energy is strain energy numerically produced and proportional to the energy used to control the distortion of brick finite elements (solid element). As recommended by the LS-DYNA user manual, the brick elements perform best during the solution when the hourglass energy is limited to less than 10% of the internal energy.

Sliding Energy - The sliding energy plots represent the efficiency of the contact interface and the level of penetration between adjacent parts. A negative sliding energy indicates that the contact interface is not working well with a high degree of part penetrations. The contact interface control parameters must be revised to allow the use of different contact algorithms to prevent parts penetrations and pass-through. A positive sliding energy indicates the contact interface is working well and no penetrations are present.

2.12.1.11.1. Case 1 End Drop Benchmark

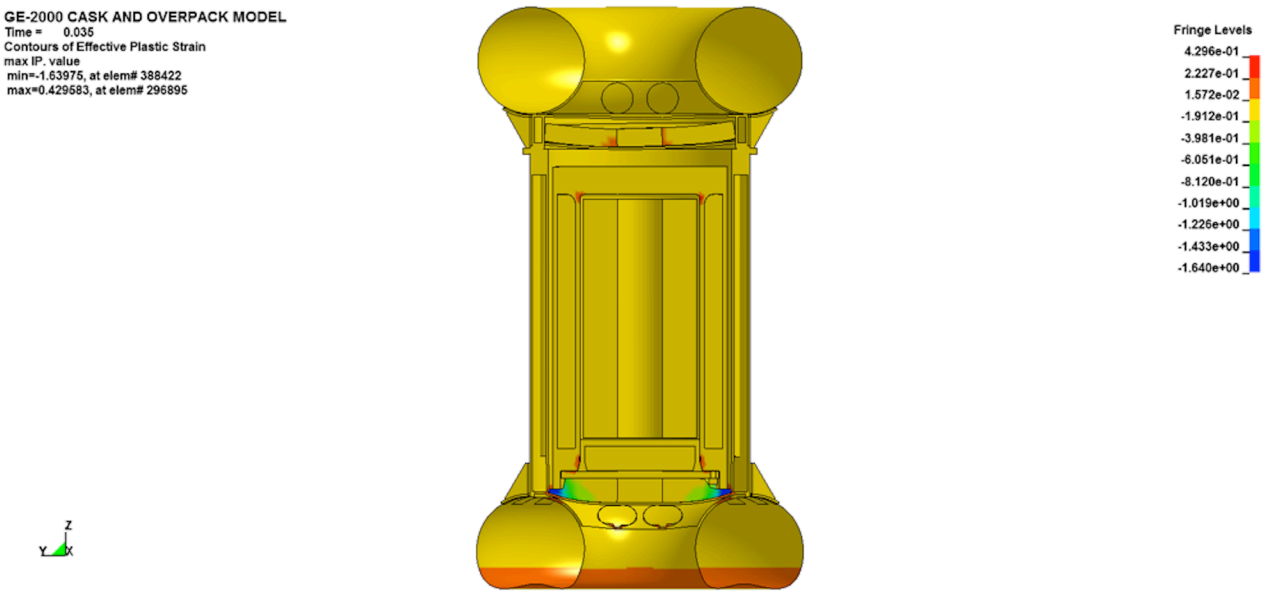

Figure 2.12.1.11-1. Case 1 Deformed Overpack Shape (Effective Plastic Strain)

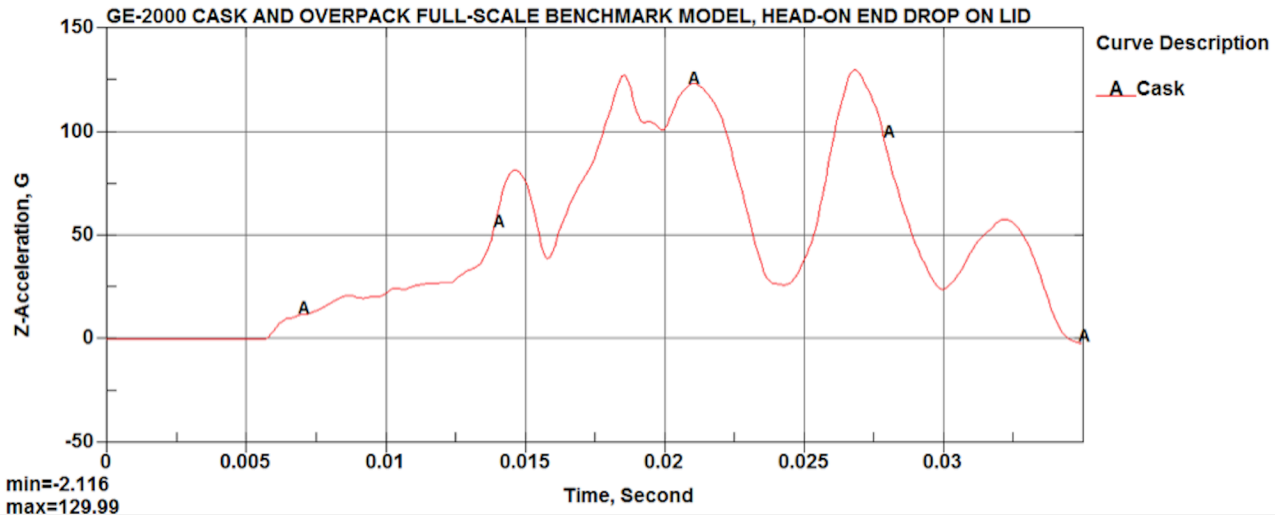

Figure 2.12.1.11-2. Case 1 Payload Acceleration Time History

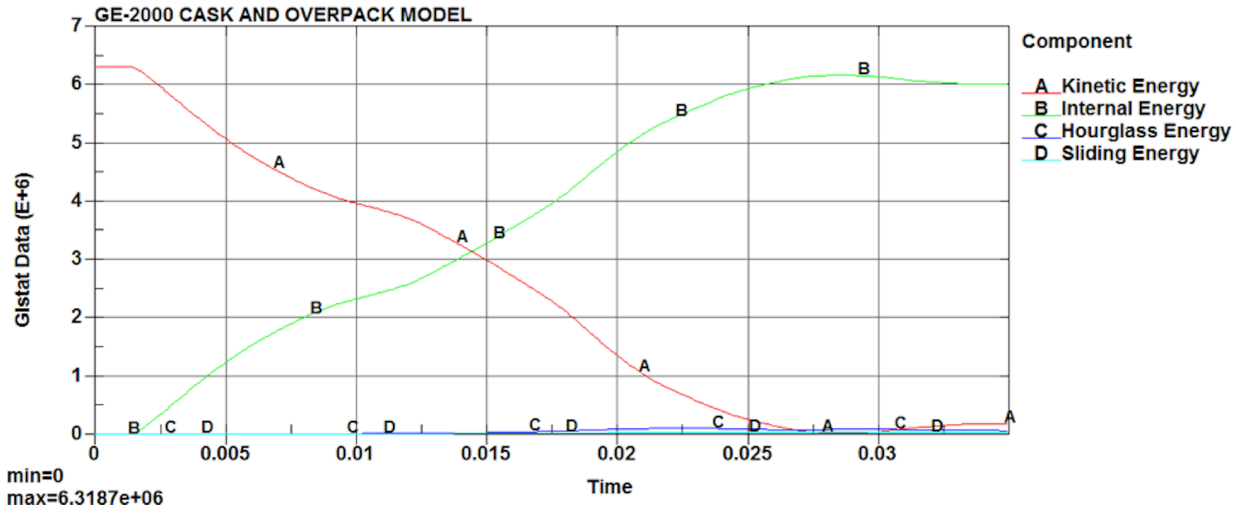

Note: time in Seconds

Figure 2.12.1.11-3. Case 1 Impact Energy Plot

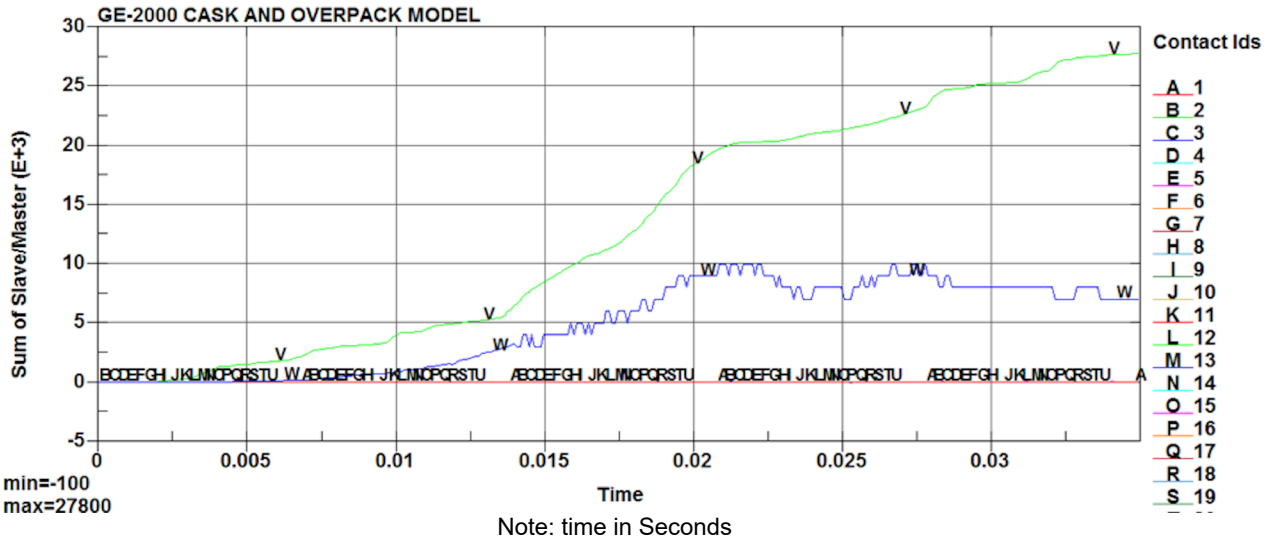

Note: time in Seconds

Figure 2.12.1.11-4. Case 1 Interface Sliding Energy Time History

2.12.1.11.2. Case 2 Side Drop Benchmark

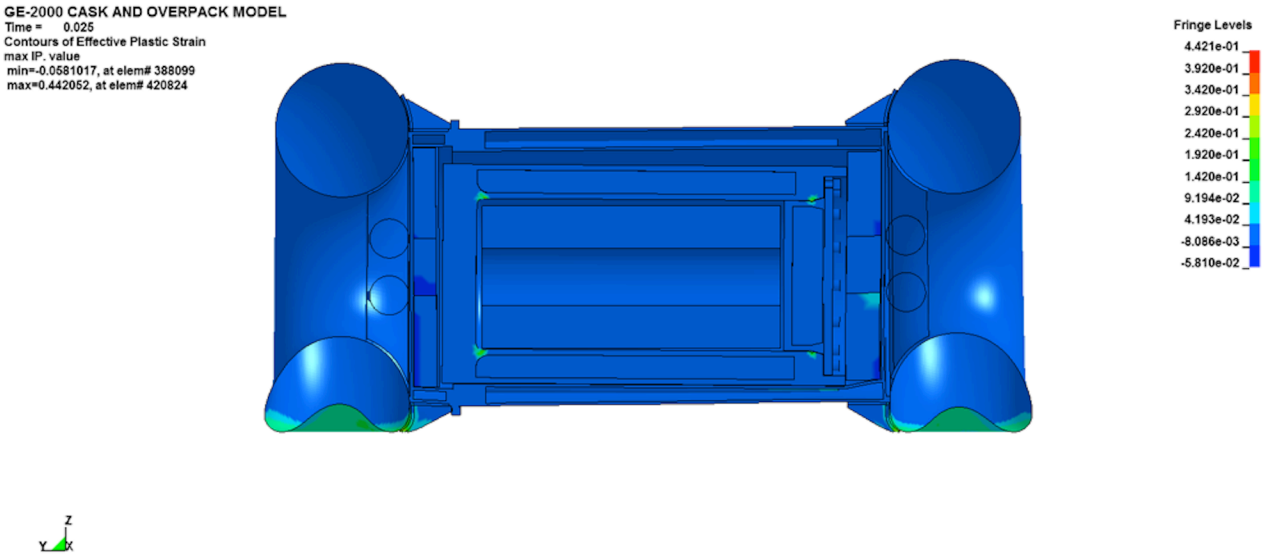

Figure 2.12.1.11-5. Case 2 Deformed Overpack Shape (Effective Plastic Strain)

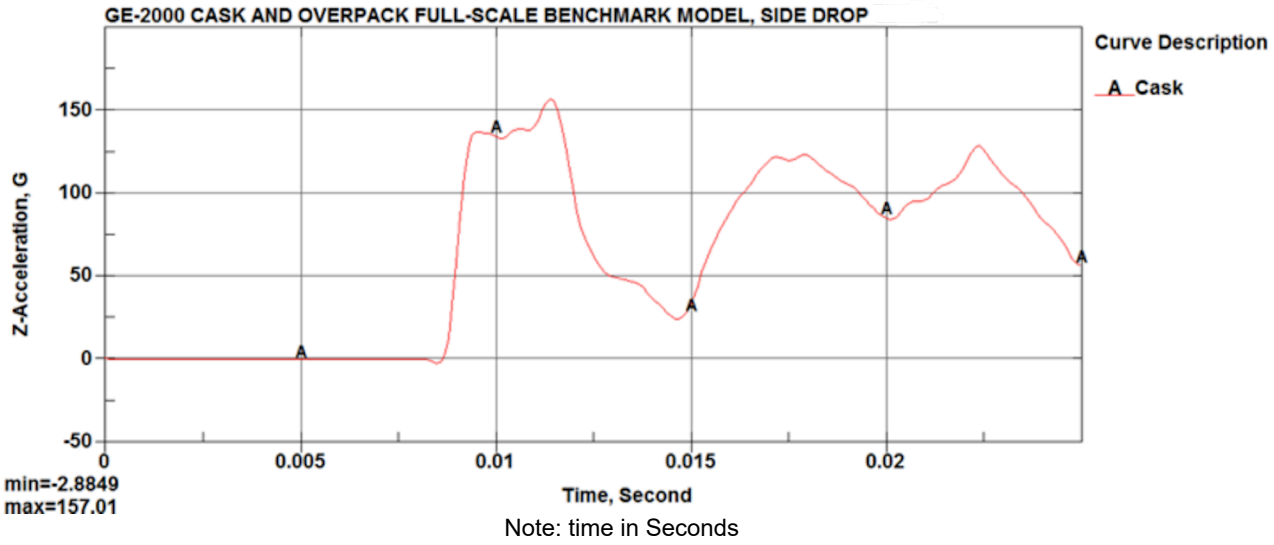

Note: time in Seconds

Figure 2.12.1.11-6. Case 2 Payload Acceleration Time History

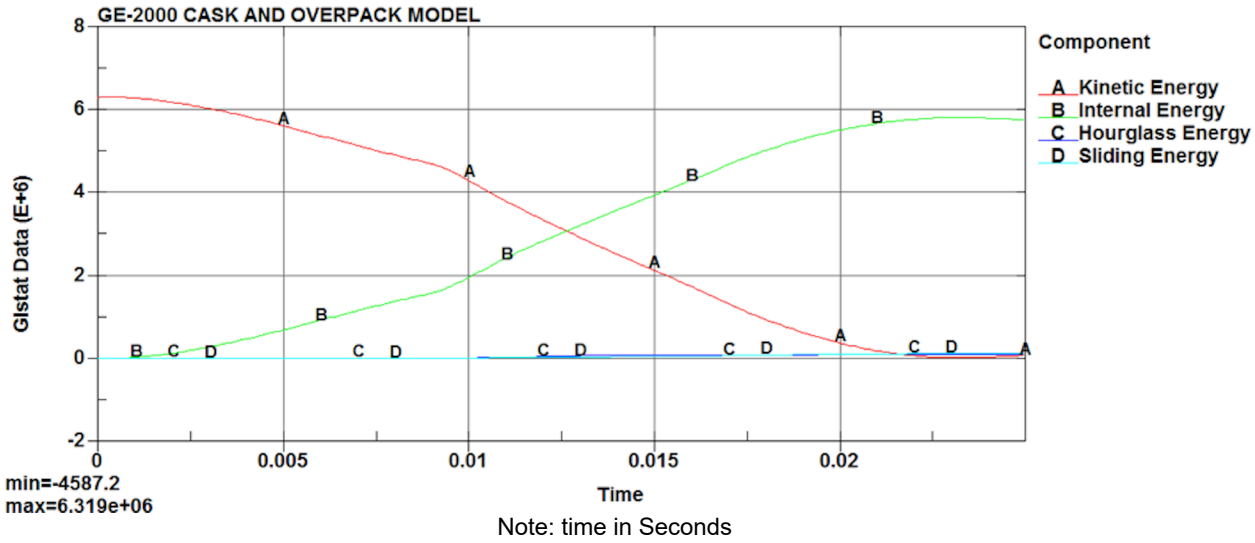

Figure 2.12.1.11-7. Case 2 Impact Energy Plot

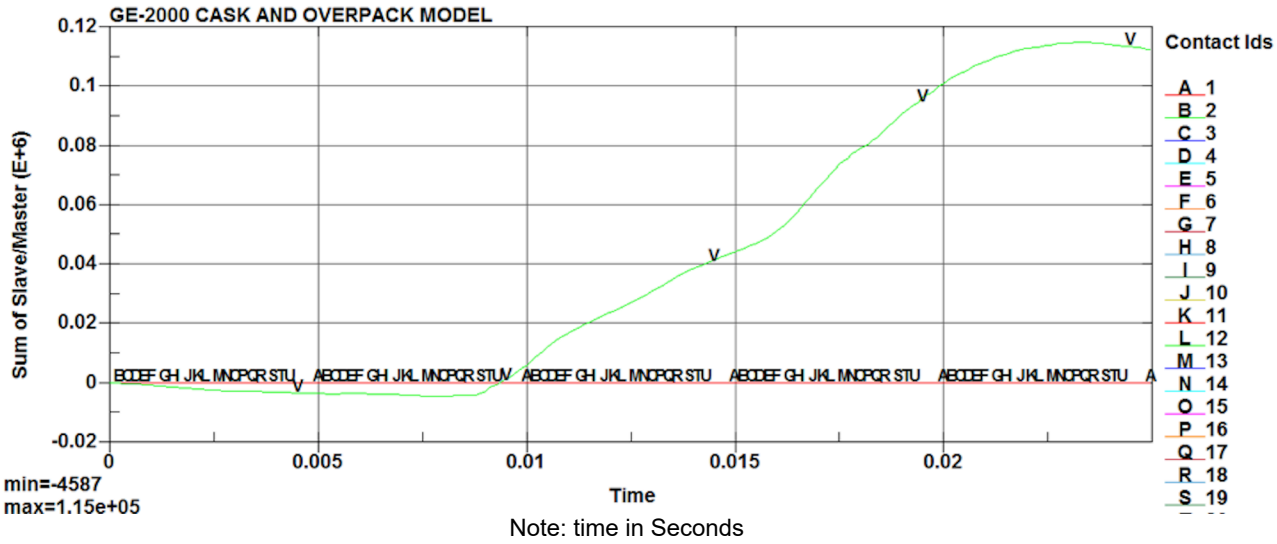

Figure 2.12.1.11-8. Case 2 Interface Sliding Energy Time History

2.12.1.11.3. Case 3 C.G. over Corner Drop Benchmark

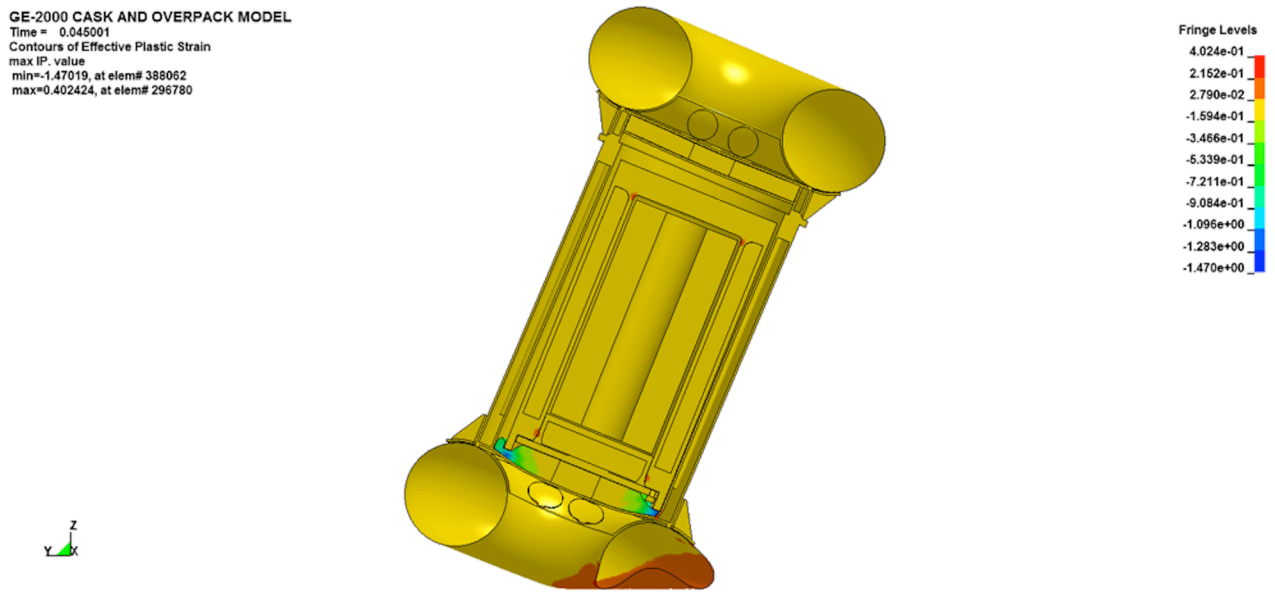

Figure 2.12.1.11-9. Case 3 Deformed Overpack Shape (Effective Plastic Strain)

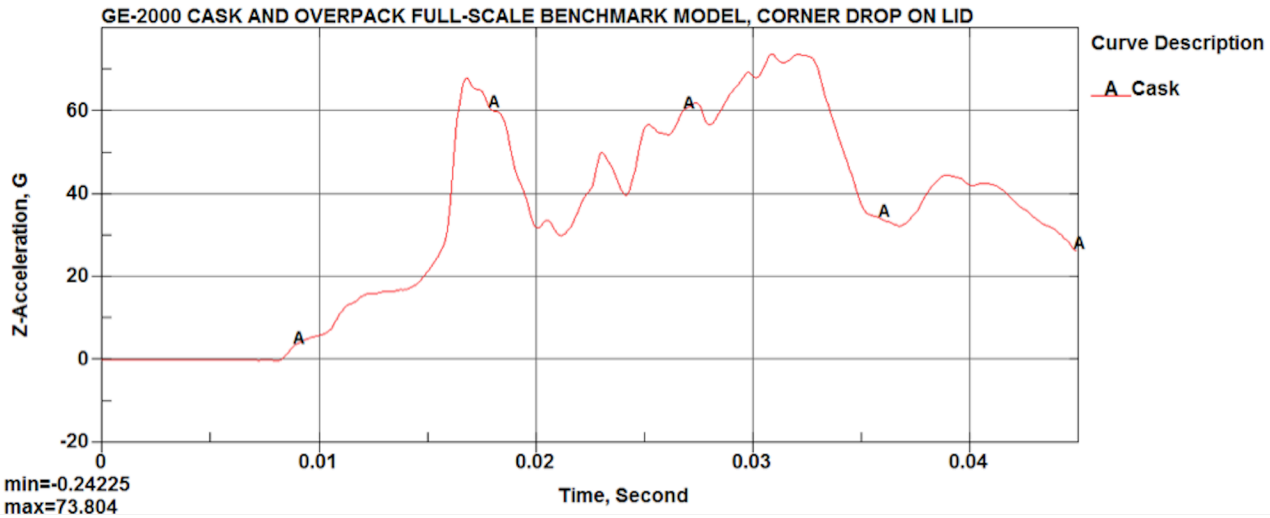

Note: time in Seconds

Figure 2.12.1.11-10. Case 3 Payload Acceleration Time History

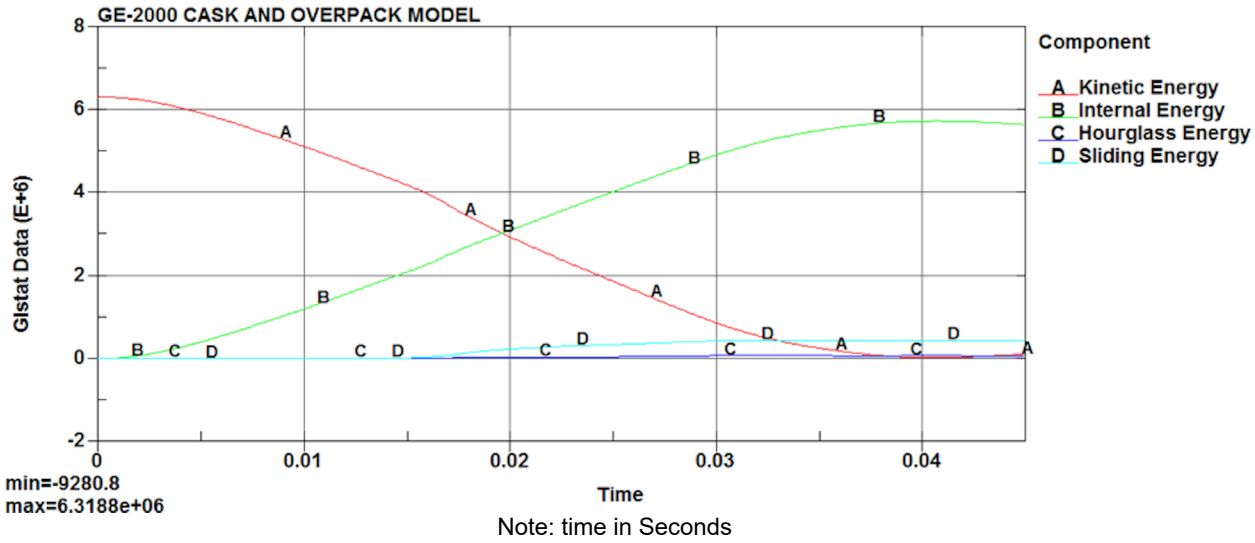

Figure 2.12.1.11-11. Case 3 Impact Energy Plot

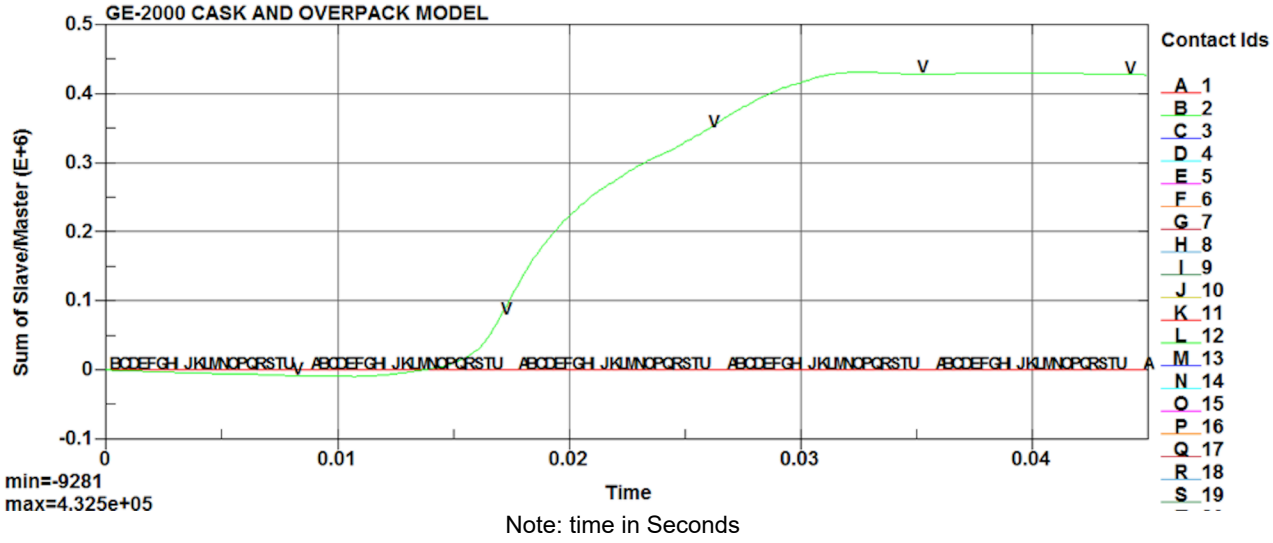

Figure 2.12.1.11-12. Case 3 Interface Sliding Energy Time History

2.12.1.11.4. Case 4 NCT End Drop with Thick Shell, Cold Condition and Light Payload

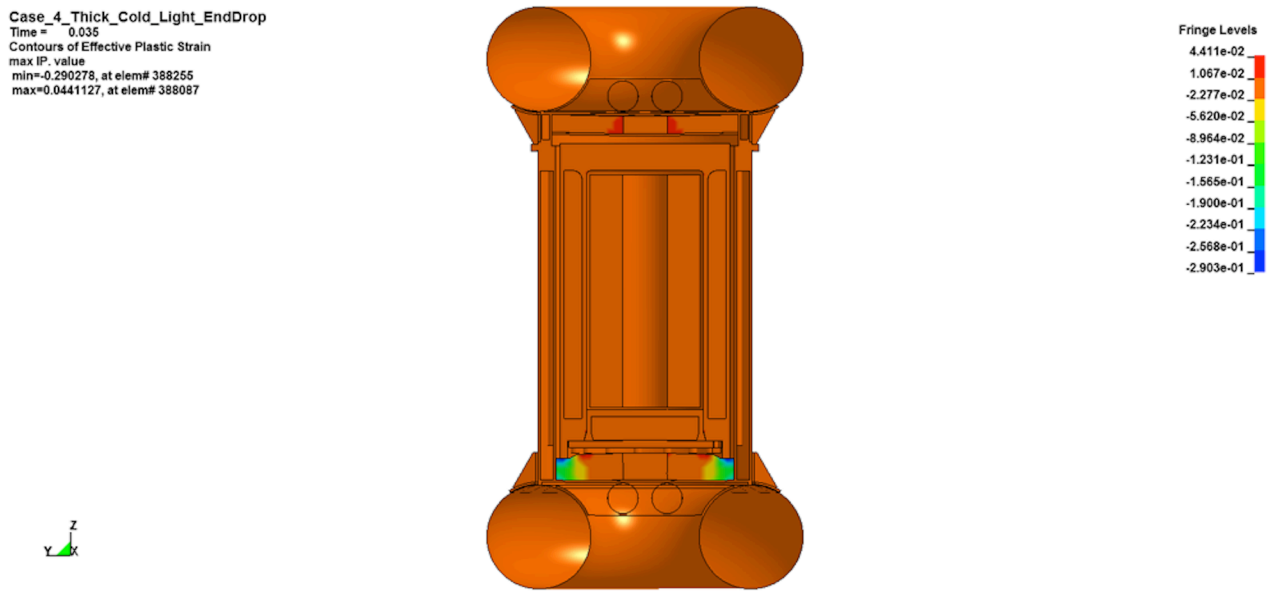

Figure 2.12.1.11-13. Case 4 Deformed Overpack Shape (Effective Plastic Strain)

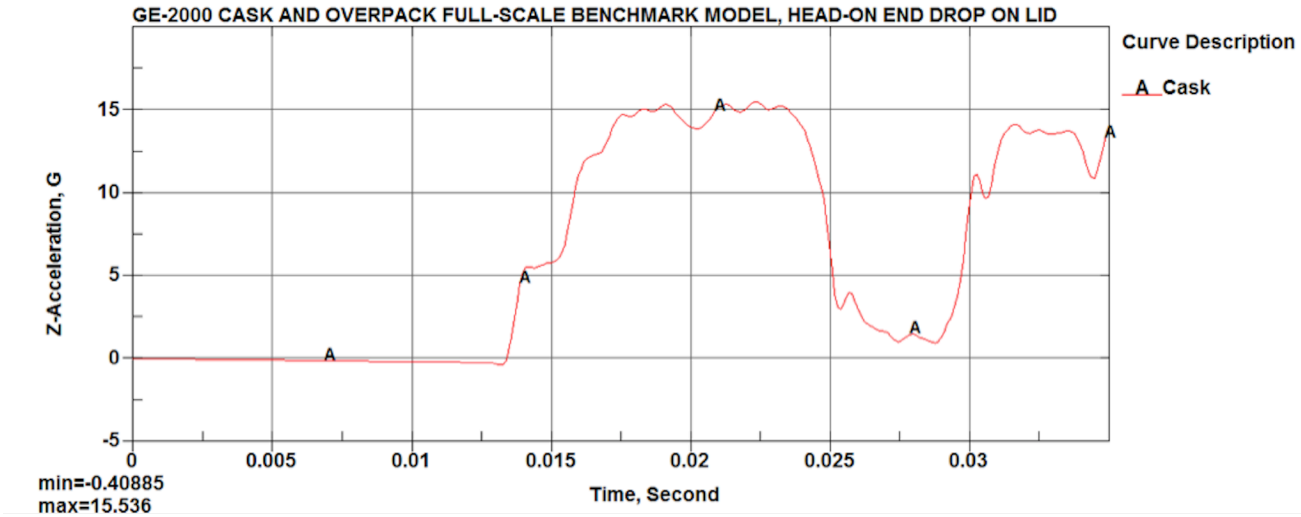

Figure 2.12.1.11-14. Case 4 Payload Acceleration Time History

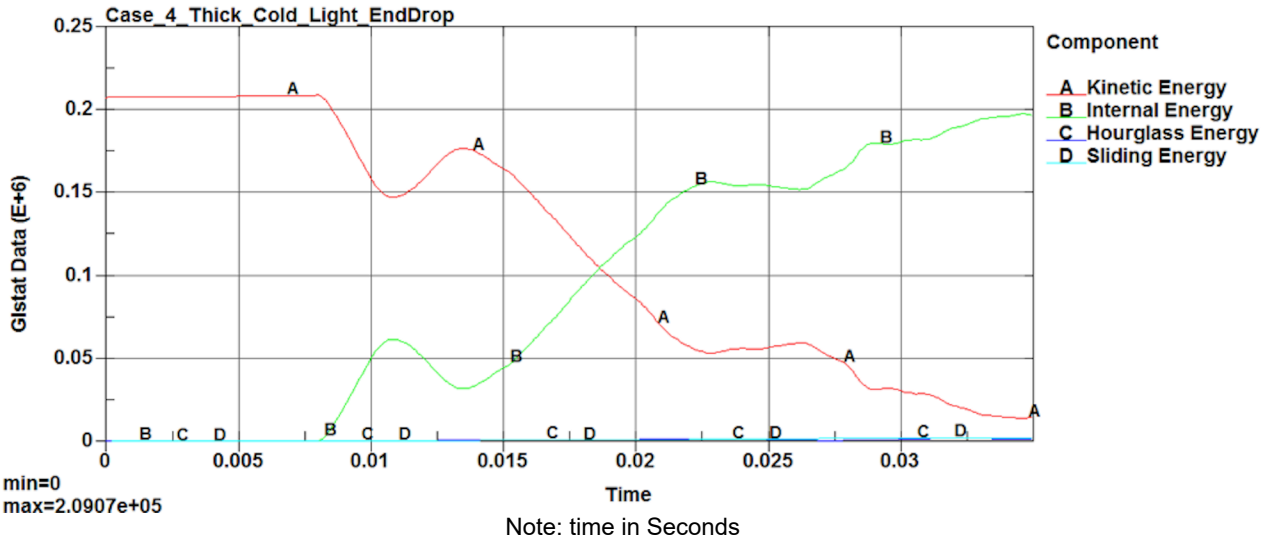

Note: time in Seconds

Figure 2.12.1.11-15. Case 4 Impact Energy Plot

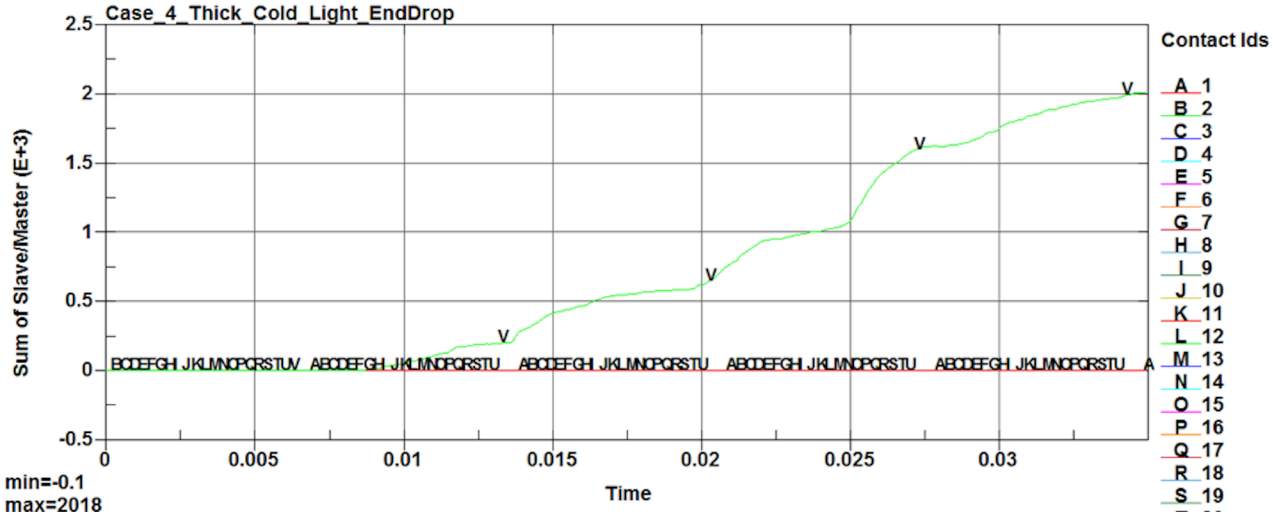

Note: time in Seconds

Figure 2.12.1.11-16. Case 4 Interface Sliding Energy Time History

2.12.1.11.5. Case 5 NCT Side Drop with Thick Shell, Cold Condition and Light Payload

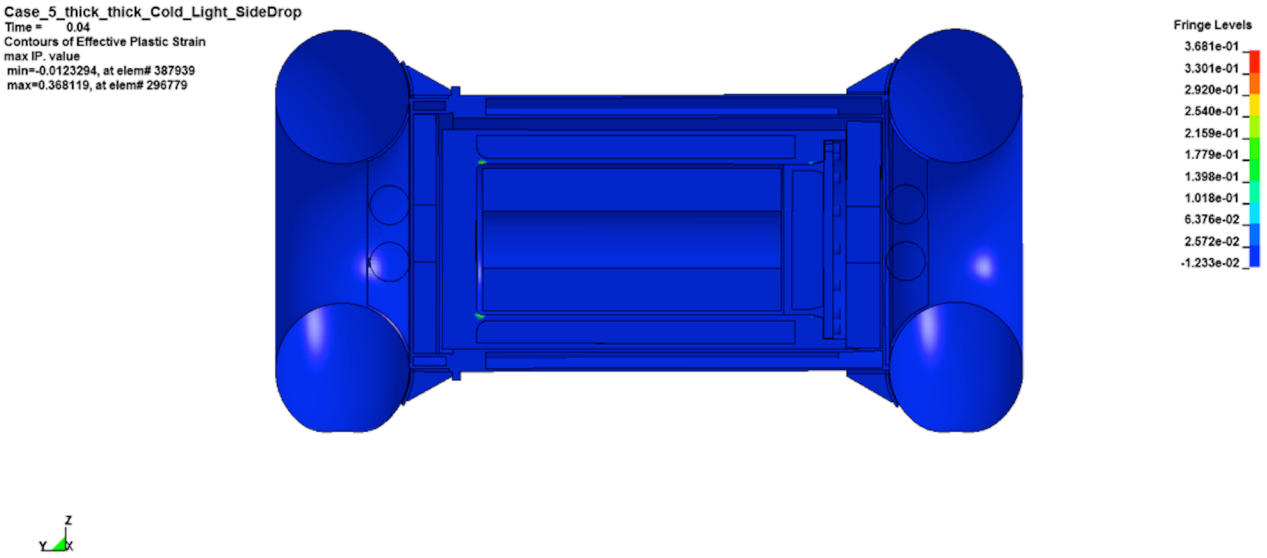

Figure 2.12.1.11-17. Case 5 Deformed Overpack Shape (Effective Plastic Strain)

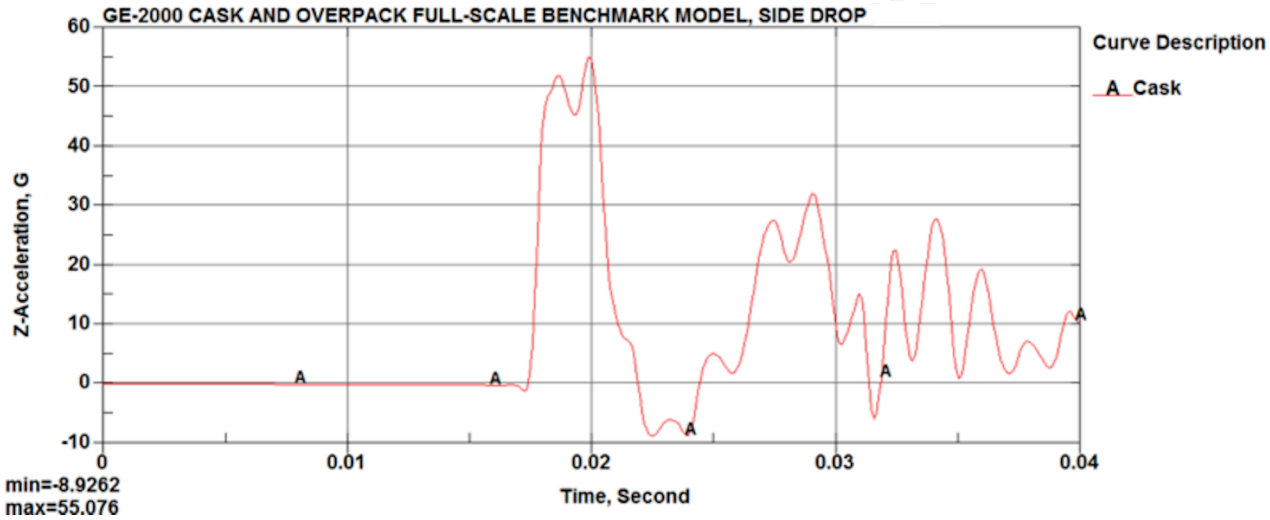

Figure 2.12.1.11-18. Case 5 Payload Acceleration Time History

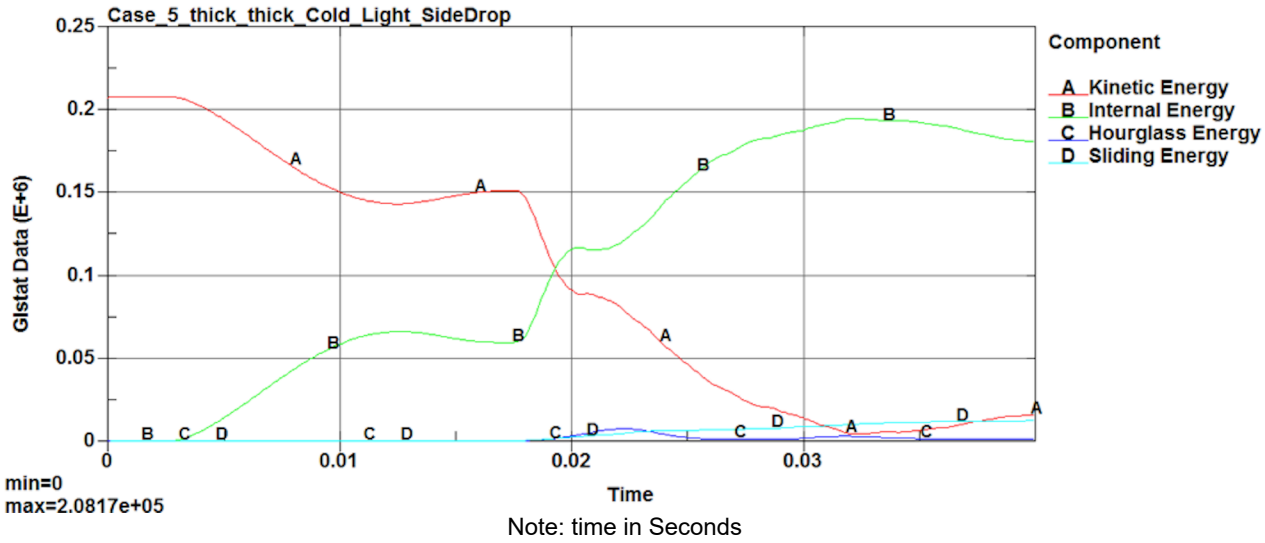

Note: time in Seconds

Figure 2.12.1.11-19. Case 5 Impact Energy Plot

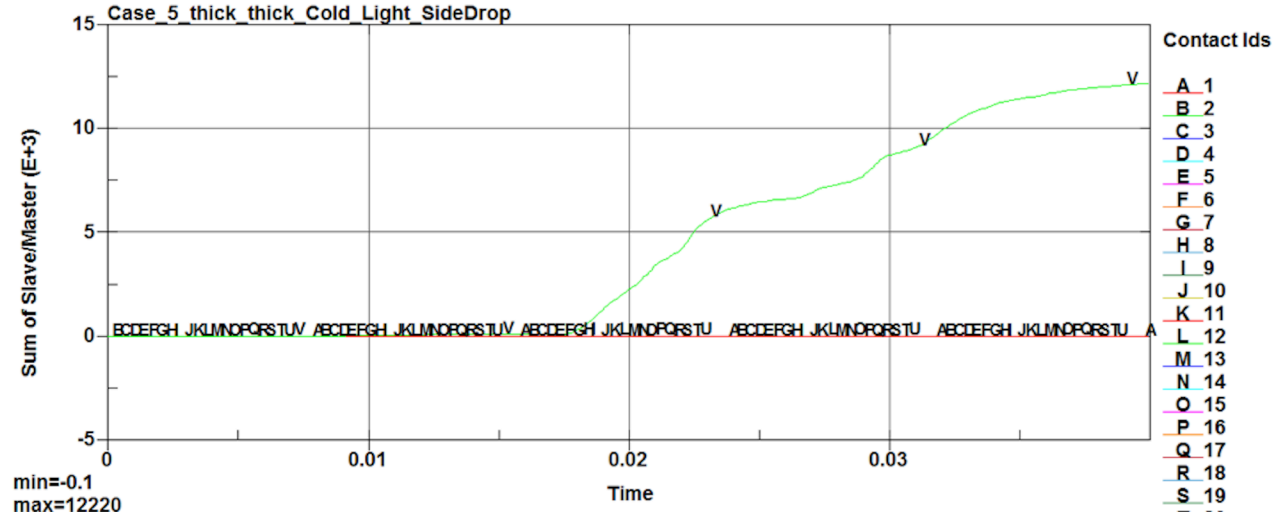

Note: time in Seconds

Figure 2.12.1.11-20. Case 5 Interface Sliding Energy Time History

2.12.1.11.6. Case 6 NCT Corner Drop with Thick Shell, Cold Condition and Light Payload

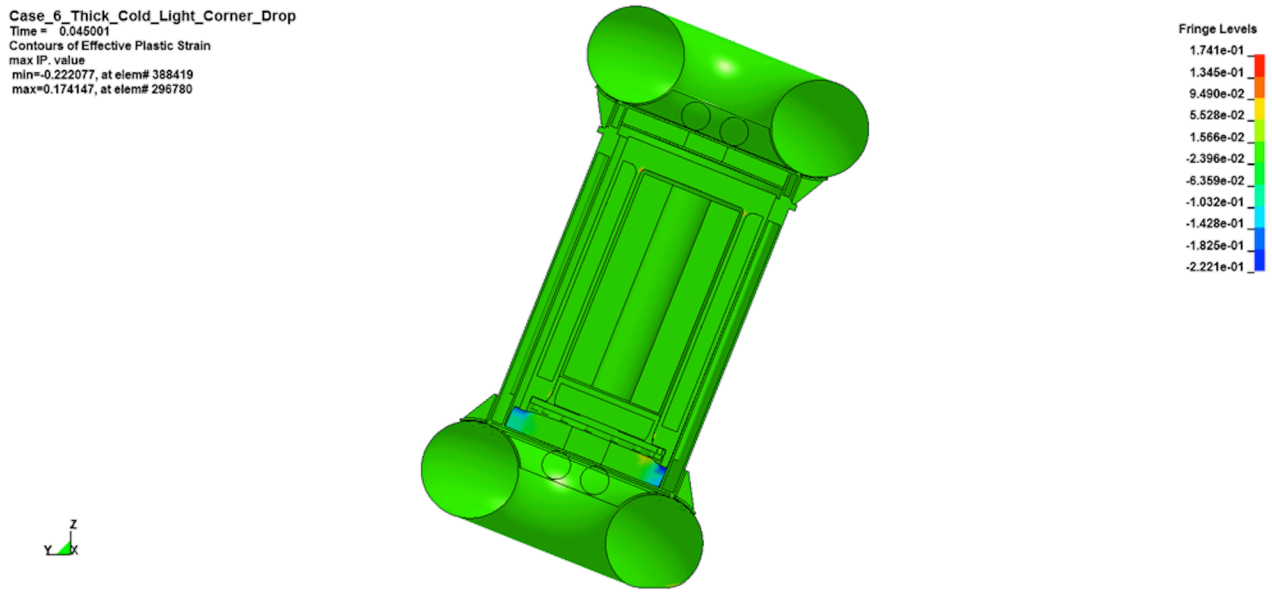

Figure 2.12.1.11-21. Case 6 Deformed Overpack Shape (Effective Plastic Strain)

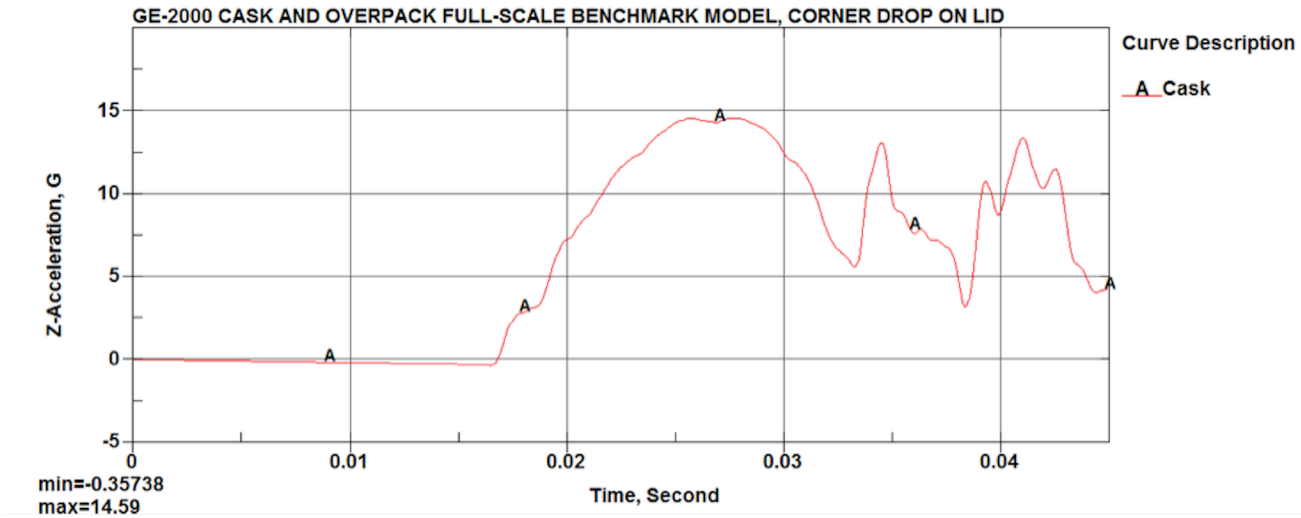

Figure 2.12.1.11-22. Case 6 Payload Acceleration Time History

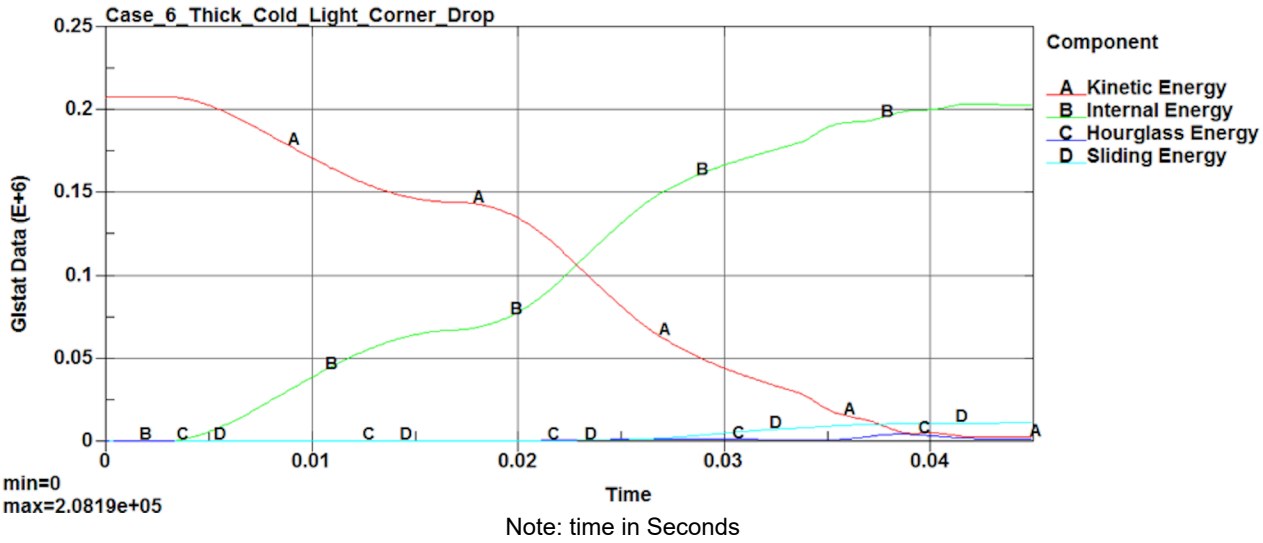

Note: time in Seconds

Figure 2.12.1.11-23. Case 6 Impact Energy Plot

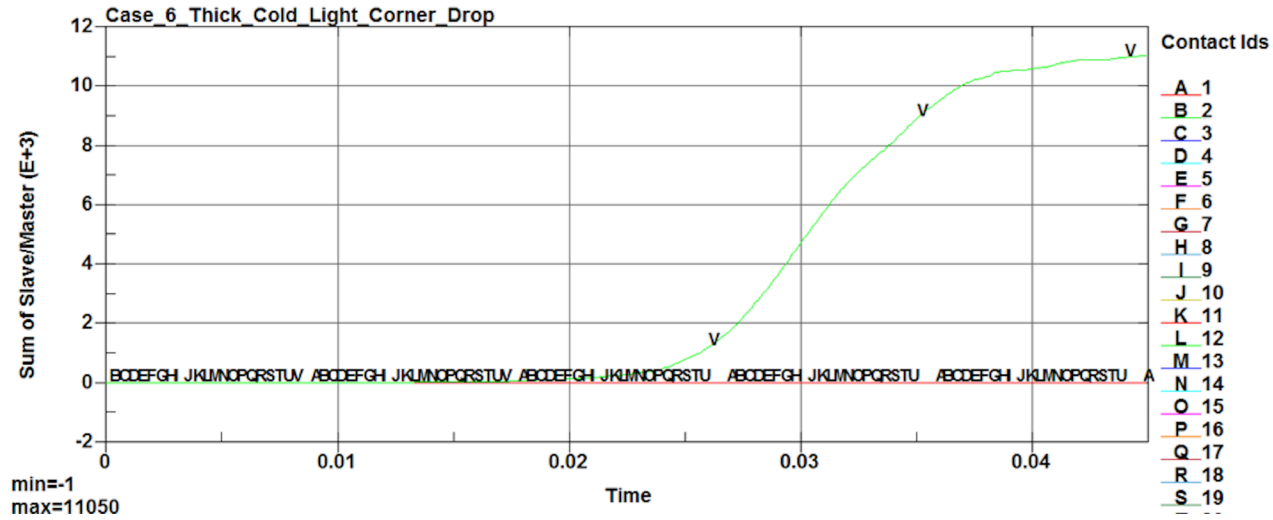

Note: time in Seconds

Figure 2.12.1.11-24. Case 6 Interface Sliding Energy Time History

2.12.1.11.7. Case 7 HAC End Drop with Thick Shell, Cold Condition and Light Payload

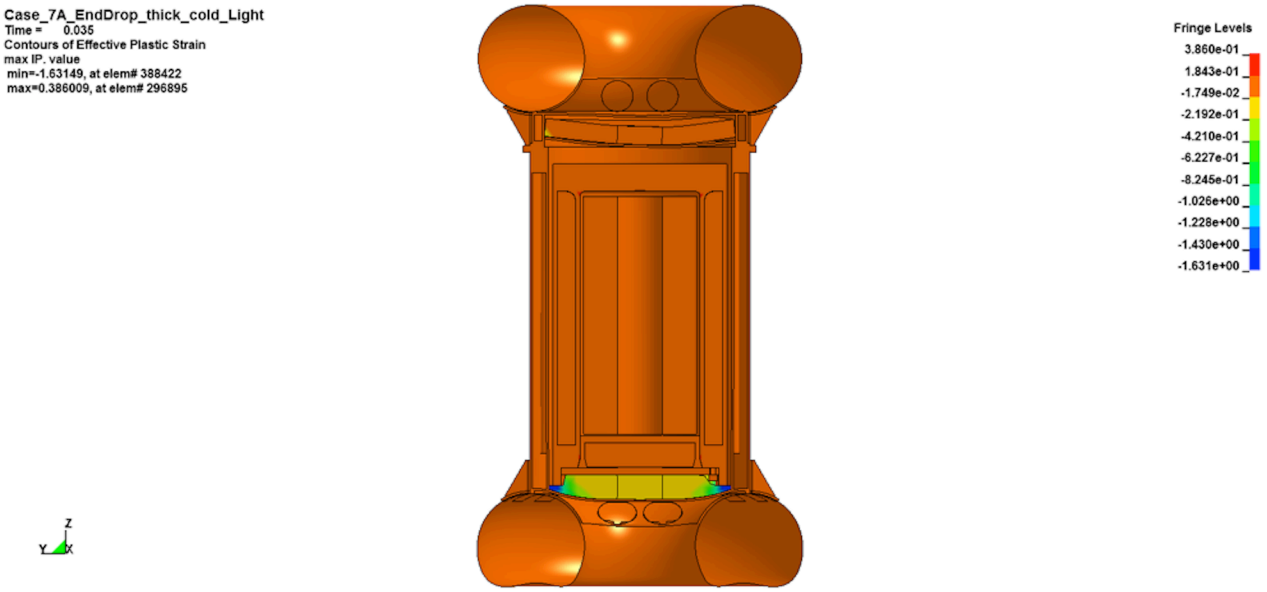

Figure 2.12.1.11-25. Case 7 Deformed Overpack Shape (Effective Plastic Strain)

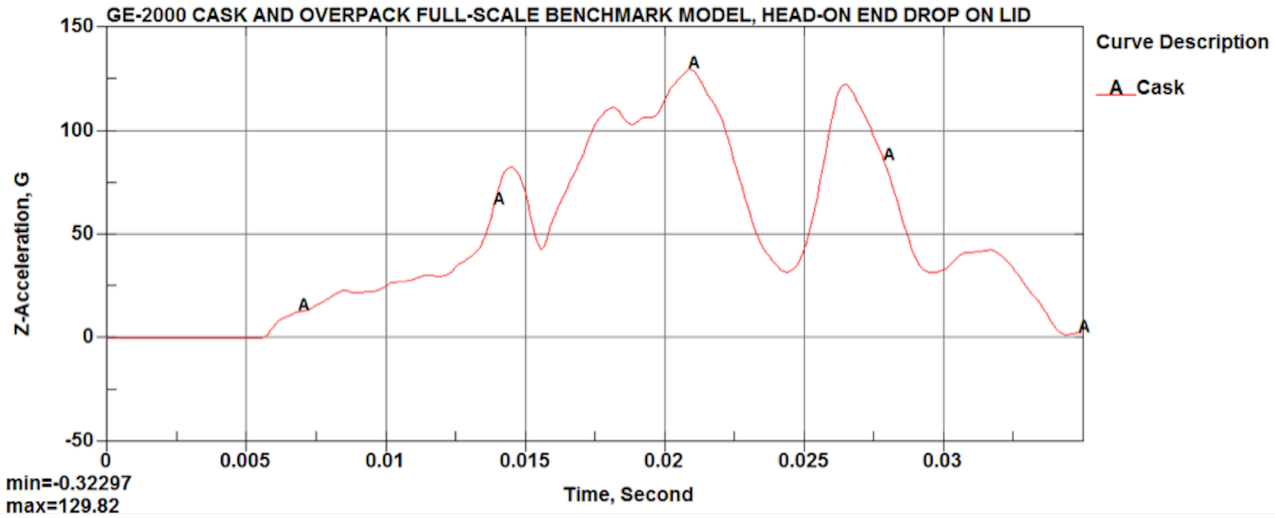

Figure 2.12.1.11-26. Case 7 Payload Acceleration Time History

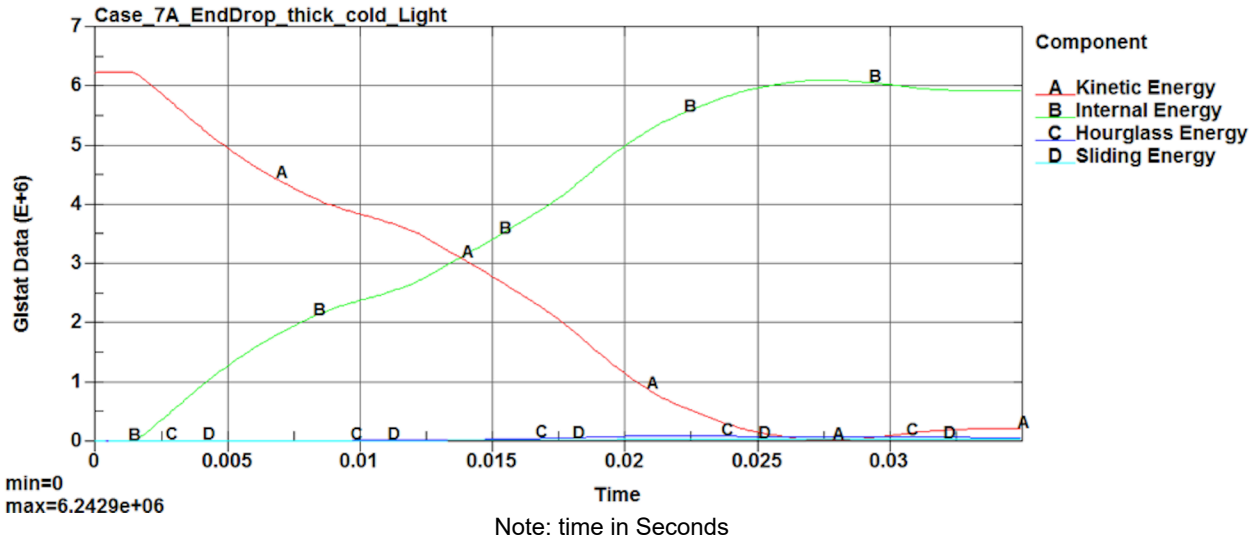

Note: time in Seconds

Figure 2.12.1.11-27. Case 7 Impact Energy Plot

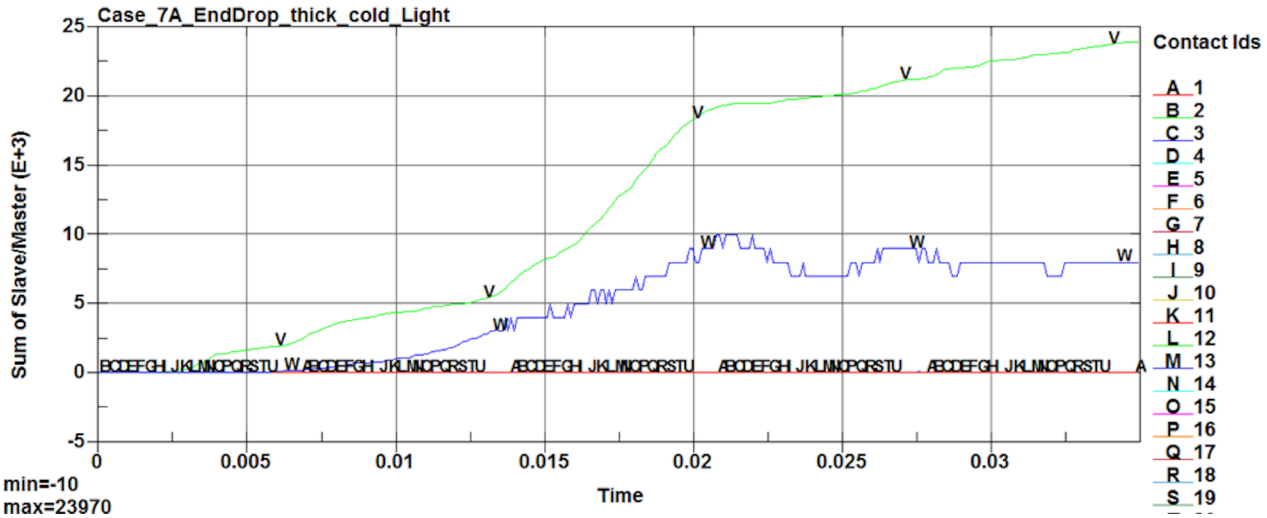

Note: time in Seconds

Figure 2.12.1.11-28. Case 7 Interface Sliding Energy Time History

2.12.1.11.8. Case 8 HAC End Drop with Thick Shell, Hot Condition and Heavy Payload

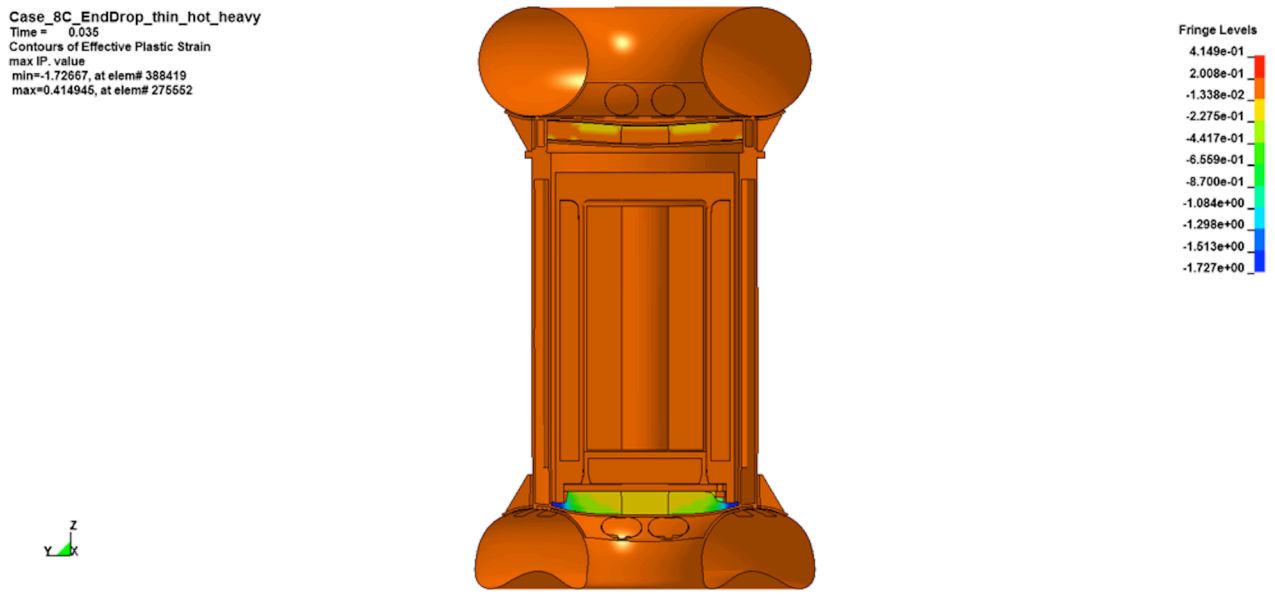

Figure 2.12.1.11-29. Case 8 Deformed Overpack Shape (Effective Plastic Strain)

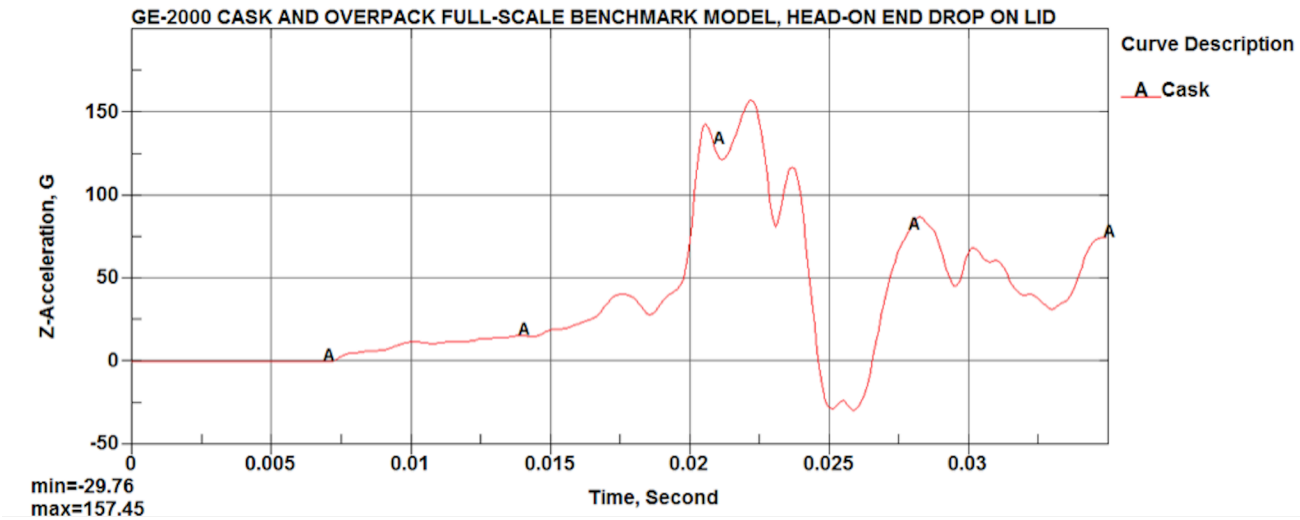

Figure 2.12.1.11-30. Case 8 Payload Acceleration Time History

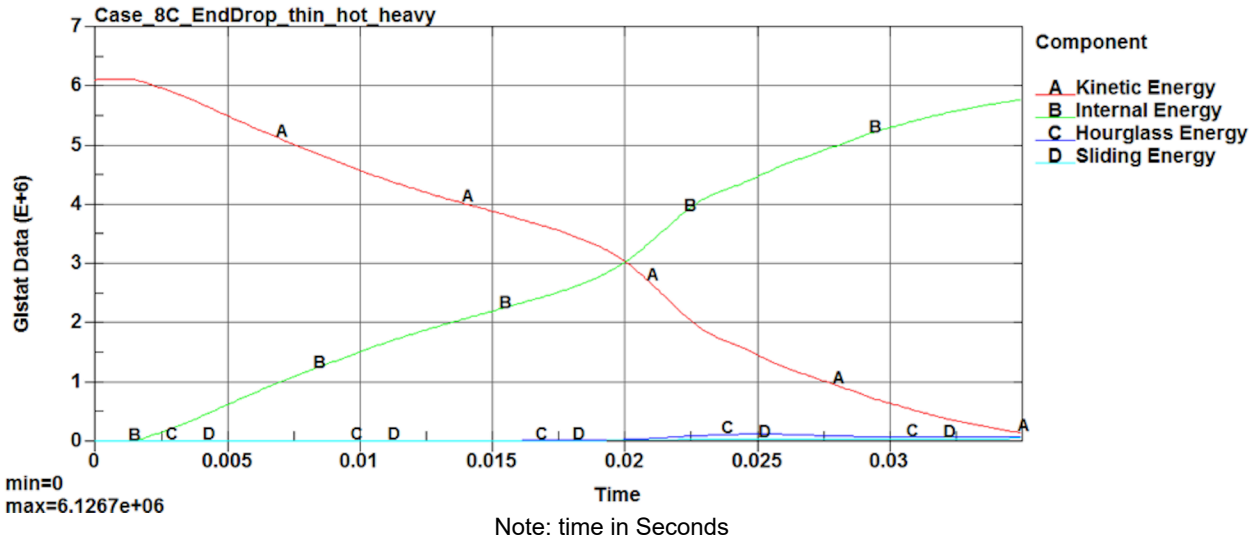

Note: time in Seconds

Figure 2.12.1.11-31. Case 8 Impact Energy Plot

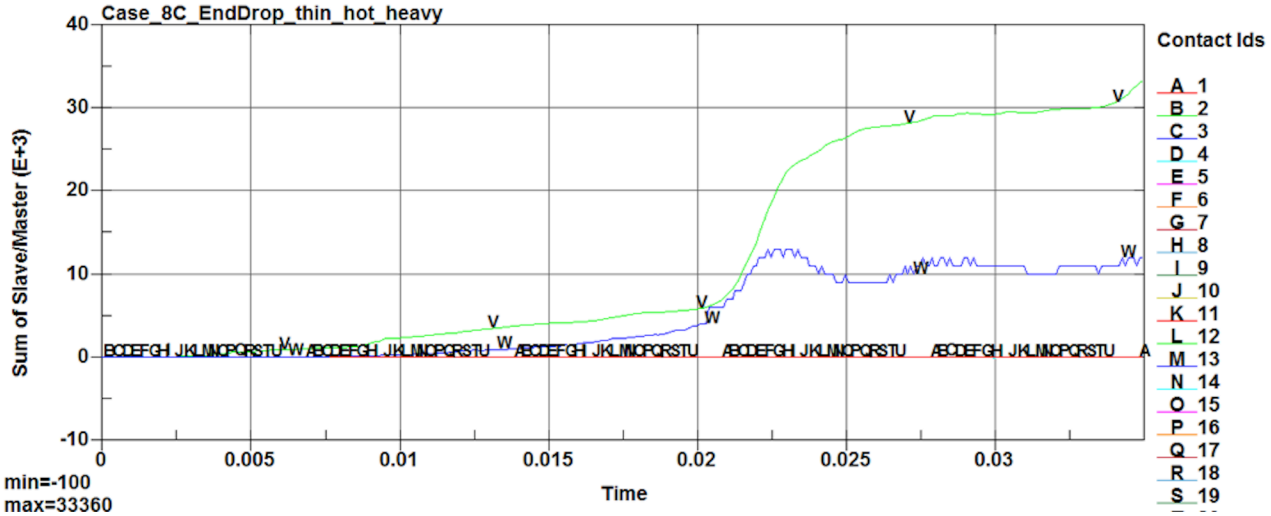

Note: time in Seconds

Figure 2.12.1.11-32. Case 8 Interface Sliding Energy Time History

2.12.1.11.9. Case 9 Side Drop with Thick Shell, Cold Condition and Light Payload

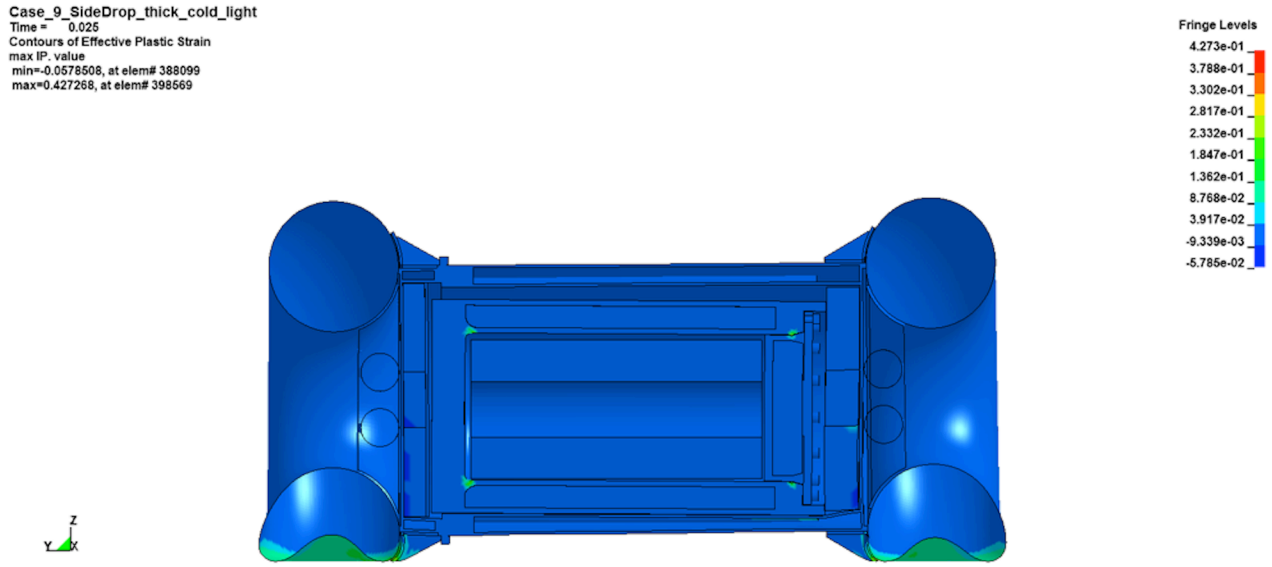

Figure 2.12.1.11-33. Case 9 Deformed Overpack Shape (Effective Plastic Strain)

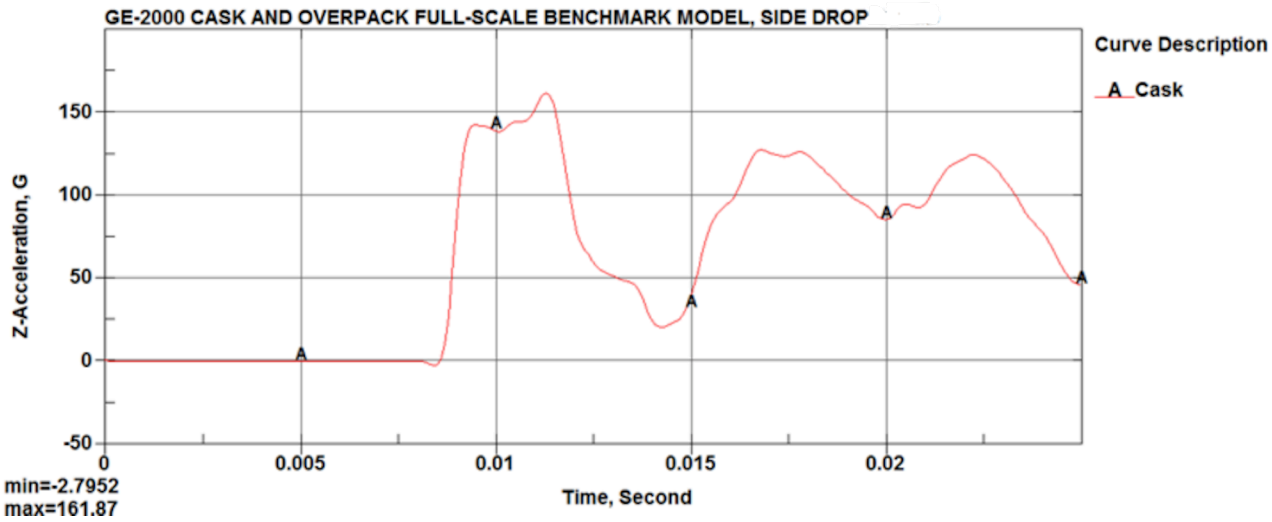

Figure 2.12.1.11-34. Case 9 Payload Acceleration Time History

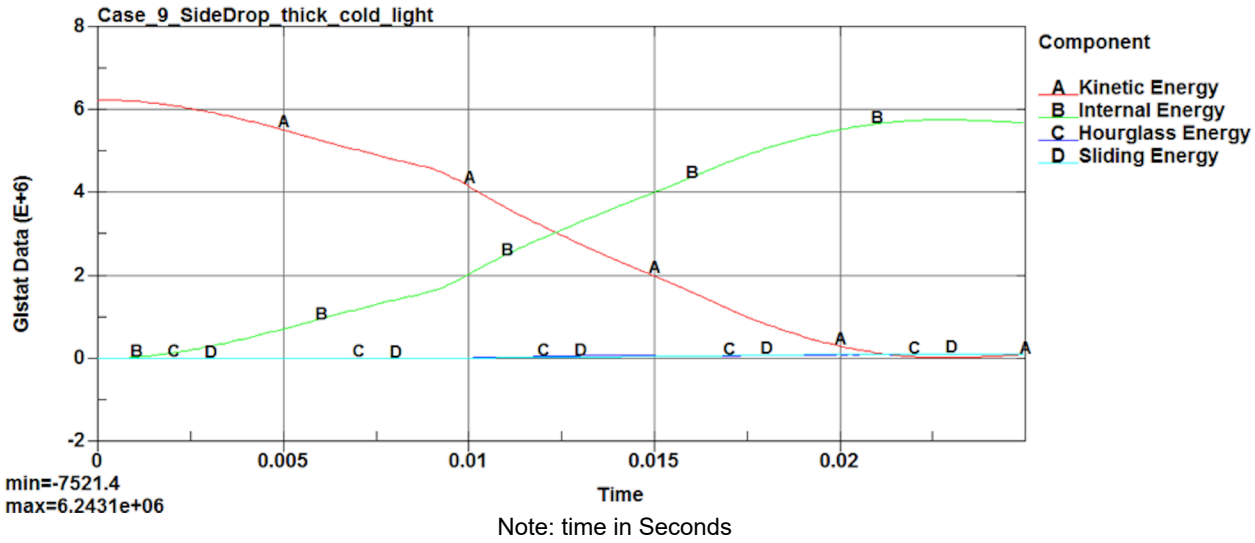

Note: time in Seconds

Figure 2.12.1.11-35. Case 9 Impact Energy Plot

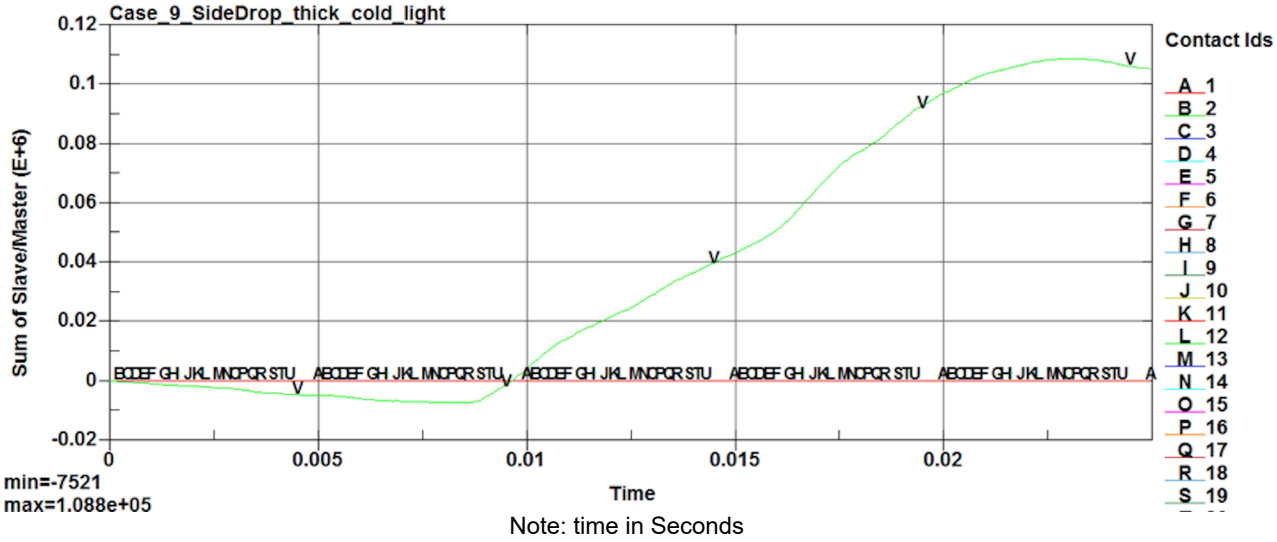

Note: time in Seconds

Figure 2.12.1.11-36. Case 9 Interface Sliding Energy Time History

2.12.1.11.10. Case 10 Side Drop with Thin Shell, Hot Condition and Heavy Payload

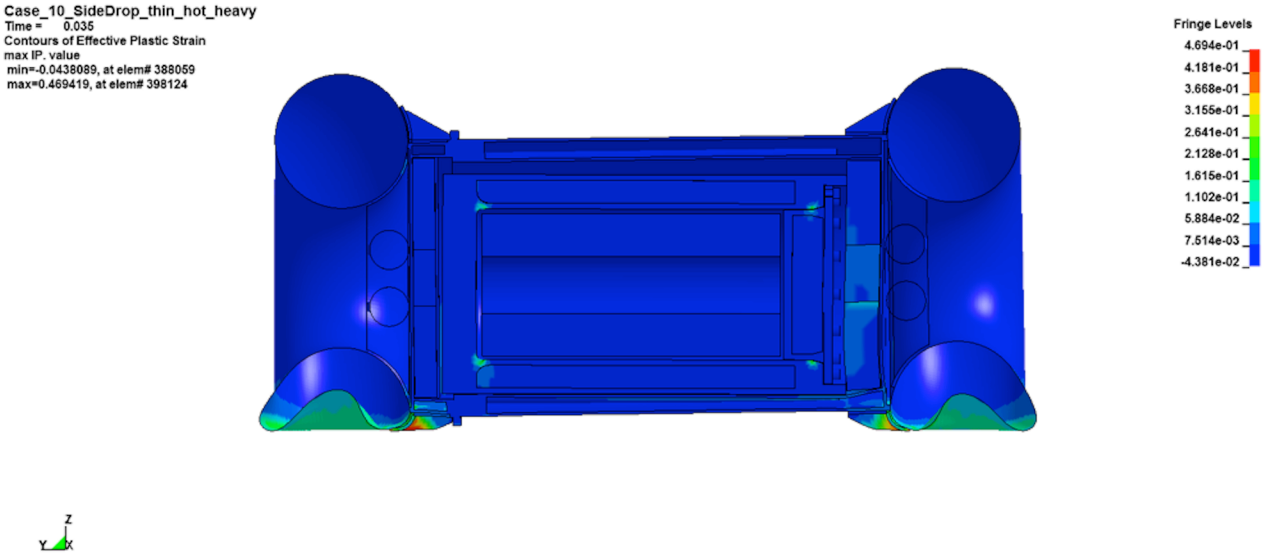

Figure 2.12.1.11-37. Case 10 Deformed Overpack Shape (Effective Plastic Strain)

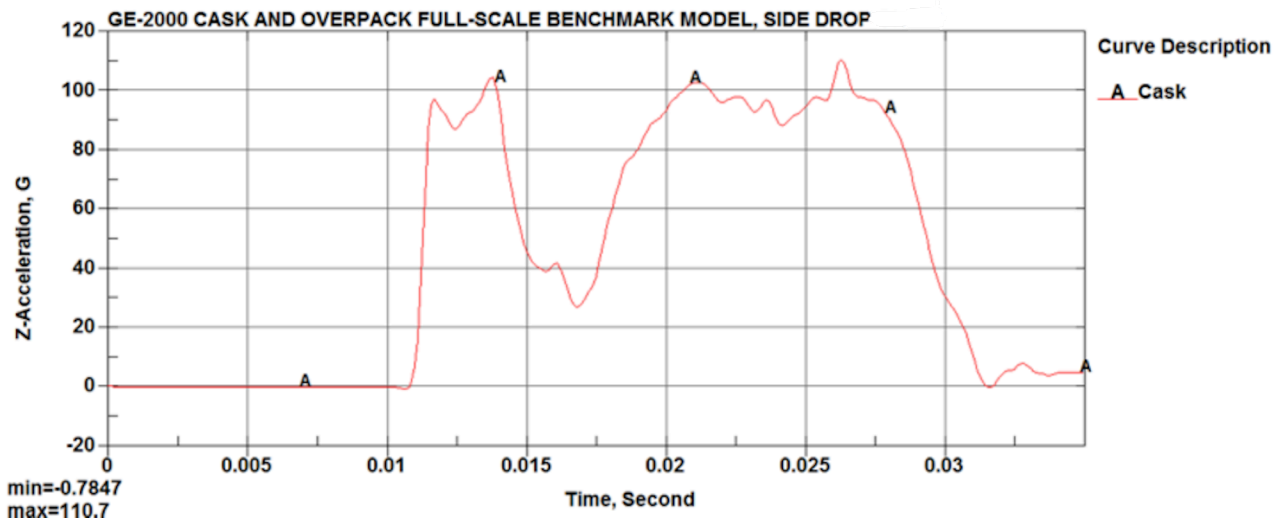

Figure 2.12.1.11-38. Case 10 Payload Acceleration Time History

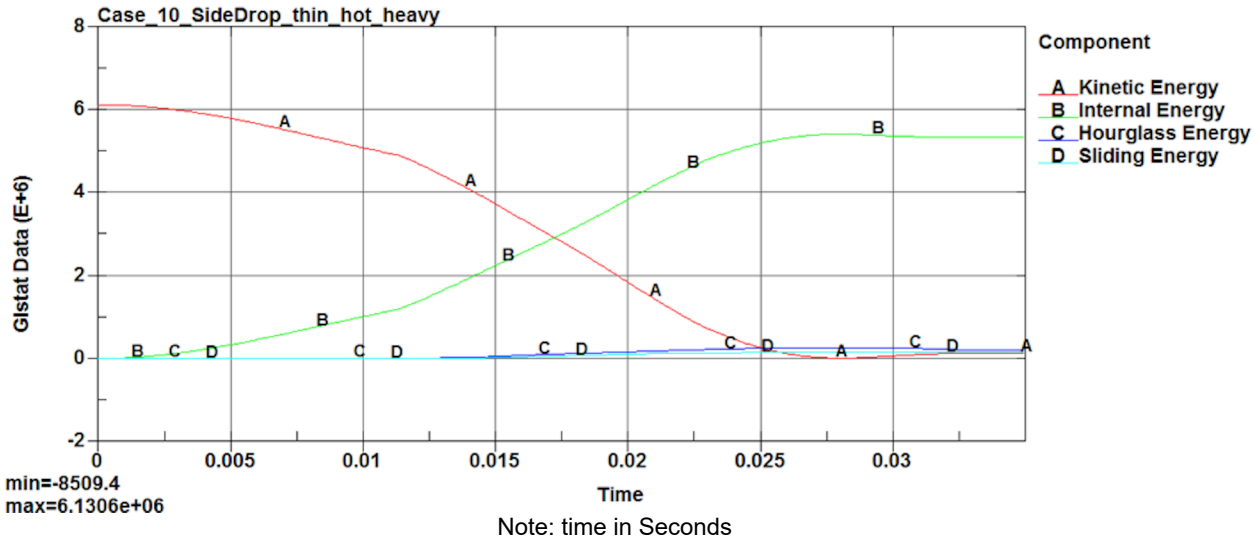

Note: time in Seconds

Figure 2.12.1.11-39. Case 10 Impact Energy Plot

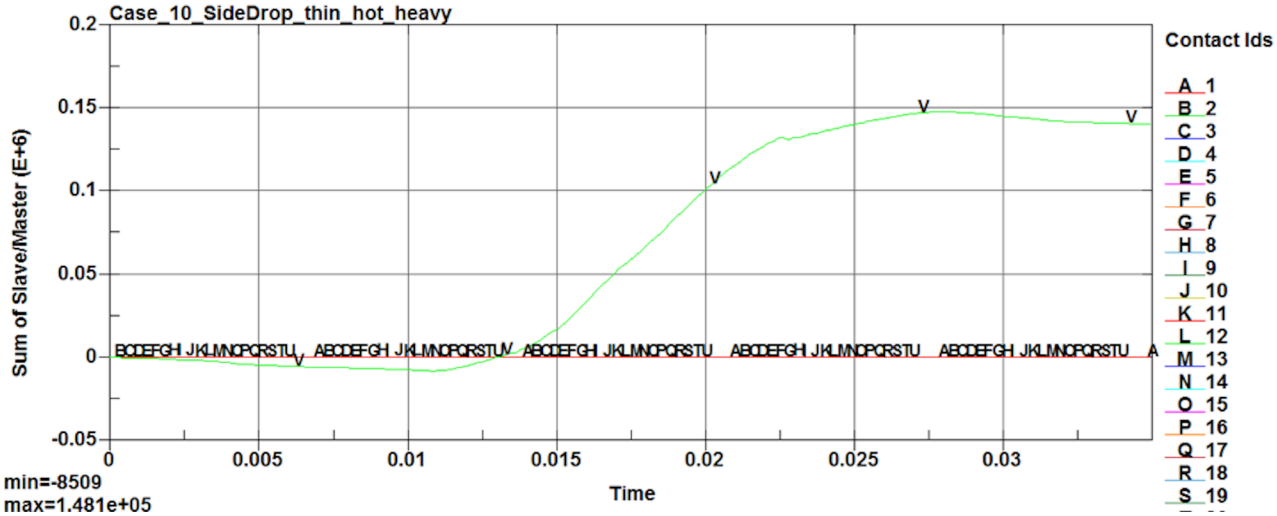

Note: time in Seconds

Figure 2.12.1.11-40. Case 10 Interface Sliding Energy Time History

2.12.1.11.11. Case 11 Corner Drop with Thick Shell, Cold Condition and Light Payload

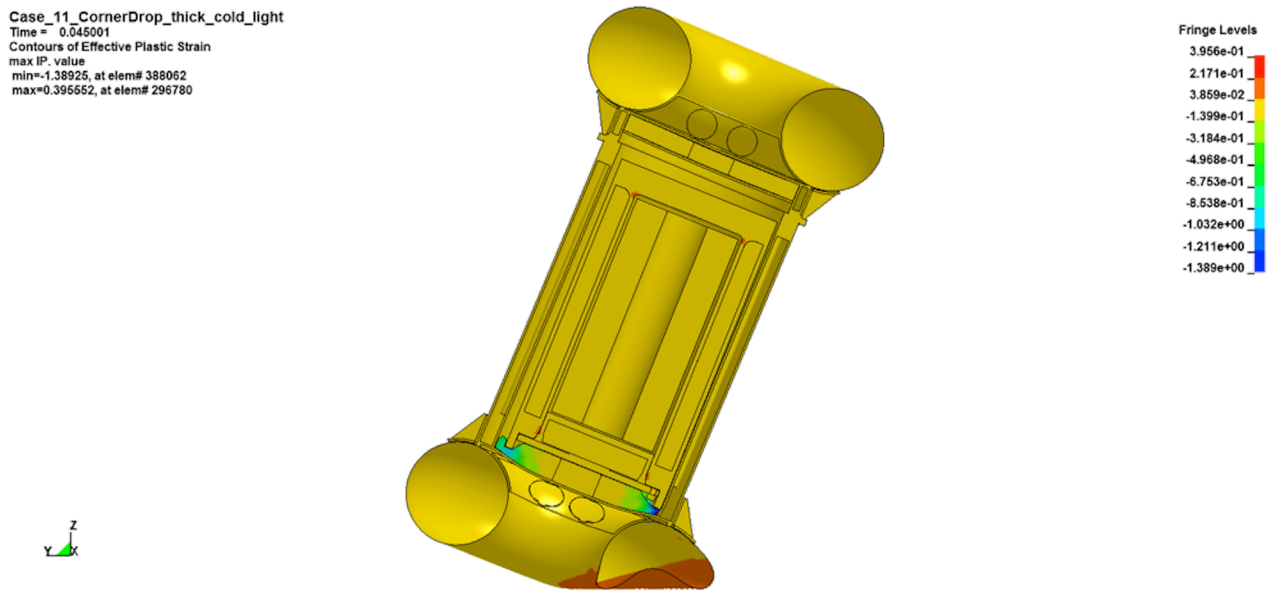

Figure 2.12.1.11-41. Case 11 Deformed Overpack Shape (Effective Plastic Strain)

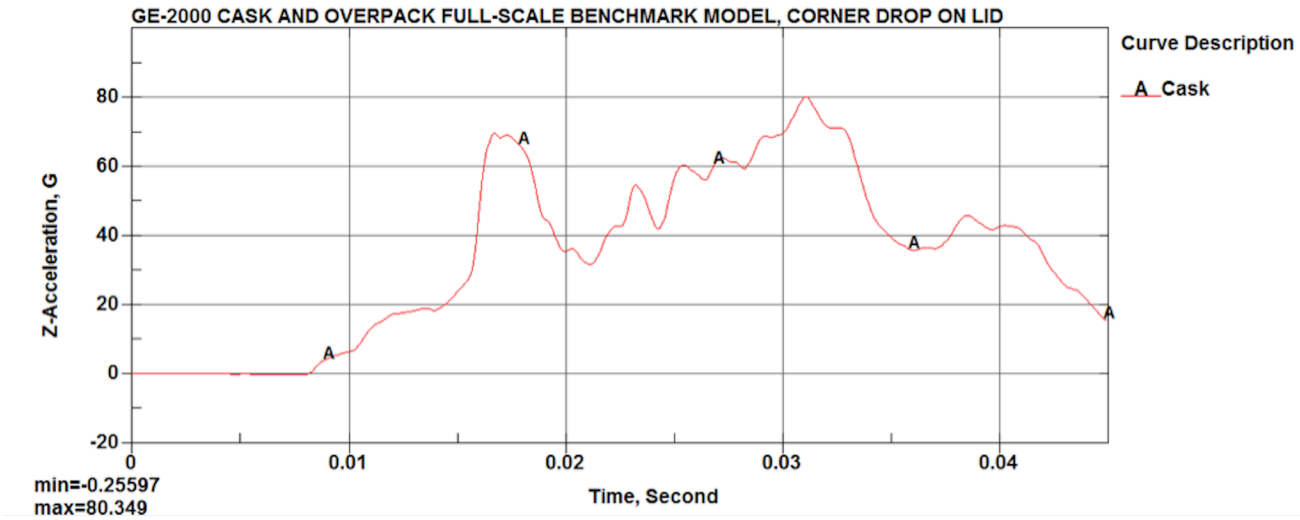

Figure 2.12.1.11-42. Case 11 Payload Acceleration Time History

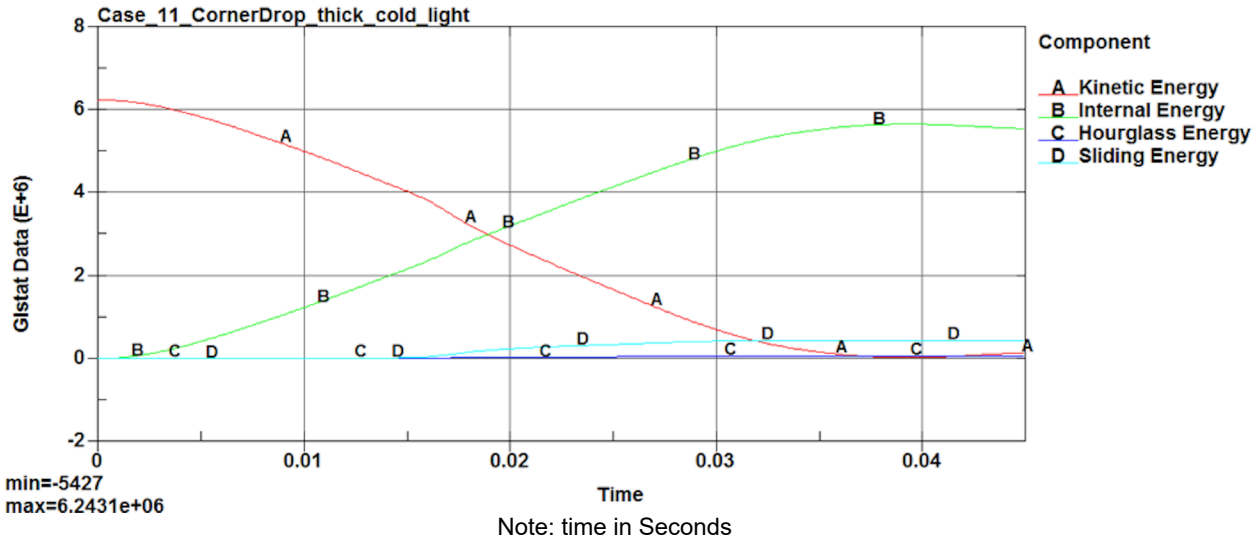

Note: time in Seconds

Figure 2.12.1.11-43. Case 11 Impact Energy Plot

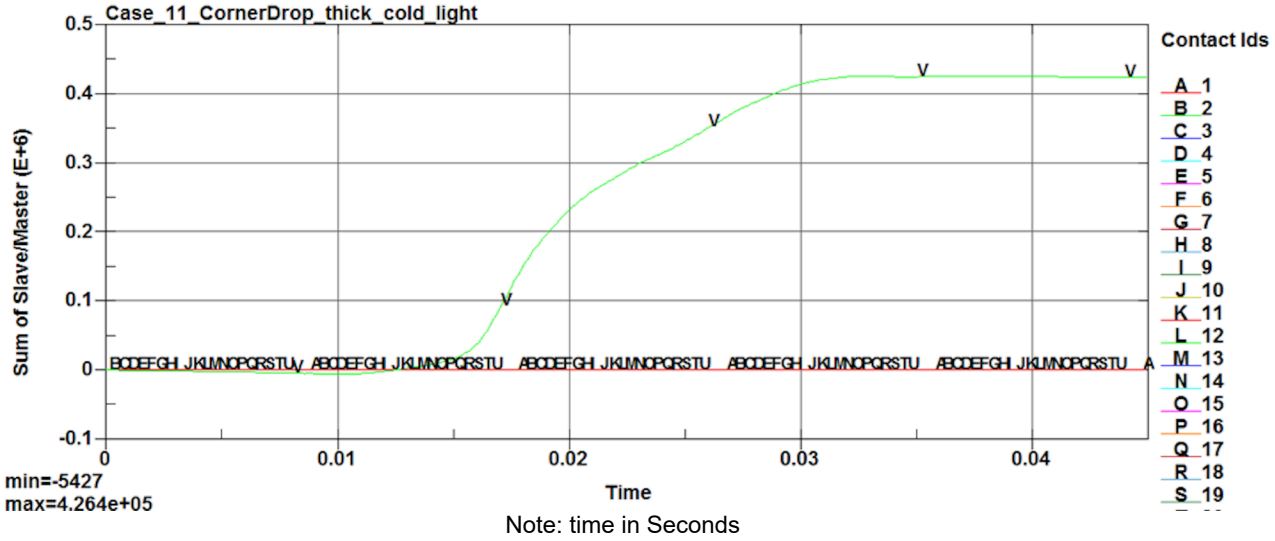

Note: time in Seconds

Figure 2.12.1.11-44. Case 11 Interface Sliding Energy Time History

2.12.1.11.12. Case 12 Corner Drop with Thin Shell, Hot Condition and Heavy Payload

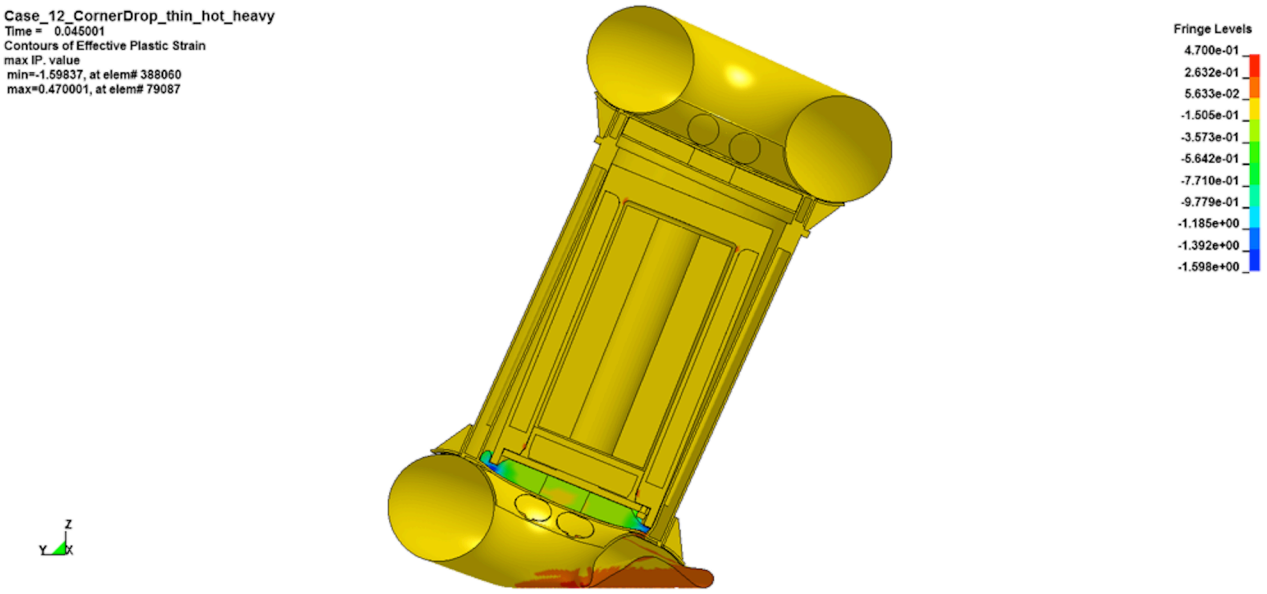

Figure 2.12.1.11-45. Case 12 Deformed Overpack Shape (Effective Plastic Strain)

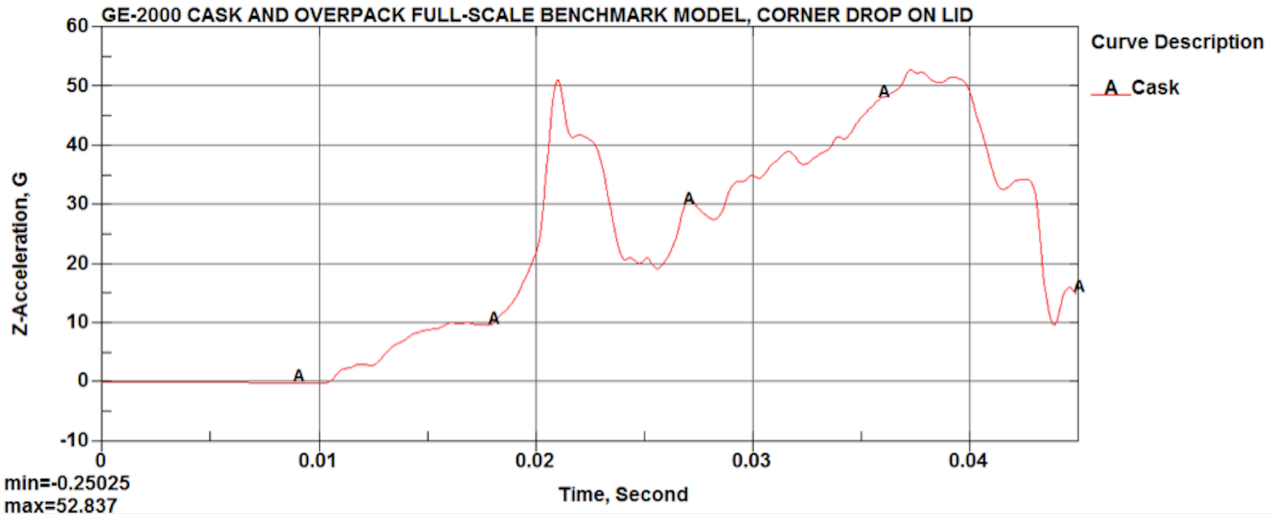

Note: time in Seconds

Figure 2.12.1.11-46. Case 12 Payload Acceleration Time History

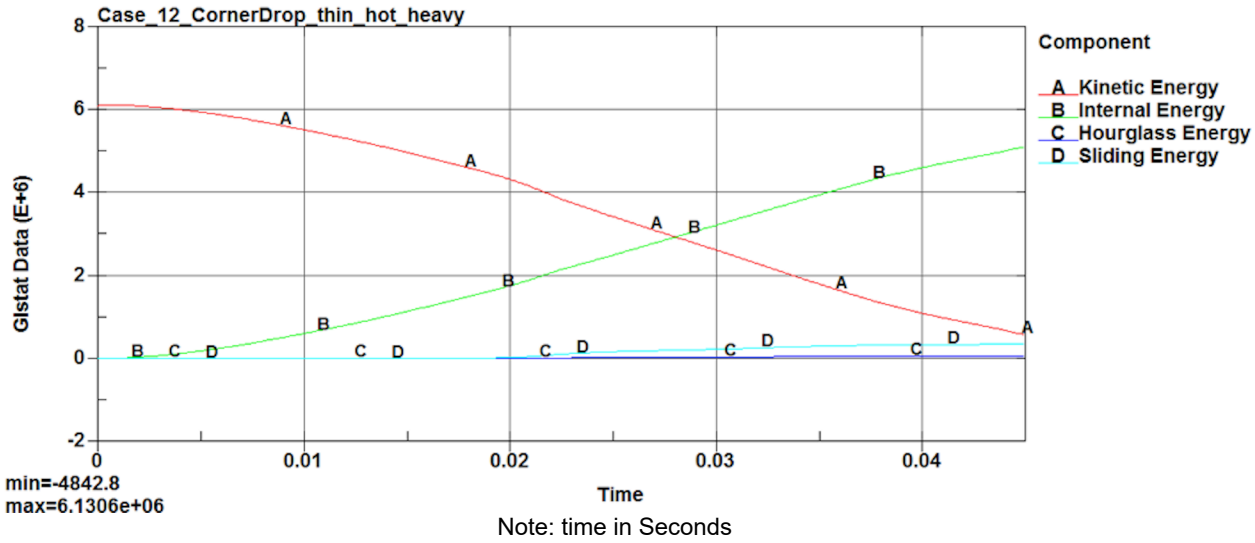

Figure 2.12.1.11-47. Case 12 Impact Energy Plot

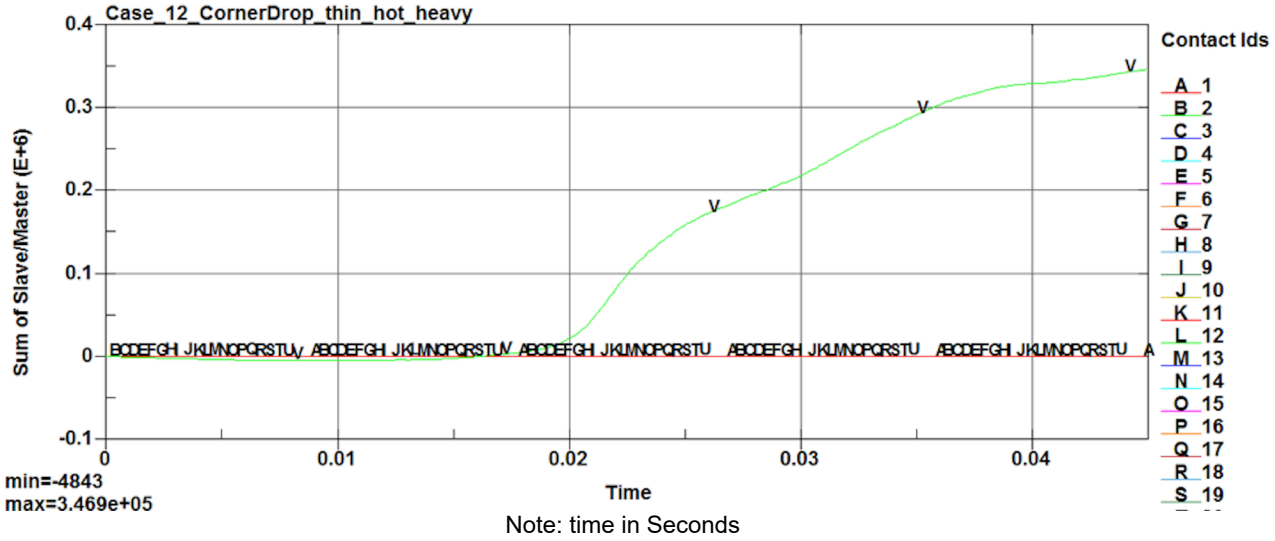

Figure 2.12.1.11-48. Case 12 Interface Sliding Energy Time History

2.12.1.11.13. Case 13 Slapdown Drop (5°), Thick Shell, Ambient Condition and Nominal Payload

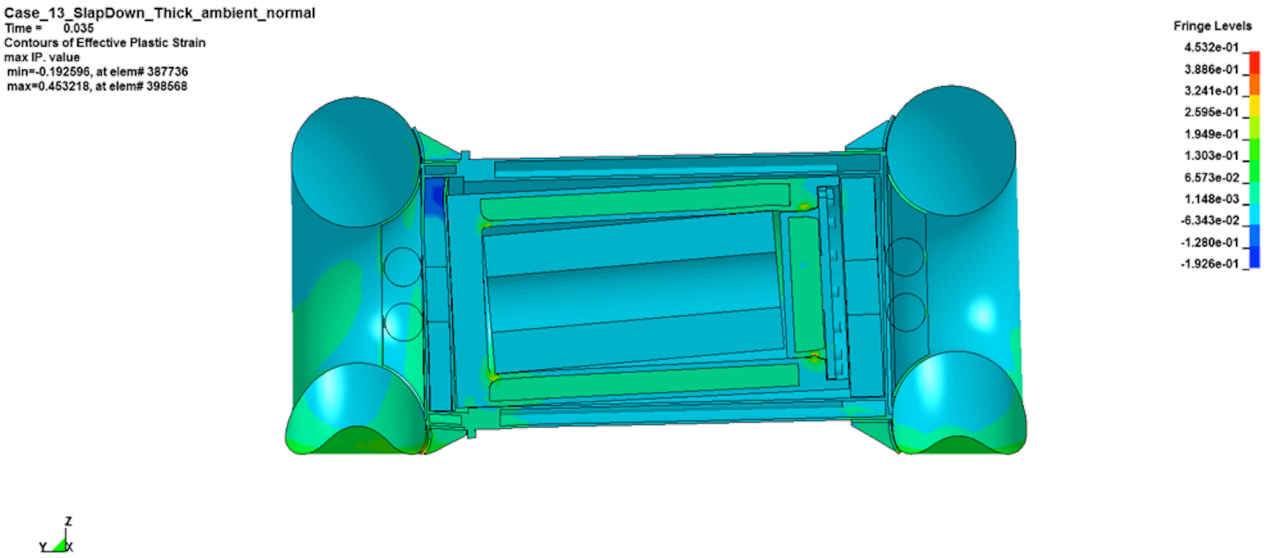

Figure 2.12.1.11-49. Case 13 Deformed Overpack Shape (Effective Plastic Strain)

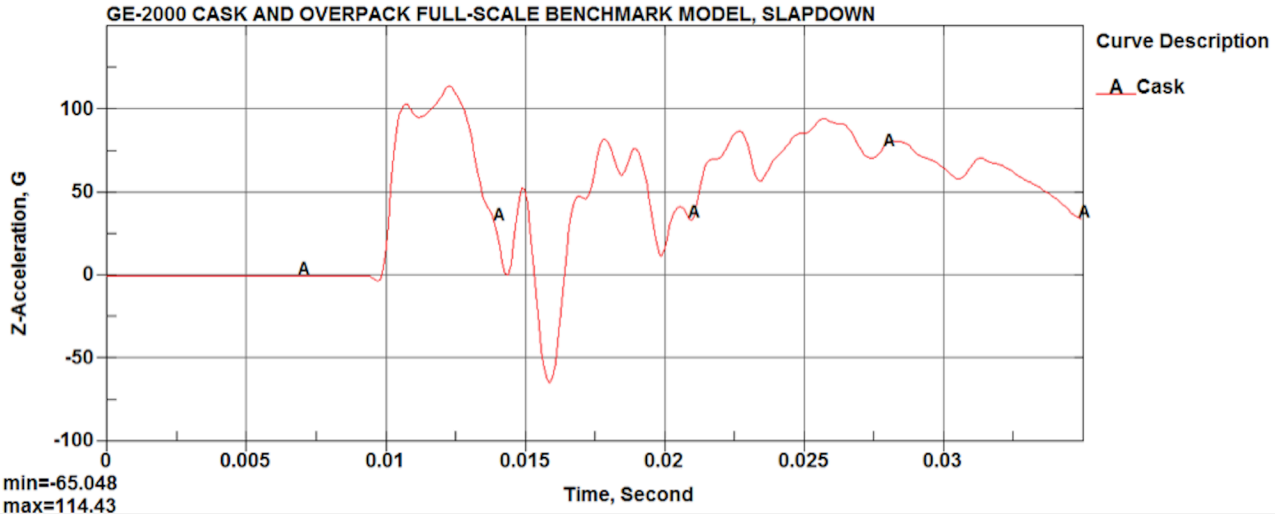

Note: time in Seconds

Figure 2.12.1.11-50. Case 13 Payload Acceleration Time History

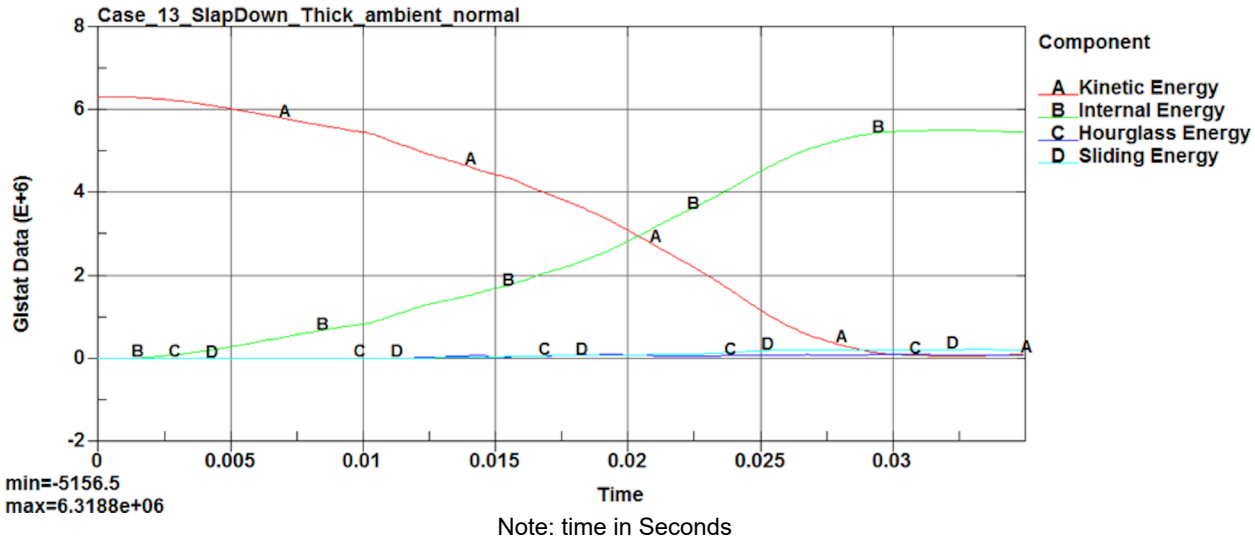

Figure 2.12.1.11-51. Case 13 Impact Energy Plot

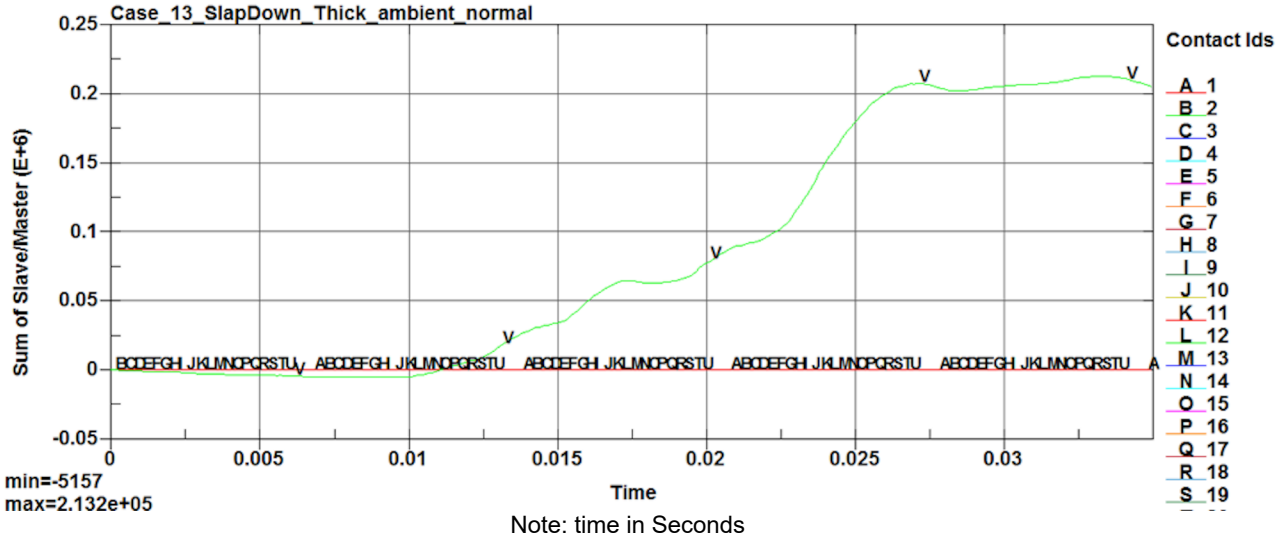

Figure 2.12.1.11-52. Case 13 Interface Sliding Energy Time History

2.12.1.11.14. Case 14 Slapdown Drop (10°), Thick Shell, Ambient Condition and Nominal Payload

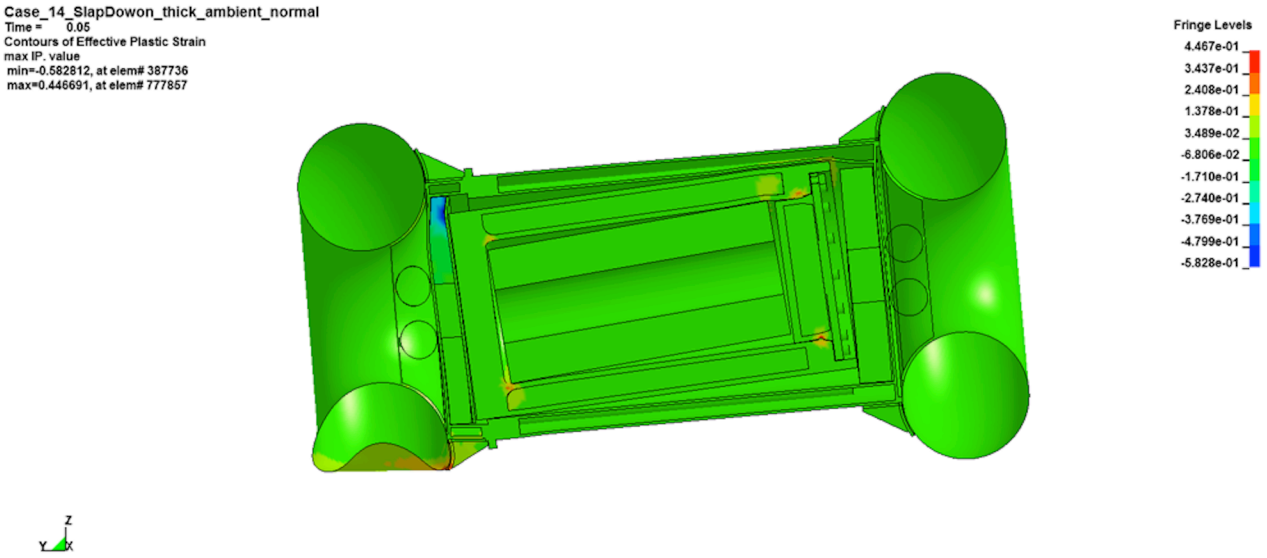

Figure 2.12.1.11-53. Case 14 Deformed Overpack Shape (Effective Plastic Strain)

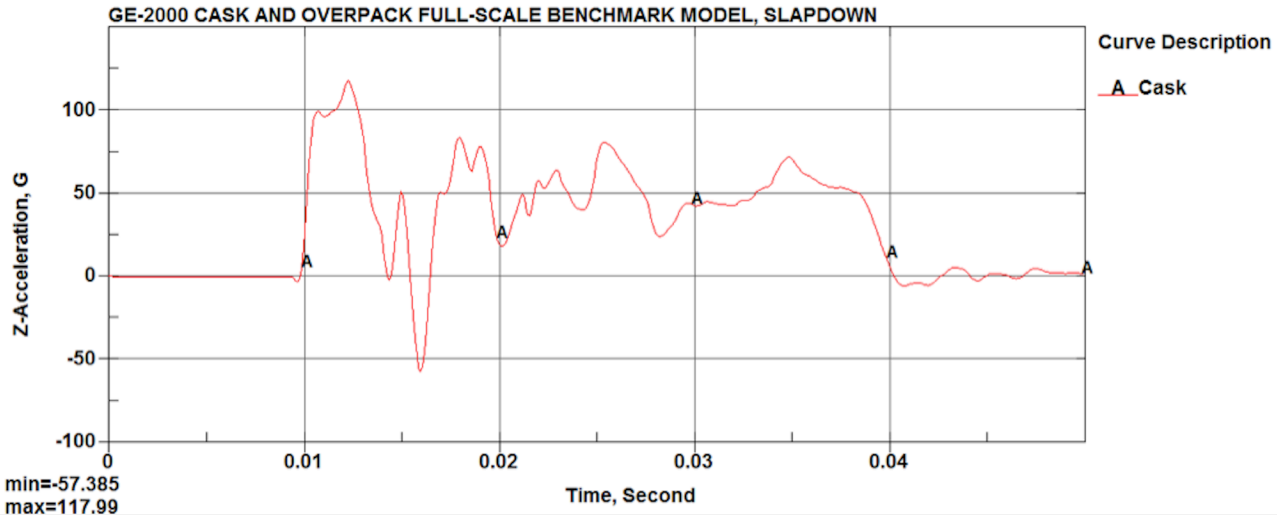

Figure 2.12.1.11-54. Case 14 Payload Acceleration Time History

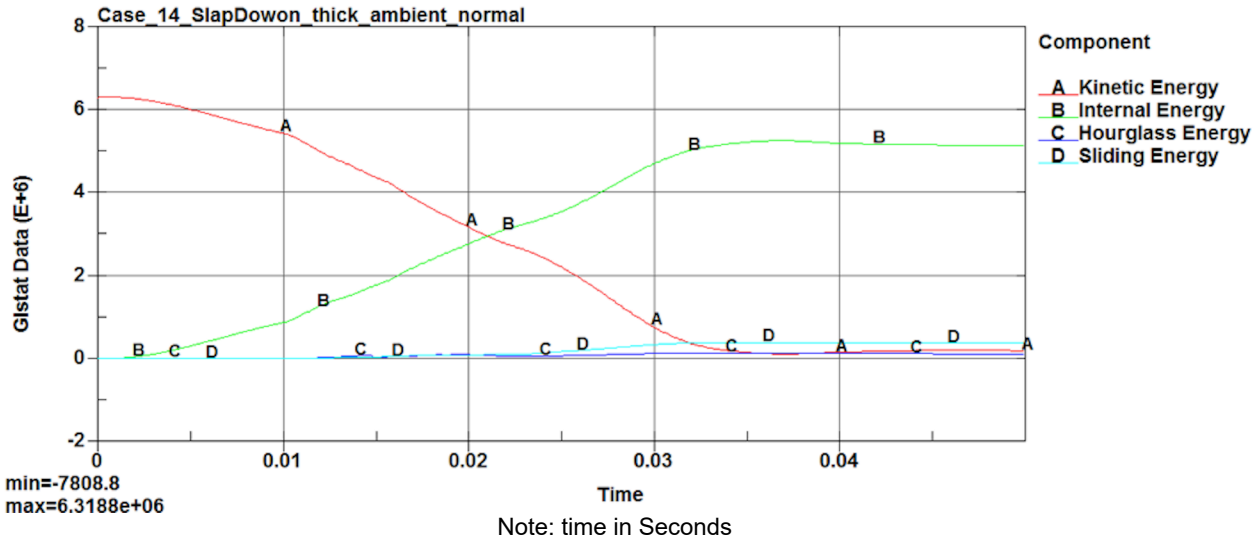

Note: time in Seconds

Figure 2.12.1.11-55. Case 14 Impact Energy Plot

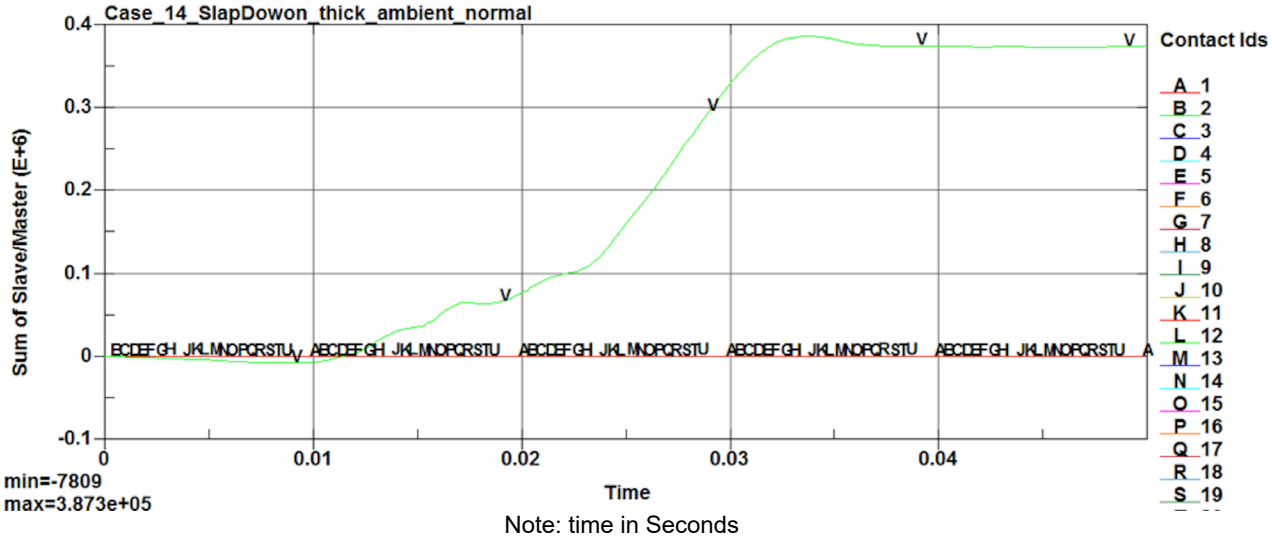

Note: time in Seconds

Figure 2.12.1.11-56. Case 14 Interface Sliding Energy Time History

2.12.1.11.15. Results for 30 ft Drop Followed and 40 in Pin Puncture Drop Sequence

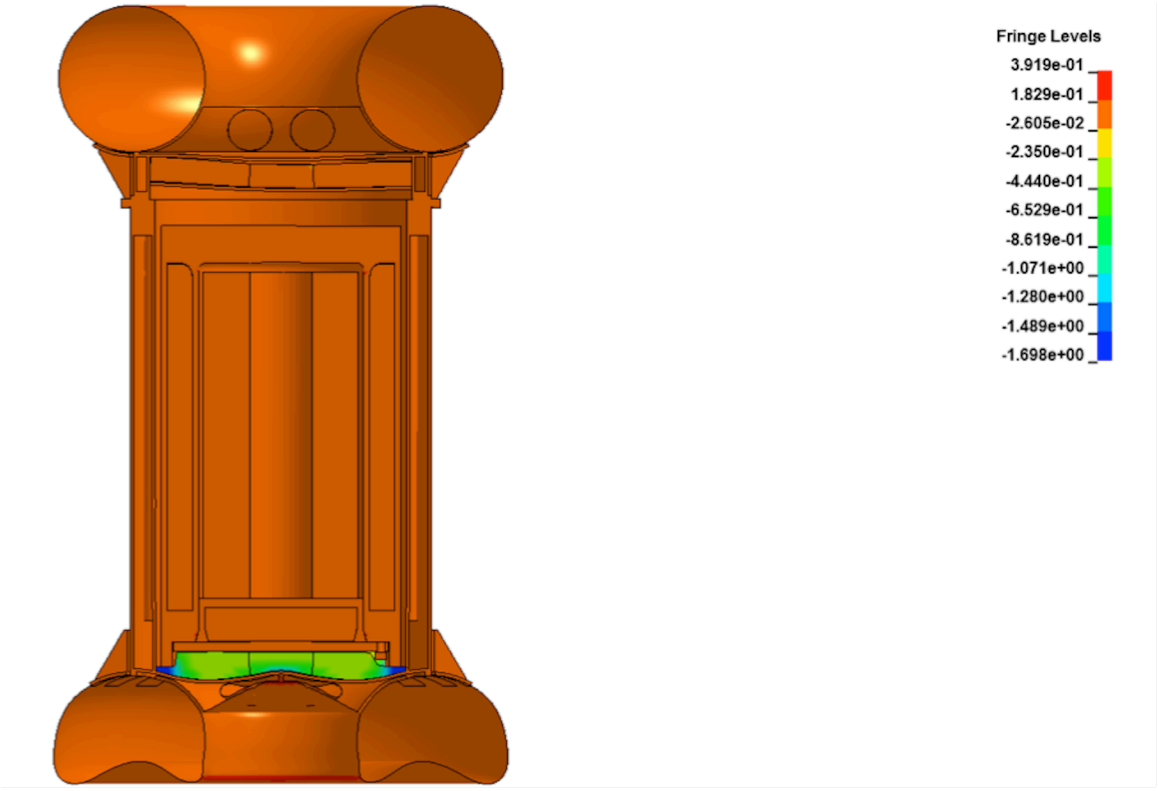

Figure 2.12.1.11-57. Strain Contour of Package after 30 ft End Drop and Pin Puncture Sequence

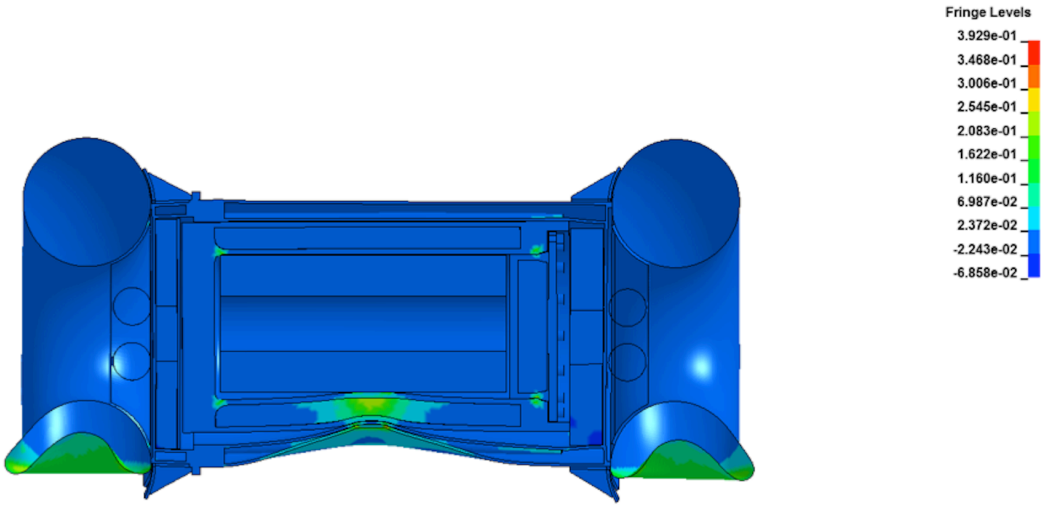

Figure 2.12.1.11-58. Strain Contour of Package after 30 ft Side Drop and Pin Puncture Sequence

2.12.1.12. Summary of Impact Analysis Results

Conservative impact analyses of the Model 2000 cask during the NCT and HAC impact events were performed to evaluate the performance of impact limiter design. This report summarizes the results of structural analyses of the Model 2000 Transport Package during NCT per 10 CFR 71.71 and HAC per 10 CFR 71.73. The summary of results for the bounding drop cases are presented in Table 2.12.1-1.

The worst-case HAC accelerations occur during the cold/thick/light side drop and the hot/thin/heavy bottom end drop. For the bottom end drop, the acceleration trend showed that the accelerations dropped until the honeycomb temperature was increased to 400°F and the honeycomb fully compresses. Because the average temperature of the honeycomb is less than 350°F, the honeycomb has sufficient capacity to protect the package during hot conditions.

The results of the evaluations presented in this section show that the Model 2000 overpack provides sufficient protection of the cask and contents.

2.12.1.12.1. Benchmark Tests

The peak accelerations of the benchmark analysis results from Drop Cases 1 through 3 are compared with the drop test results from Section 2.12.5 in Table 2.12.1-14.

Table 2.12.1-14. Comparison of Benchmark Simulations and Drop Tests Acceleration

Drop Case No.	Drop Configuration	LS-DYNA Analysis	Drop Test[1] Measurements	Notes
1	30-ft End Drop	130.0 g	408/4 = 102 g	Quarter-scale model
2	30-ft Side Drop	157.0 g	Not available	Instrument failure, No result
3	30-ft Corner Drop	70.9 g	156/4 = 39 g	Quarter-scale model

Note: 1. Section 2.12.5.

The comparison of ¼-scale drop test deformation results and the LS-DYNA benchmark simulation is provided in Table 2.12.1-15.

Table 2.12.1-15. Comparison of Benchmark Simulations and Drop Tests Deformations

Drop Case No.	Drop Configuration	LS-DYNA Analysis	Drop Test[1] Measurements
1	30-ft End Drop	3.5 in	2.255×4 = 9.0 in
2	30-ft Side Drop	9.4 in	3.18×4 = 12.7 in
3	30-ft Corner Drop	11.8 in	5.3×4 = 21.2 in

Note: 1. Section 2.12.5.

The comparison of measured accelerations and deformations with LS-DYNA analysis results for each drop orientation shows that the LS-DYNA model is stiffer, which results in higher accelerations.

2.12.1.12.2. Shallow Angle Drops—Slap Down

Two shallow angle drop simulations are also performed. The drop configurations include nominal payload at ambient temperature with thick toroidal shell thickness (t=0.76 inches) to compare with the side-drop test performed for the benchmarking test. The two shallow angles are 5° and 10° slapdown drops that are designated as Drop Cases 13 and 14. The results of shallow angle drops for the 0° (Drop Case 2, side drop), 5° (Drop Case 13) and 10° (Drop Case 14) conclude that the side drop (Drop Case 2) bounds the shallow angle cases with and acceleration of 157 g. Table 2.12.1-16 provides a summary of results for the shallow angle analyses.

Table 2.12.1-16. Comparison of Shallow Angle Drop Analyses

Drop Case No.	Shallow Angle Drop Angle	Peak Acceleration
2	0°	157.0 g
13	5°	115.0 g
14	10°	118.0 g

2.12.1.12.3. Pin Puncture

Besides the 30-foot drop configurations, two HAC drop configurations (side drop and end drop) are selected to perform the code-required pin puncture test, where the cask is dropped 30-feet and then followed by a drop height of 40 inches onto a rigid pin 6 inches in diameter. Evaluation of the pin puncture results shows that the maximum strain is limited to local area and will not result in the degradation of the containment boundary. As the figures show, the maximum strain is 39%. However, review of results show the maximum strain is limited to local deformation of the overpack. The maximum strain in the outer shell of the cask is 31% and limited to the puncture area. Therefore, no gross deformations of the cask are predicted. Additionally, results for the combined 30-foot impact and pin puncture are used as input for the HAC thermal evaluation.

2.12.1.12.4. Containment Integrity

Based on the analyses presented in the calculation, there are no gross structural deformations of the cask body or containment boundary. Therefore, the containment integrity of the cask is maintained.

2.12.2. Lead Slump Calculation

The following sections provide a detailed analysis for lead slump. Section 2.12.2.1 assesses the thermal expansion of the lead at the operating temperature of the lead shielding. Subsequently, in Sections 2.12.2.2 and 2.12.2.3, the shielding capability of the Model 2000 cask is evaluated for the potential of lead slump during a bottom end drop using classic methods to support the shielding analysis assumptions. Further, Sections 2.12.2.4 through 2.12.2.6 assess the thermal contraction of the lead and the lead deformation that results at the NCT extreme cold ambient temperature of -40°F (-40°C).

2.12.2.1. Thermal Expansion of Lead Shielding at Operating Temperature

It is possible that during fabrication an air gap will develop between the lead and the outer steel shell of the cask (Reference 2-24), which could potentially result in a lead slump condition, meanwhile noting that the lead is inspected during fabrication. However, during NCT the operating temperature of the lead is taken at 500°F (260°C) (see Section 3.3.1.1) to envelope all conditions. The change in the outer radius of the lead shield due to thermal expansion is calculated as follows:

$$r_{final} = r_0 (1 + \alpha\Delta T) = 18.40 \text{ in (467.4 mm)}$$

where

r_0 = 18.25 in
= Outside radius of lead shield
α = 1.90×10^{-5} in/in/°F
= Coefficient of thermal expansion at 500°F
ΔT = 500°F-70°F =430°F
= Temperature difference

NOTE: Coefficient of thermal expansion for lead extrapolated from data provided in Section 2.2.1.

For the outer steel shell the thermal expansion for the inside radius is:

$$r_{final} = r_i (1 + \alpha\Delta T) = 18.33 \text{ in (465.6 mm)}$$

where

r_i = 18.25 in
= Inside radius of steel shell
α = 9.70×10^{-6} in/in/°F
= Coefficient of thermal expansion at 500°F
ΔT = 500°F-70°F = 430°F
= Temperature difference

Comparing the final outside radius of the lead shield to the inner radius of the outer shell, the difference is -0.07000 inches (1.800 mm), which indicates that the lead expands more than the steel shell during NCT. Further, this demonstrates the temperature sensitivity of lead and steel at high temperatures. Relative expansion of the lead exceeds the expansion of the steel. Therefore, any existing gap that may have formed during fabrication will close, minimizing the potential for lead slump.

2.12.2.2. Compressive Stress in Lead Slump During Bottom End Drop

The previous section shows that the relative change in thermal expansion does not create a void. However, if the lead shield column did not bond to the mating steel shells during the fabrication process, compressive stress will develop in the column. The maximum stress occurs at the bottom of the column and progressively decreases as the elevation increases. The maximum compressive stress is

$$\sigma_{max} = \frac{P}{A} = 3{,}613.6 \text{ psi}$$

where

P	=	Total load
	=	$W \times G$ = 1.476×10^6 lb
	=	Weight of lead shield
W	=	$V \times \rho$ = 9370.2 lb
V	=	Volume of lead shield
	=	$A \times h$ = 22870.8 in³
A	=	Cross-sectional area of lead shield
	=	$\pi(r_o^2 - r_i^2)$ = 408.4 in²
r_o	=	Outside radius of lead shield
	=	18.25 in
r_i	=	Inside radius of lead shield
	=	14.25 in
h	=	Height of lead column
	=	56 in
ρ	=	Density of lead
	=	0.4097 lb/in³
G	=	End drop acceleration
	=	157.5 g

NOTE: Value for the height of the lead column is rounded up to the nearest integer for conservatism.

Table 2.12.2-1 shows the stresses varying along the length of the lead column. The yield strength at 500°F is 189 psi. However, lead is sensitive to the strain-rate effects of the material. During the end drop, the estimated strain-rate is 12 in/in/sec (see Section 2.12.1). The yield strength varies from 823 psi at 0.002 in/in to 6,279 psi at 0.30 in/in. Therefore, during the end drop if yielding of the lead occurs it is localized to a small region near the bottom of the column.

NOTE: Yield strength of lead shielding at 500°F is extrapolated from data provided in Section 2.2.1.

2.12.2.3. Elastic Deformation During Bottom Impact

The elastic deformation is calculated assuming the cask lead shield column is unsupported by the steel inner and outer shells during an end drop event. The response of the lead shield is determined by multiplying the shield weight by the HAC end drop acceleration of 1,57.5 g. Therefore, an estimate of lead slump during HAC free drop conditions is (Reference 2-19):

$$y_{max} = \frac{P}{k} = 0.075 \text{ in (1.91 mm)}$$

where

k = Effective stiffness of the lead shield
$= \frac{A \times G}{h} = 1.98 \times 10^7$ lb/in
G = Bulk modulus of lead
$= \frac{E}{3(1-2\nu)} = 2.72 \times 10^6$ psi
A = Cross-sectional area of lead shield
$= \pi(r_o^2 - r_i^2) =$ 408.4 in²
W = Weight of lead shield
= 9370.2 lb
P = Total load
$= W \times g = 1.476 \times 10^6$ lb
g = End drop acceleration
= 157.5 g
h = Height of lead column
= 56 in
E = 1.63×10^6psi
= Modulus of elasticity of lead at 500°F
ν = Poisson's ratio for lead
= 0.4

The calculation shows that this estimate of lead slump is small for an unsupported lead shield. With the lead fully supported by the inner and outer shells of the cask, the actual lead slump is even smaller.

Table 2.12.2-1. Compressive Stress in Lead Shield

Column Height from Bottom	Compressive Stress / G (psi)	Compressive Stress (psi)
55.0	0.4	64.5
50.0	2.5	387.2
45.0	4.5	709.8
40.0	6.6	1032.4
35.0	8.6	1355.1
30.0	10.7	1677.7
25.0	12.7	2000.4
20.0	14.7	2323.0

2.12.2.4. Axial Thermal Expansion at NCT Extreme Cold Ambient Temperature

A small gap occurs at the top of the lead column when the cask is exposed to the extreme cold temperature of -40°F (-40°C) per the NRC requirements of 10 CFR 71.71 (c)(2). This is due to changes at the molecular level that cause the materials to contract. This reduction in the height of the lead shield is represented by the following equation:

$$h_{lead} = h_{0\text{-}lead}\,(1 + \alpha_{lead}\,\Delta T) = 55.904 \text{ in (1420.0 mm)}$$

where

$h_{0\text{-}lead}$ = Initial lead shield height
= 56 in
α_{lead} = Lead coefficient of thermal expansion at -40°F
= $1.56E^{-05}$ in/in/°F
ΔT = Temperature difference
= -40°F – 70°F = -110°F

The same calculation can be made to determine the reduction in the height of the steel shells:

$$h_{steel} = h_{0\text{-}steel}\,(1 + \alpha_{steel}\,\Delta T) = 55.95 \text{ in (1421.1 mm)}$$

where

$h_{0\text{-}steel}$ = Initial steel shell height
= 56 in
α_{steel} = Steel coefficient of thermal expansion at -40°F
= $8.09E\text{-}0^{6}$ in/in/°F
ΔT = Temperature difference
= -40°F – 70°F = -110°F

2.12.2.5. Radial Thermal Expansion at NCT Extreme Cold Ambient Temperature

The radial gaps that occur during exposure to NCT extreme cold conditions can also be calculated in a similar manner by taking the initial radius prior to exposure and then adding the change in radius due to thermal expansion. The outside radius of the lead shield at -40°F is:

$$r_o = r_{0\text{-}outer}(1 + \alpha_{lead}\,\Delta T) = 18.22 \text{ in (462.8 mm)}$$

where

$r_{0\text{-}outer}$ = Initial outside radius of the lead shield
= 18.25 in (463.6 mm)

Accordingly, the inside radius of the lead shield at -40°F is:

$$r_i = r_{0\text{-}inner}(1 + \alpha_{lead}\,\Delta T) = 14.23 \text{ in (361.3 mm)}$$

where

$r_{0\text{-}inner}$ = Initial inside radius of the lead shield
= 14.25 in (362 mm)

Now the decrease in radius is evaluated for the steel shells starting with the inside radius of the outer steel shell at -40°F:

$$R_o = R_{0\text{-}outer}\,(1 + \alpha_{steel}\,\Delta T) = 18.23 \text{ in (463.1 mm)}$$

where

$R_{0\text{-outer}}$ = Initial inside radius of the outer steel shell
= 18.25 in (463.6 mm)

The decrease in the outside radius of the inner steel shell at -40°F is:

$$R_i = R_{0\text{-inner}}(1 + \alpha_{steel}\Delta T) = 14.24 \text{ in (361.6 mm)}$$

where

$R_{0\text{-inner}}$ = Initial outside radius of the inner steel shell
= 14.25 in (362 mm)

2.12.2.6. Lead Slump Due to Impact After NCT Extreme Cold Ambient Temperature

A small gap occurs during extreme cold exposure due to the contraction of components in relation to each other as determined by the calculations in the previous section. In order to determine the magnitude of lead slump, the reduced height of the lead column based on the net gap is calculated and then the difference between the reduced height of the lead column and the height of the annular region is taken. The volume of the lead column at the extreme cold conditions (-40°F) is:

$$V_{f\text{-lead}} = A_{f\text{-lead}} \times h_{lead}$$
$$= (407.011 \text{ in}^2 \times 55.904 \text{ in}) = 22{,}753.59 \text{ in}^3 \text{ (3.73E+08 mm}^3\text{)}$$

where

$$A_{f\text{-lead}} = \pi(r_o^2 - r_i^2)$$
$$= \pi[(18.22 \text{ in})^2 - (14.23 \text{ in})^2] = 407.011 \text{ in}^2 \text{ (262,587.22 mm}^2\text{)}$$

The cross-sectional area of the annulus between the outer and inner steel shells at -40°F is:

$$A_{annulus} = \pi(R_o^2 - R_i^2)$$
$$= \pi[(18.23 \text{ in})^2 - (14.24)^2] = 407.68 \text{ in}^2 \text{ (263,018.83 mm}^2\text{)}$$

The reduced height of the lead column when taking into account impact after contraction of components is:

$$h_{final} = \frac{V_f}{A_{annulus}}$$

$$= \frac{22{,}753.59\ in^3}{407.68\ in^2} = 55.81 \text{ in (1417.57 mm)}$$

Taking the difference between the reduced height of the lead shielding and the height of the annular region, the lead deformation due to impact after NCT extreme cold (-40°F) is:

$$h_{slump} = h_{steel} - h_{final}$$
$$= 55.95 \text{ in} - 55.81 \text{ in} = 0.14 \text{ in (3.56 mm)}$$

2.12.3. Lifting and Tie-Down Analysis

2.12.3.1. Model 2000 Transport Package Lifting Analysis

The purpose and scope of this analysis is to demonstrate the structural integrity of the lifting ears and lid-lifting lug on the Series 2000 shielded shipping casks.

There are two types of ear designs employed during the handling of the Model 2000 cask, standard and auxiliary (see Figure 2.12.3-1). The ear design identified as standard is used for crane and fork truck lifting, and only one pair is required for these operations. The auxiliary ear is used in crane lifting only, and two pairs or four ears are required. The user may combine the different types of ears as follows:

1. 2 Standard/2 Auxiliary
2. 4 Auxiliary
3. 2 Standard

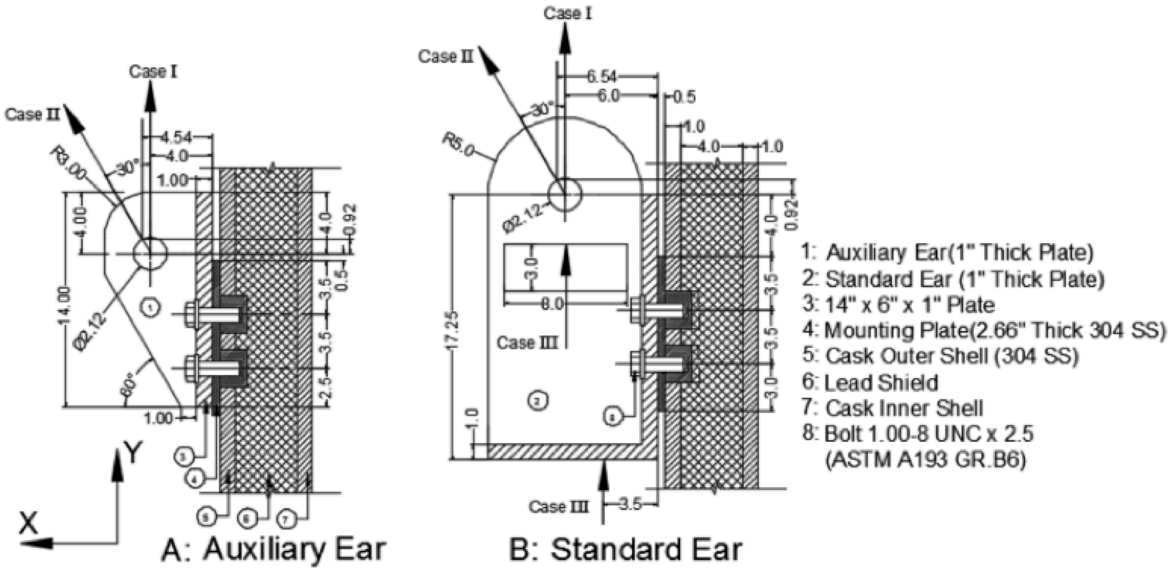

Figure 2.12.3-1. Structural Locations for Ear Analysis

Both ear designs (Auxiliary and Standard) are attached to the cask outer shell by means of four ASTM A193-B6 1-8 UNC-2-1/2 attaching bolts; only two bolts are shown. Also on this figure, the line of action of the different lifting forces is drawn. The different lifting forces are: Case I, straight up by crane; Case II, angular lift 30° from vertical, also by crane; and Case III, fork truck lift at two different points on the standard ear only. This analysis mainly considers Case II and I. The loading conditions are the following:

- The design rated load, W, shall be 23,630 pounds. This includes the dead weight of the cask (1 body, lid, 2 standard ears, and 2 auxiliary ears) and the cask payload including the liner.
- The two pairs of auxiliary ears (Auxiliary) are to support 3W such that the lifting cable does not make an angle of more than +30° measured from the vertical.

- The pair of standard ears (Standard) is to support 3W.
- These ears are removed from the cask during transport and are shipped separately.

Material properties are based upon 250°F for the outer cask. The 249°F temperature is the maximum temperature under normal conditions for the cask outer surface. Both types of ears, standard and auxiliary, and the cask outer shell are ASTM A240, Type 304 stainless steel. The attaching bolt material is ASTM A193-B6.

The standard ear individual load is obtained by dividing the weight of the cask and content (23,630 lbs.) by 2 (only two standard ears are used), and multiplying the resulting value by 3. The auxiliary ear load is obtained in a similar manner with the weight divided by 4 instead of 2 because 4 ears are used when this design is employed. Case III represents the fork truck loading condition on the standard ear, and it has a magnitude equal to that of Case I for the standard ear. Case III loading is not shown in Figure 2.12.3-2.

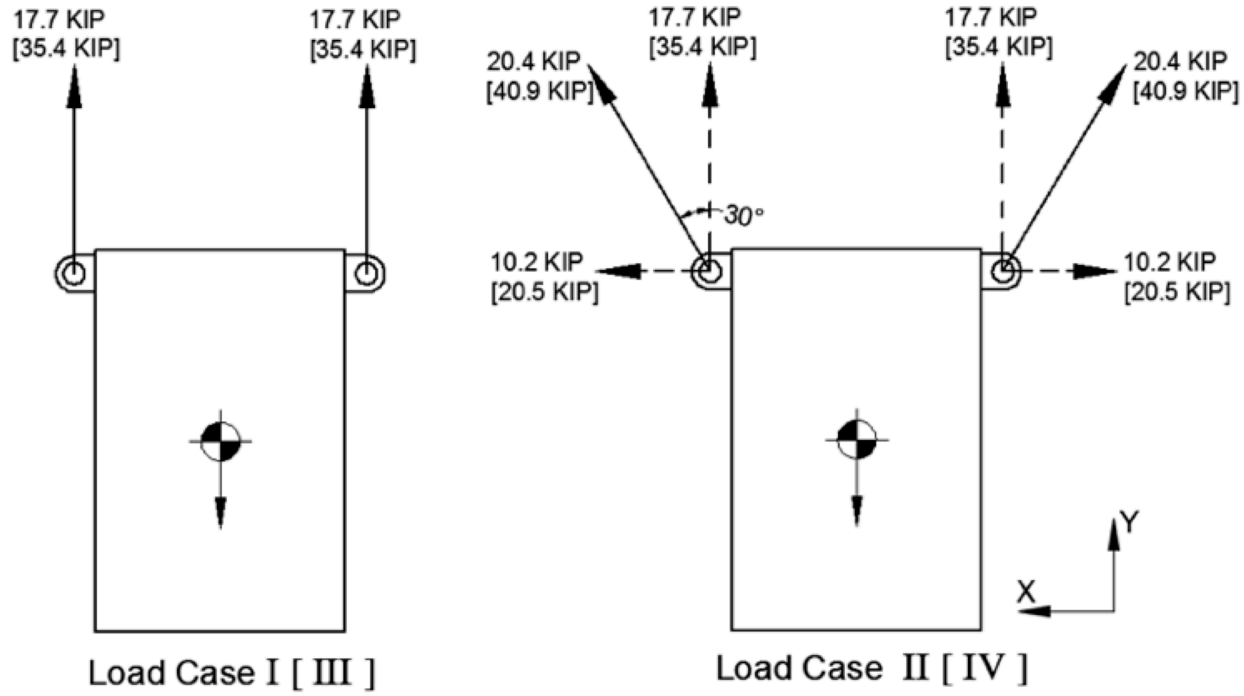

Figure 2.12.3-2. Magnitude and Direction of Loading in Model 2000 Cask

The following modes of failure are investigated for both ear designs:

- Shear tearout of lifting hole
- Tensile failure of ear plate
- Bearing of shackle pin on ear
- Yielding of weld joint
- Yielding of attaching bolt
- Shearing of bolt threads
- Shearing of tapped threads
- Yielding of cask outer shell

- SHEAR TEAR-OUT OF LIFTING HOLE-AUXILIARY AND STANDARD DESIGNS

Auxiliary Ear Design

For Load Case I, the shear tearout stress is computed as follows:

$$\tau = \frac{F}{A}$$ Reference 2-25 page 89.

where

F = 17.7 kip (see Figure 2.12.3-2) and

A = cross sectional area along the force line of action

$$= \left(4 - \frac{2.12}{2}\right) \times 1$$ (see Figure 2.12.3-1) = 2.94 in²

$$\tau = \frac{F}{A} = \frac{17.7}{2.94} = 6.02 \text{ ksi} < 15 \text{ ksi}$$

Standard Ear Design

For Load Case I, the shear tearout stress is:

$$\tau = \frac{F}{A} = \frac{35.4}{\left(5 - \frac{2.12}{2}\right) \times 1} = 8.98 \text{ ksi} < 15 \text{ ksi}$$

- TENSILE FAILURE OF EAR PLATE

  Auxiliary Ear Design

  In order to compute tensile failure for Load Case II, the internal forces that react to the lifting force are resolved into planes containing the minimum ligament cross-sectional area, as illustrated in Figure 2.12.3-3.

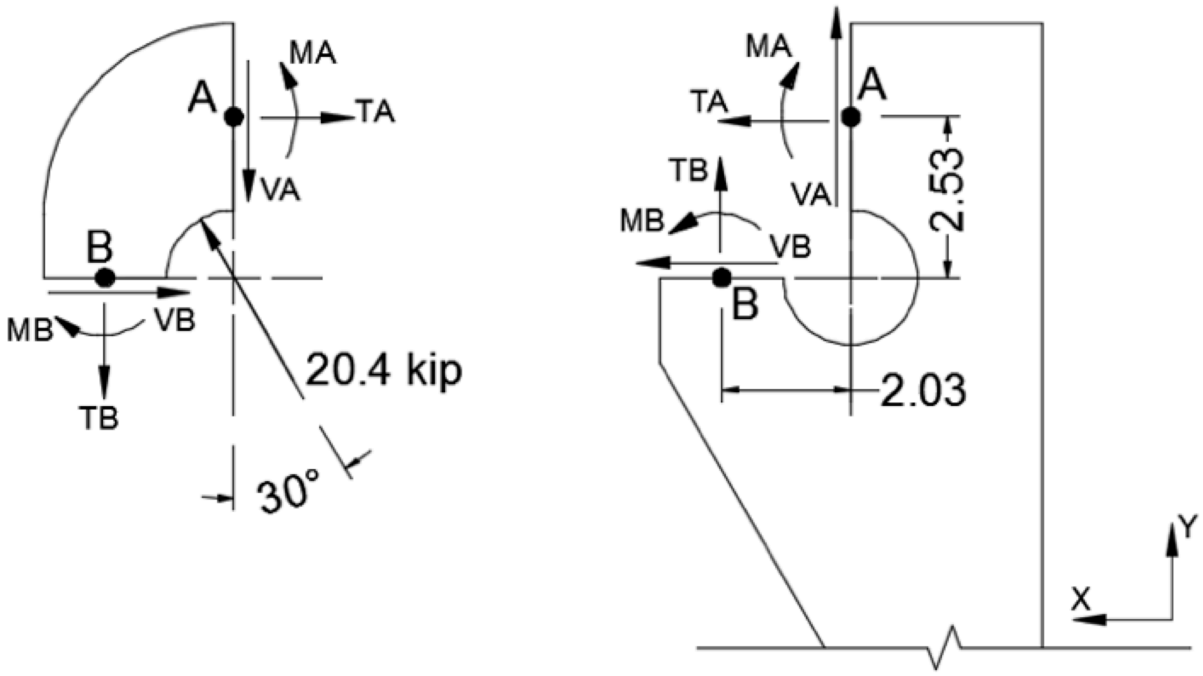

Figure 2.12.3-3. Ear Hole Cross Section

FH = 20.4 (sin 30°) = 10.2 kip
FV = 20.4 (cos 30°) = 17.7 kip

Equilibrium:

Eq. I $\sum$Mo = 0 = MA - MB - 2.53 TA + 2.03TB
Eq. II $\sum$FV = 0 =17.7 - VA - TB
Eq. III $\sum$FH = 0 = 10.2 - TA - VB

This is a statically indeterminate problem; however, by making some conservative simplifying assumptions, a solution may be obtained without resorting to indeterminate analysis methods. For the evaluation of primary stresses, we may conservatively assume MA = MB = 0. Also, on the basis of relative stiffness, TA > VB; consequently, it may be conservatively assumed that TA = VB. Therefore, we may write the following:

From Eq. III,

TA = VB = $\frac{10.2}{2}$ = 5.1 kip

From Eq. I,

TB = $\frac{2.53}{2.03}$ TA = 6.35 kip

From Eq. II,

VA = 17.7 - TB = 11.35kip

The principal stresses will now be calculated at point A.

From Reference 2-25, page 81, the principal stresses are calculated using:

$$\sigma_1, \sigma_2 = \frac{\sigma}{2} \pm \sqrt{\left(\frac{\sigma}{2}\right)^2 + \tau^2}$$

$$\sigma = \frac{TA}{A} = \frac{5.1}{2.94} = 1.735 \text{ ksi}$$

$$\tau = \frac{VA}{A} = \frac{11.35}{2.94} = 3.86 \text{ ksi}$$

$$\sigma_1 = \frac{1.735}{2} + \sqrt{\left(\frac{1.735}{2}\right)^2 + 3.86^2} = 4.82 < 23.7 \text{ ksi}$$

Standard Ear Design

Load Case I or III

Standard ear dimensions and loading are shown in Figure 2.12.3-4. The critical tensile section is at Section X-X, see Figure 2.12.3-4. The exact force distribution cannot be determined without a detailed analysis that would include all of the stiffness characteristics (e.g., a finite element analysis). However, it can be deduced that the limiting load at the critical section (i.e., point "A") will not exceed P/2. Then the tensile stress is:

$$\sigma_T = \frac{P/2}{A} = \frac{35.4/2}{1x1} = 17.7 \text{ ksi} < 23.7 \text{ ksi}$$

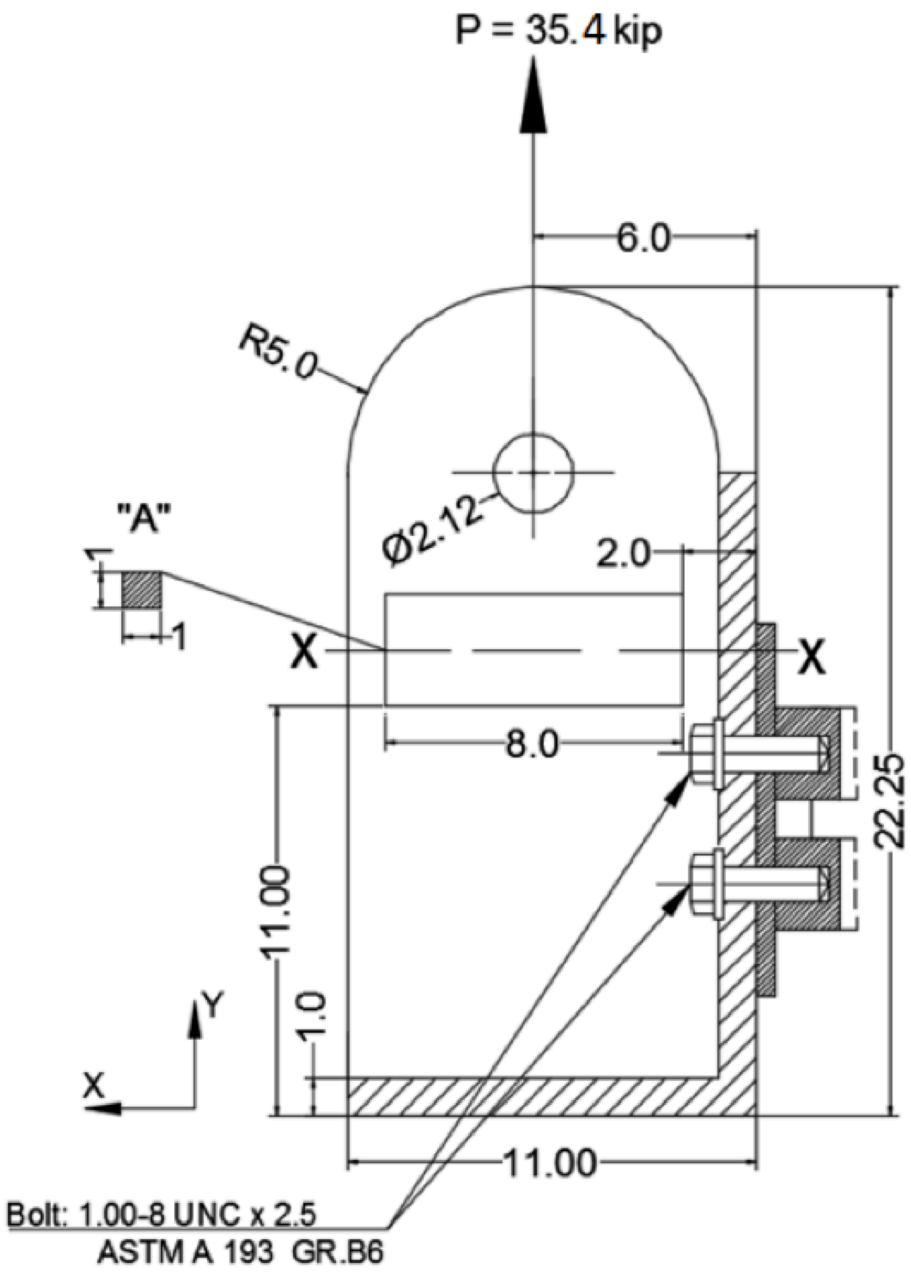

Figure 2.12.3-4. Standard Ear Load Case I or III

- BEARING OF SHACKLE PIN ON EAR

Auxiliary Ear Design

The bearing stress is computed assuming that the force is uniformly distributed over the projected contact area of the pin. This gives a stress:

$$\sigma = \frac{F}{A}$$

Where the projected area for the pin is A = t x d. Here, t is the thickness of the ear plate (1″) and d is the pin diameter (2″).

$$\sigma = \frac{20.4}{1 \times 2} = 10.2 \text{ ksi} < 23.7 \text{ ksi}$$

Standard Ear Design

Case I

$$\sigma = \frac{35.4}{1 \times 2} = 17.7 \text{ ksi} < 23.7 \text{ ksi}$$

Case III

$$\sigma = \frac{35.4}{1 \times 7.5} = 4.72 \text{ ksi} < 23.7 \text{ ksi}$$

- YIELDING OF WELD JOINTS

Auxiliary Ear Design

Figure 2.12.3-5 shows a free-body diagram of the ear with the lifting force acting through the center of the hole for Load Case I and Case II. The center of gravity of the weld group and of the bottom of the bracket point A is G. The force FG is the force of the weld group acting on the ear. Because FG has a different line of action than the lifting force, there is also a moment M.

Load Case I

The moment M produces a bending stress in the welds. The force F_G produces shear throughout the weld. These effects are:

$$M = 17.7 \times 3 = 53.10 \text{ k-in}$$

$$F_G = 17.7 \text{ kip}$$

- WELD GEOMETRY AND CROSS SECTION PROPERTIES

Weld throat area (A_w)

$$A_w = 1.414\ (0.375)(6.75 + 2.0 + 2.25) = 5.833 \text{ in}^2$$

Centroid of weld group (G)

$$\bar{Y} = \frac{\sum_1^3 (\bar{Y}_i A_i)}{\sum_1^3 A_i} = \frac{((1.125 \times 2.25 \times 0.375) + (4.75 \times 2 \times 0.375) + (10.625 \times 6.75 \times 0.375))}{(2.25 \times 0.375 + 2 \times 0.375 + 6.75 \times 0.375)} = 7.614 \text{ in}$$

Unit moment of inertia (I_u):

$$Iu = \sum(I_o + A_i d_i^2)$$

$$= 2\times\left\{\left(\frac{2.25^3}{12} + 2.25 \times 6.488^2\right) + \left(\frac{2^3}{12} + 2\times 2.863^2\right) + \left(\frac{6.75^3}{12} + 6.75\times 3.012^2\right)\right\}$$

$$= 399.17 \text{ in}^3$$

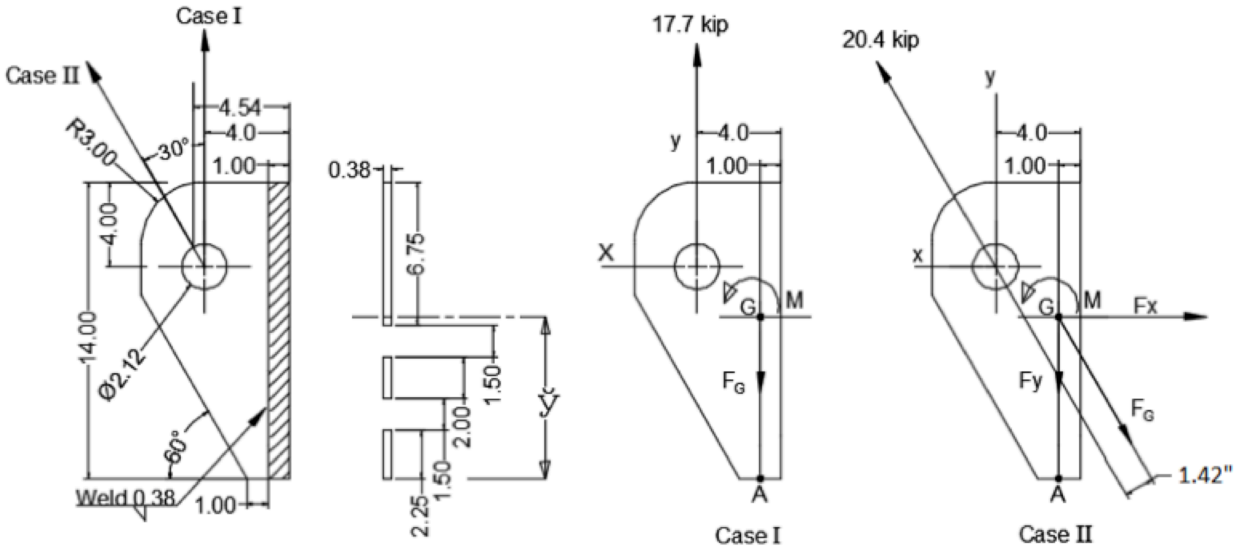

Figure 2.12.3-5. Auxiliary Ear, Case I and Case II Weld Stresses

Then the moment of inertia about an area through G parallel to area Z is:

$$I = 0.707\ hIu = 0.707\ (0.375)\ (399.17) = 105.83 \text{ in}^4$$

For the weld metal the normal stress at point A:

$$\sigma_x = \frac{Mc}{I} = \frac{53.10(7.614)}{105.83} = 3.82 \text{ ksi}$$

The shear stress is:

$$\tau_{xy} = \frac{F}{A} = \frac{17.7}{5.833} = 3.03 \text{ ksi}$$

The resulting Von Mises stress in the weld metal is:

$$\sigma' = \sqrt{\sigma_X^2 + 3\tau_{xy}^2} = \sqrt{3.82^2 + 3(3.03)^2} = 6.5 \text{ ksi} < 75 \text{ ksi}$$

CALCULATION OF STRESS IN THE PARENT METAL:

The area subject to shear is :

$A = 0.375\ (6.75 + 2.0 + 2.25) = 4.125\ in^2$

$\tau_{xy} = \frac{17.7}{4.125} = 4.29\ ksi$

The section modulus of the ear at the weld interface is:

$\frac{I}{C} = \frac{hI_u}{C} = \frac{0.375 \times 0.5 \times 399.17}{7.614} = 9.83\ in^3$

Thus, the tensile stress at A in the parent metal is:

$\sigma_x = \frac{M}{I/C} = \frac{53.10}{9.83} = 5.4\ ksi$

$\sigma' = \sqrt{\sigma_X^2 + 3\tau_{xy}^2} = \sqrt{5.4^2 + 3(4.29)^2} = 9.19\ ksi < 23.7\ ksi$

Load Case II

Figure 2.12.3-5 (Case II) shows a free body diagram of the ear for the Load Case II.
The moment M produces a bending stress in the welds.
The force component Fx produces tension throughout the weld.
The force component Fy produces shear throughout the weld.
These effects are:

$M = 20.4\ (1.42) = 28.97$ k-in.
$Fx = 10.2kip$
$Fy = 17.7kip$
$Aw = [(2.25 + 2 + 6.75)\ x\ 0.375\ x\ 0.707] \times 2 = 5.833\ in^2$

At the point A the bending stress and tensile stress due to Fx add. For the weld metal the total normal stress is:

$\sigma_x = \frac{F_X}{A} + \frac{M_C}{I} = \frac{10.2}{5.83} + \frac{28.97(7.614)}{105.84} = 3.83\ ksi$

The shear stress is:

$\tau_{xy} = \frac{F_y}{A} = \frac{17.7}{5.83} = 3.03\ ksi$

Thus, the Von Mises stress in the weld is:

$\sigma' = \sqrt{\sigma_X^2 + 3\tau_{xy}^2} = \sqrt{3.83^2 + 3(3.03)^2} = 6.51\ ksi < 23.7\ ksi$

The stresses in the parent metal are:

A_{pm} = (2.25 + 2 + 6.75) x 0.375 = 4.125

$\tau_{xy} = \frac{F_y}{A} = \frac{17.7}{4.125} = 4.29$ ksi

$\sigma_x = \frac{F_X}{A} + \frac{M}{I/C} = \frac{10.2}{4.125} + \frac{28.97}{9.83} = 5.42$ ksi

$\sigma' = \sqrt{\sigma_X{}^2 + 3\tau_{xy}{}^2} = \sqrt{5.42^2 + 3(4.29)^2} = 9.2$ ksi < 23.7 ksi

Standard Ear Design

Figure 2.12.3-6 shows a detailed sketch of the standard ear design. It includes dimensions, weld lines identification diagram, and a free body diagram of the ear plate for load conditions Case I and Case II. The investigation of stress on the welds is conducted conservatively by considering only welds A and B are active, in this part the welds are analyzed for both load conditions Case I and Case II. Case III was not analyzed because the resultant force in this case acts along the same line of action as the force in Case I.

Load case I

Figure 2.12.3-6 (Case I) shows a free body diagram of the standard ear for Load Case I.

Centroid of weld group ($\overline{Y}$)

$\bar{Y} = \frac{\sum_1^2(\bar{Y}_i A_i)}{\sum_1^2 A_i} = \frac{(2.25 \times 0.375 \times 0.19) + (15.87 \times 0.375 \times 7.935)}{2.25 \times 0.375 + 15.87 \times 0.375} = 6.97$ in

Unit moment of inertia (I_u):

$I_u = \sum(I_o + A_i d_i{}^2)$

$= 2 \times \left\{ \left(\frac{15.87^3}{12} + 15.87 \times (7.935 - 6.97)^2 \right) + (2.25 \times 6.97^2) \right\} = 914.13$ in^3

Then the moment of inertia about an axis through G parallel to axis Z through the weld minimum effective throat is:

$I = 0.707\ h\ I_u = 0.707 \times (0.375) \times 914.13 = 242.36$ in^4

For the weld metal the normal stress at point A:

$\sigma_x = \frac{Mc}{I} = \frac{35.4\ (5) 6.97}{242.36} = 5.09$ ksi

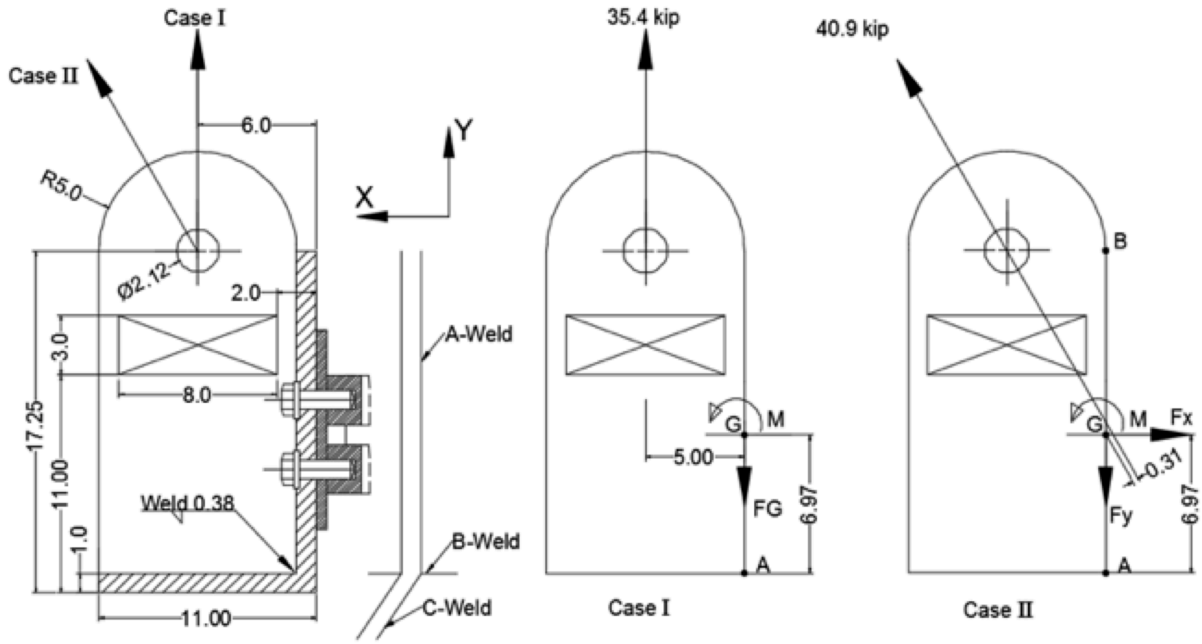

Figure 2.12.3-6. Standard Ear, Case I and Case II Weld Stresses

The shear stress is:

$$\tau_{xy} = \frac{F_G}{A} = \frac{35.4}{2(0.707)(2.25\ x\ 0.375+15.87\ x\ 0.375)} = 3.68 \text{ ksi}$$

The resulting von Mises stress in the weld metal is.

$$\sigma' = \sqrt{\sigma_X{}^2 + 3\tau_{xy}{}^2} = \sqrt{5.09^2 + 3(3.68)^2} = 8.16 \text{ ksi} < 23.7 \text{ ksi}$$

CALCULATION OF STRESS IN THE PARENT METAL:

The area subject to shear is:

$$A = 2 \times (0.375) \times (2.25 + 15.87) = 13.59 \text{ in}^2$$

Thus, the shear stress on the parent metal is:

$$\tau_{xy} = \frac{F_G}{A} = \frac{35.4}{13.77} = 2.6 \text{ ksi} < 13.7 \text{ ksi}$$

The section modulus of the ear plate at the weld interface is:

$$\frac{I}{C} = \frac{0.38 \times 914.33}{6.97} = 49.85 \text{ in}^3$$

Thus, the tensile stress at A in the parent metal is:

$$\sigma_x = \frac{35.4\ (5)}{49.85} = 3.6 \text{ ksi}$$

$$\sigma' = \sqrt{\sigma_x^2 + 3\tau_{xy}^2} = \sqrt{3.6^2 + 3(2.6)^2} = 5.77 \text{ ksi} < 23.7 \text{ ksi}$$

Load Case II

Figure 2.12.3-6 (Case II) shows a free body diagram of the standard ear for Load Case II.

$$A = 2(0.707)\ (0.375)(2.25 + 15.87) = 9.61 \text{in}^2$$
$$M = 40.9\ (0.31) = 12.68 \text{ k-in}$$
$$Fx = 20.5 \text{ kip}$$
$$Fy = 35.4 \text{ kip}$$

At the point B the bending stress and the tensile due to Fx add. For the weld metal the total normal stress is:

$$\sigma_x = \frac{F_x}{A} + \frac{Mc}{I} = \frac{20.5}{9.61} + \frac{12.68(16.25 - 6.97)}{242.36} = 2.62 \text{ ksi}$$

The shear stress is:

$$\tau_{xy} = \frac{F_y}{A} = \frac{35.4}{9.61} = 3.68 \text{ ksi}$$

Thus, the von Mises stress in the weld is:

$$\sigma' = \sqrt{\sigma_x^2 + 3\tau_{xy}^2} = \sqrt{2.62^2 + 3(3.68)^2} = 6.9 \text{ ksi} < 23.7 \text{ ksi}$$

The stresses in the parent metal are:

$$A = 2 \times (0.375) \times (2.25 + 15.87) = 13.59 \text{ in}^2$$

$$\tau_{xy} = \frac{35.4}{13.59} = 2.6\ ksi$$

$$\sigma_x = \frac{20.5}{13.59} + \frac{12.68}{49.85} = 1.77 \text{ ksi}$$

$$\sigma' = \sqrt{1.77^2 + 3(2.6)^2} = 4.85 \text{ ksi} < 23.7 \text{ ksi}$$

- YIELDING OF ATTACHING BOLT AND SHEARING OF BOLT AND TAPPED THREAD

Bolt Loading Auxiliary Ear Design

For the auxiliary ear design, the external bolt force produced by the lifting condition is:

Load Case I

The moment applied to the bolts is:

$$M = 17.7(4.00) = 70.8 \text{ k-in}$$

The tensile stress σ_{tb} at the bottom of contact area due to the applied moment is:

$$\sigma_{tb} = \frac{Md/2}{I} = \frac{Md/2}{bd^3/12} = \frac{6M}{bd^2}$$

Where b and d are the base and height dimensions of the contact area. The tensile load on the bolt is the area A_{tb} of each fastener times σ_{tb}.

$$F_T = \frac{6M}{bd^2} A_{tb}$$

Where A_{tb} for the bottom row bolt is:

$$A_{tb} = 3.00 \times (2.5+1.75) = 12.75 \text{ in}^2$$

$$F_T = \frac{6(70.8)}{6.0 \text{ x } 9.5^2} \times 12.75 = 10.00 \text{ kip}$$

Load Case II

The moment for this Load Case is reduced by the action of the horizontal component as follows:

$$M = 17.7 \times (4.54) - 10.2 \times (0.92 + 0.50 + 3.50 + 1.75) = 12.32 \text{ k-in.}$$ see Figure 2.12.3-1.

The tensile load on the bolt is:

$$F_T = \frac{6M}{bd^2} \times A_{tb} + \frac{F_H}{4} = \frac{6(12.32)(12.75)}{6.0(9.5)^2} + \frac{10.2}{4} = 1.74 + 2.55 = 4.29 \text{ kip}$$

Bolt Loading, Standard Ear Design

Load Case I and Case III (Slot Lift)

The moment applied to the bolt is:

$$M = 35.4(6.00) = 212.4 \text{ k-in}$$

$$A_{tb} = 3.00(3+1.75) = 14.25 \text{ in}^2$$

The tensile load F_t per bolt at the bottom row of bolts due to the applied moment is:

$$F_t = \frac{6MA_{tb}}{bd^2} = \frac{6(212.4)(14.25)}{6.0(10.0)^2} = 30.27 \text{ kip}$$

Load Case II

The moment for Load Case II is:

$$M = 35.4\ (6.54) - 20.5\ (0.92 + 7.75 + 3.50 + 1.75) = -53.84 \text{ k-in}$$

The tensile load F_t per bolt at the top row of bolts is:

$$A_{tb} = 3.00(3.5 + 1.75) = 15.75 \text{ in}^2$$

$$F_t = \frac{6(53.84)(15.75)}{6.0(10.0)^2} + \frac{20.5}{4} = 13.61 \text{ kip}$$

Load Case III ear base lift is not considered because the moment area is less than that of Load Case I and the load acts on the same directions as Load Case I.

Table 2.12.3-1 presents a summary of bolt loading for each of the ear designs (auxiliary and standard). Because the standard design under Load Case I, straight lift, imposes the largest tensile load on the bolt than in the other conditions, this load value (30.27 kip) is used in the analysis of the bolt.

Table 2.12.3-1. Bolt Loading Per Ear Design and Load Case

Ear Design	Bolt Loading (kip)			Yield Strength (ksi)	Shear Strength (ksi)
	Load Case				
	I	II	III (Slot Lift)		
Auxiliary	10	4.29	N/A	85	51
Standard	30.27	13.61	30.27	85	51

Bolt Analysis

Bolt and thread section properties use in the analyses for both internal and external threads are evaluated for a standard 1-8 UNC x 2-1/2 in bolt as follows.

Tensile stress area (A_t) for high strength bolt with σ_{tb} > 100ksi, as provided in *Machineries Handbook* , Reference 2-26, Page 1490 is:

$$A_t = \pi\left(\frac{E_{s_{min}}}{2} - \frac{0.16238}{n}\right)^2$$

where:

$E_{s_{min}}$ = Minimum pitch diameter = 0.9188 inches

n = Number of threads per inch = 8

$$A_t = \pi\left(\frac{0.9188}{2} - \frac{0.16238}{8}\right)^2 = 0.61 \text{ in}^2$$

Shear area of the external (A_s) and the internal (A_n) threads, Machineries Handbook, Reference 2-26, Page 1491.

$$A_s = \pi n L_e K_{n_{max}} \left[\frac{1}{2n} + 0.57735\,(E_{s_{min}} - K_{n_{max}})\right]$$

where:

n = 8

L_e = Length of engagement = 1.680 inches

$K_{n_{max}}$ = Maximum minor diameter of internal thread = 0.8795 inches

$$A_s = \pi\,(8)(1.680)(0.8795)\left[\frac{1}{2(8)} + 0.57735\,(0.9188 - 0.8795)\right] = 3.164 \text{ in}^2$$

$$A_n = \pi n L_e D_{s_{min}} \left[\frac{1}{2n} + 0.57735\,(D_{s_{min}} - E_{n_{max}})\right]$$

where:

$D_{s_{min}}$ = Minimum major diameter of external thread = 0.9848 inches

$E_{n_{max}}$ = Maximum pitch diameter of internal thread = 0.9242 inches

$$A_n = \pi\,(8)(1.680)(0.9848)\left[\frac{1}{2(8)} + 0.57735\,(0.9848 - 0.9242)\right] = 4.05 \text{ in}^2$$

Bolt Preload

J.E. Shigley and L.D. Mitchell (Reference 2-27) recommend the bolt preload (F_i) be between 60% and 90% of the proof load. The proof load is equal to 85% of the yield strength (S_y) multiplied by the tensile stress area (A_t). For a torque of 600±20 ft-lbs, the corresponding preload, proof load and percent of proof load are determined as follows:

$F_i = T/(kd)$

% proof load = [F_i / proof load] x 100%

Where:

T = torque = 600±20 ft-lb = 7,200±240 in-lb

d = bolt thread nominal diameter = 1.0 in (GEH drawings 101E8718 and 105E9520)

k = torque coefficient = 0.2 (Reference 2-27)

proof load = proof strength x A_t = 43,762 lbs

proof strength = 0.85 S_y = 72,250 psi

A_t = thread tensile area = 0.6057 in^2

S_y = yield strength at room temperature = 85,000 psi (Table 2.2-8)

Table 2.12.3-2 summarizes the bolt preload, bolt proof load and % proof load for all three lifting ear bolt torque values. As indicated, maximum, nominal, and minimum torques produce loads within the recommended range of 60% to 90% of the proof load.

Table 2.12.3-2 Lifting Ear Bolt Percent Proof Load

Lifting Ear Bolt Torque	Torque Value (ft-lbs)	Bolt Preload (lb)	Proof Load (lb)	Percent Proof Load
Maximum	620	37,200	43,762	85%
Nominal	600	36,000		82%
Minimum	580	34,800		80%

Stresses produced by preload:

Bolt tension

$$\sigma = \frac{F_i}{A_t} = \frac{37.20}{0.606} = 61.42 \text{ ksi}$$

Bolt thread stripping

$$\tau = \frac{F_i}{A_s} = \frac{37.20}{3.164} = 11.76 \text{ ksi}$$

Tapped thread stripping

$$\tau = \frac{F_i}{A_n} = \frac{37.20}{4.054} = 9.18 \text{ ksi}$$

Minimum Bearing stress between cask and ear

$$\sigma_{ib} = \frac{(\#of\ bolt)(F_i)}{Contact\ Area} = \frac{4(34.80)}{6.0(10.0)} = 2.32 \text{ ksi}$$

The initial bearing pressure, σ_{ib}, previously calculated, is assumed to be uniform over the contact area. The bearing pressure should not be exceeded by tensile stress, σ_{tb}. Figure 2.12.3-7 shows the bearing stresses at the lifting ear contact region.

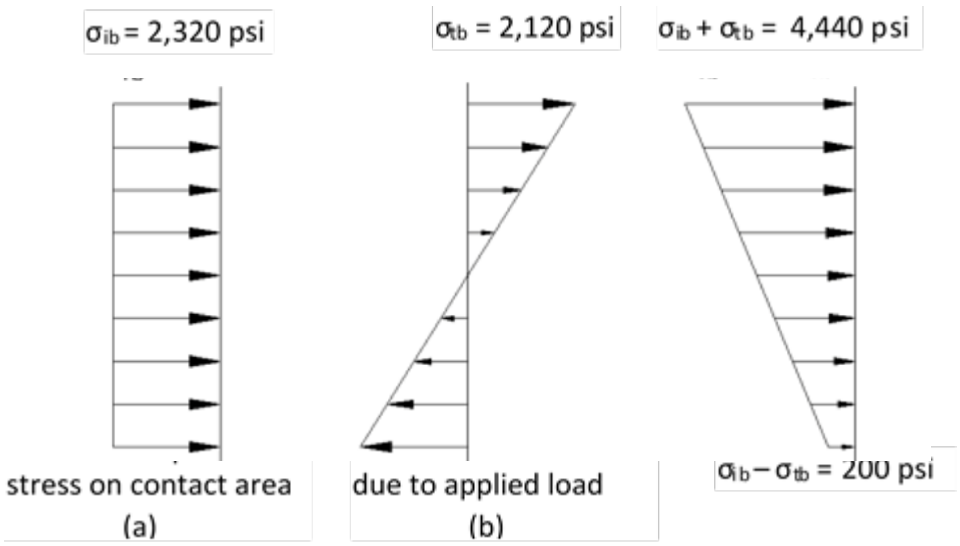

Figure 2.12.3-7. Lifting Ear Contact Bearing Stresses

$$\sigma_{tb} = \frac{6M}{bd^2} = \frac{6(212.4)}{6(10.0)^2} = 2.12 \text{ ksi}$$

$$\sigma_{ib} > \sigma_{tb}$$

The moment M (212.4 k-in) is produced by Load Case I or III on the standard ear design attaching bolt as previously calculated.

The nominal tensile stress, σ_t, in the bottom row bolts is:

$$\sigma_t = \frac{F_t}{A_t}$$

As previously calculated the tensile load for Load Case I is 30.27 kip per bolt.

$$\sigma_t = \frac{30.27}{0.606} = 49.95 \text{ ksi} < 85 \text{ ksi}$$

and the direct-shear component is:

$$\tau = \frac{35.4}{4(0.606)} = 14.6 \text{ ksi} < 51 \text{ ksi}$$

The interaction equation for the strength of a connection with bolts in combined shear and tension may be approximated by the elliptical relationship:

$$\left(\frac{\sigma_t}{\sigma_y}\right)^2 + \left(\frac{\tau}{0.6\sigma_y}\right)^2 \leq 1.0$$

$$\left(\frac{49.95}{85.0}\right)^2 + \left(\frac{14.60}{0.6(85)}\right)^2 \leq 1.0$$

$$0.43 \leq 1.0$$

Therefore, the selected bolts are adequate to carry the lifting load.

For the shearing of the bolt threads due to tensile load F_t.

$$\tau = \frac{F_t}{A_s} = \frac{30.27}{3.164} = 9.57\ ksi < 51.0\ ksi$$

For the shearing of the tapped threads due to tensile load F_t.

$$\tau = \frac{F_t}{A_n} = \frac{30.27}{4.054} = 7.47\ ksi < 51.0\ ksi$$

Bolt Fatigue Analysis

Bolt and Load Data:

1-8 UNC-2A, ASTM A193-B6

Yield Strength:	85 ksi (minimum)
Operating Temperature:	250°F
Modulus of Elasticity:	28.1 (10^6) psi
Maximum Tensile Stress:	61.42 ksi (Preload)
Maximum Shear Stress:	14.6 ksi

(Shear neglects the reducing effect of friction between ear and cask body.)

The maximum cycle of stress is due to a combination of the preload stress, 61.42 ksi, and the shear stress (14.6 ksi) due to lifting. These give a maximum principal stress of:

$$\sigma_{max} = \frac{61.42}{2} + \sqrt{\left(\frac{61.42}{2}\right)^2 + 14.6^2} = 64.71 \text{ ksi}$$

From ASME Section III NB 3232.3, the fatigue strength reduction factor to be used is 4.0. Because the fatigue curve (ASME Section III, Figure I-9.4 (Reference 2-18)) is based on modulus of elasticity of 30(10^6) psi and the bolt has a modulus of elasticity of 28.1(10^6) psi, the stress range is given by:

$$S = (64.71 \text{ ksi}) \times 4(30(10^6)/28.1(10^6)) = 276.34 \text{ ksi}$$

To select the correct fatigue curve, the stress intensity value, S_m, of 26.5 ksi is used at 250°F. Calculating the alternating stress:

$$S_a = \frac{1}{2} S = \frac{1}{2}(276.34) = 138.17 \text{ ksi}$$

Using the fatigue curve for a maximum nominal stress $\leq 2.7\ S_m$ the fatigue limit is ≅ 530 cycles as provided in Figure 2.12.3-8. Assuming an average of four ear lifts per usage and 12 usages per year, this gives a bolt life of:

$$\frac{530}{\left(12\frac{usages}{year}\right)\left(4\frac{cyc.}{usage}\right)} = 11 \text{ yrs.}$$

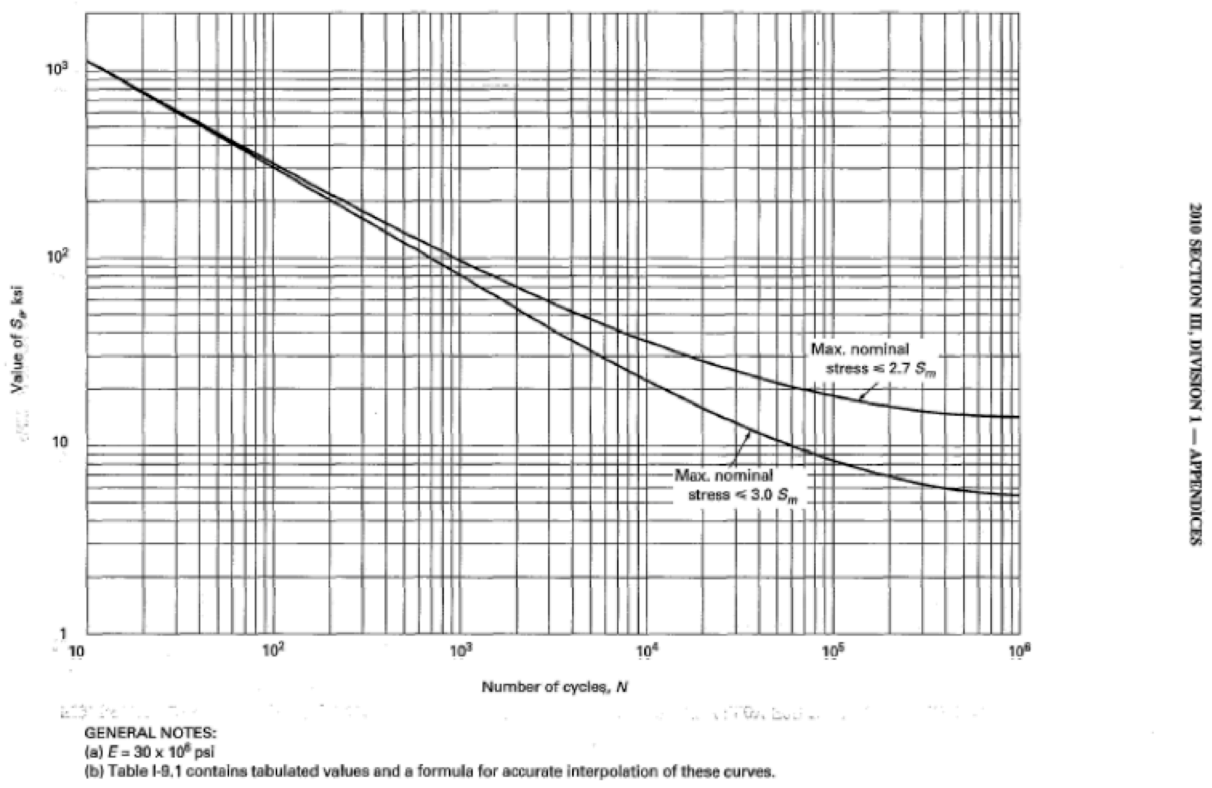

Figure 2.12.3-8. Design Fatigue Curves For High Strength Steel Bolting Above 700°F

(from Reference 2-18)

- YIELDING OF CASK OUTER SHELL

The lifting ears are mounted to the outer shell of the cask on a mounting plate embedded to the cask. The mounting plate is embedded about 1.75 inches into the cask through the outer shell and the lead shield. However, 1 inch thickness of the outer shell and the maximum vertical load of 35.4 kip (standard ear) are conservatively considered for yielding due to the lifting load.

$$\sigma_c = \frac{F_c}{A} = \frac{35.4}{7.5} = 4.72\ ksi$$

where Area (A) = thickness of shell x width of mounting plate = 1 x 7.5 = 7.5 in²

$$\tau = \frac{F}{As} = \frac{35.4}{12.5} = 2.83\ ksi$$

where the shear area (A) = 2 x (6.25 x 1) = 12.5 in²

$$\sigma_b = \frac{Mc}{I} = \frac{247.8\ x\ 3.125}{152.59} = 5.07\ ksi$$

where M = 35.4 x 7 = 247.8 k-in,

c = 6.25/2 = 3.125 in

$I = \frac{bh^3}{12} = \frac{7.5\ x\ 6.25^3}{12} = 152.59\ in^4$

$\sigma' = \sqrt{(4.72 + 5.07)^2 + 3x(2.83)^2} = 10.95\ ksi$

- EXCESSIVE LOAD FAILURE

The lifting devices must be designed such that their failure under excessive load would not impair the ability of the package to meet other requirements of 10 CFR 71. In this section a margin of safety (MS) is determined for each of the lifting system components based on the results presented in Table 2.12.3-3.

Table 2.12.3-3. Summary of Ear Analysis for Model 2000

Condition	Stress Level (ksi)		Allowable (ksi) Based on Yield	MS(y) Aux./Std.	Allowable Based on Su	MS(U) Aux./Std.
	Auxiliary (Aux.)	Standard (Std.)				
Shear tearout of lift hole	6.02	8.98	14	1.33/0.56	26.18	3.35/1.92
Tensile failure of ear plate	4.82	17.7	23.7	3.92/0.34	68.6	13.23/2.88
Bearing of shackle pin on ear	10.2	17.7	23.7	1.32/0.34	68.6	5.73/2.88
Yielding of weld joint	9.2	8.16	23.7	1.58/1.9	68.6	6.46/7.41
Yielding of attaching bolt	---	61.42	85	0.38	110	0.79
Shearing of bolt thread	---	11.76	51	3.34	---	---
Shearing of tapped thread	---	9.18	14	0.53	26.18	1.85
Yielding of cask outer shell	---	10.95	23.7	1.16	68.6	5.26

Note:
Bolt and bolt thread stress levels are documented in Table 2.12.3-3 for standard ear because maximum bolt loading is documented during slot lift (Case III) of the standard ear (see Table 2.12.3-1).

The margins of safety MS(y) with respect to yield is calculated as follows:

$$\text{MS (yield)} = \frac{\text{Allowable based on yield strength}}{Stress\ level} - 1$$

The ear and cask shell material is ASTM 240 type 304 stainless steel. The margins of safety with respect to ultimate failure MS(U)are:

For shear tear-out of lifting hole

$$\text{Shear Strengths} = \frac{\sigma_{ult}}{2(1+\mu)} = \frac{68.6}{2(1.31)} = 26.18\ ksi$$

τ = 8.98 ksi (Standard Ear, Load Case I)

$$MS(U) = \frac{26.18}{8.98} - 1 = 1.92$$

For tensile failure of ear plate

σ_T = 17.7 ksi (Standard Ear, Load Case III)

MS(U) = $\frac{68.6}{17.7} - 1 = 2.88$

For yielding of weld joints

σ ' = 9.2 ksi (Auxiliary Ear, Load Case II)

MS(U) = $\frac{68.6}{9.2} - 1 = 6.46$

For bolts

P_{ult} = 110 x 0.606 = 66.66 kip

Ft = 61.42(0.606) = 37.22 kip

MS(U) = $\frac{66.66}{37.22} - 1 = 0.79$

For yielding of cask outer shell

σ ' = 10.95 ksi

MS(U) = $\frac{68.6}{10.95} - 1 = 5.26$

A review of the above margin of safety indicates that, under excessive loading, the ear attaching bolts will fail before the ear plates, ear welds or cask shell. Failure of the bolts assures that the ability of the package to meet any other regulatory requirements is not impaired.

- MODEL 2000 LID LIFTING LUG ANALYSIS

The lifting lug is covered during transport. It is shown by analysis that this lifting device complies with requirements of 10 CFR 71.45(a). The lifting lug is able to support three times the weight of the lid without yielding.

The weakest part of the lifting lug is the fillet weld, which attaches the stainless steel loop to the cask lid. Using the maximum shear stress theory the weld is determined to have a factor of safety of 1.76 when analyzed for lifting 3 times the weight of the lid.

The lifting lug is analyzed by considering the rigid frame shown in Figure 2.12.3-9. The analytical model has the same height and distance between the supports as the lifting lug.

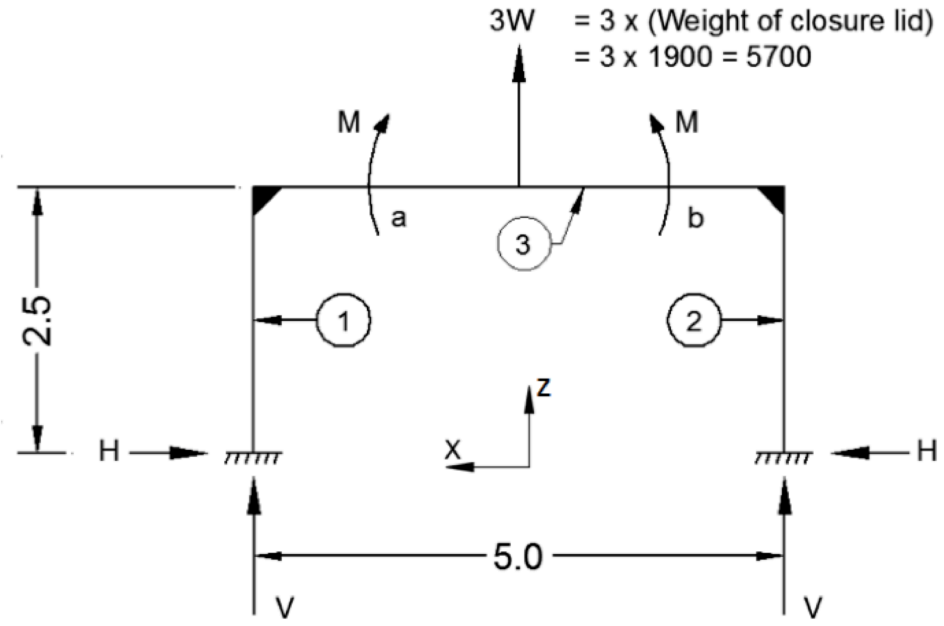

Figure 2.12.3-9. Analytical Model of Lifting Lug

The statically indeterminate forces and moments are obtained by solving the following set of equations from Reference 2-29.

$$\frac{-1/3HL^3_1}{I_1} + \frac{1/2M_1L^2_1}{I_1} = \frac{1/3HL^3_2}{I_2} - \frac{1/2M_2L^2_2}{I_2}$$

$$\frac{-1/2HL^2_1}{I_1} + \frac{M_1L_1}{I_1} = \frac{-1/3M_1L_3}{I_3} + \frac{1/6W\left(bL_3 - \frac{b^3}{L_3}\right)}{I_3} - \frac{1/6M_2L_3}{I_3}$$

$$\frac{-1/2HL^2_2}{I_2} + \frac{M_2L_2}{I_2} = \frac{1/3M_2L_3}{I_3} + \frac{1/6M_1L_3}{I_3} - \frac{1/6W\left[2bL_3 + \left(\frac{b^3}{L_3}\right) - 3b^2\right]}{I_3}$$

And by symmetry:

$M_1 = M_2 = M$

$H_1 = H_2 = H$

$V_1 = V_2 = V = 2{,}850$ lb.

Also,

$L_1 = L_2 = 2.5$

$L_3 = 5.0$

$I_1 = I_2 = I_3$

$a = b = 2.5$

Using substitution and solving the above equations simultaneously gives:

V = 2,850 lb
H = 2,671lb
M = 4,452 lb-in

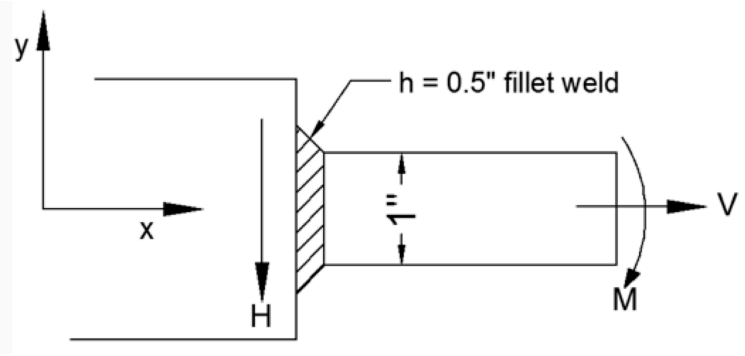

Figure 2.12.3-10. Loading on the Weld Area

The loading in the weld area is shown in Figure 2.12.3-10. The moment M produces a bending stress, σ_m, in the weld. This stress is assumed to act normal to the throat area (see Reference 2-27, P. 427).

The unit moment of inertia of the welds is from Reference 2-27, P. 429, given by:

$$I_u = \pi r^3$$

But the moment of inertia based on the weld throat is:

$$I = 0.707h\pi r^3$$

The normal stress in the weld is therefore given by:

$$\sigma = \frac{MC}{I} = \frac{MC}{0.707h\pi r^3}$$

The maximum stress occurs at the outer fibers where:

$$C = r$$

$$Z = 2\pi r$$

The maximum stress is therefore given by:

$$\sigma_m = \pm \frac{M}{0.707h\pi r^2}$$

From Reference 2-27, Equation (9.3), p. 417, the stress in the weld due to the force V is given by:

$$\tau_v = \frac{V}{0.707hZ}$$

Similarly, from Reference 2-27, Equation (a), p. 427, the stress in the weld due to the force H is given by:

$$\tau_H = \frac{H}{0.707hZ}$$

Figure 2.12.3-11 shows the stresses acting on the weld at the point where the bending moment is a maximum.

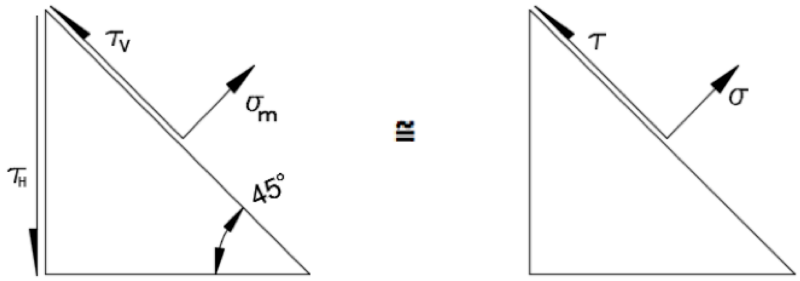

Figure 2.12.3-11. Stresses Acting on the Weld

$$\sigma = \sigma_m = \frac{4452}{0.707 \times 0.5 \times \pi \times (0.5)^2} = 16{,}035.3 \text{ psi}$$

$$\tau = \tau_v - \tau_H \cos 45°$$

$$= \frac{2{,}850}{0.707 \times 0.5 \times 2\pi \times 0.5} - \frac{2{,}671}{0.707 \times 0.5 \times 2\pi \times 0.5} \times 0.707$$

$$\tau = 2{,}566 - 1{,}700 = 866 \text{ psi}$$

From Reference 2-27, p.31, the principal stresses are found using:

$$\sigma_1, \sigma_2 = \frac{\sigma}{2} \pm \sqrt{\left(\frac{\sigma}{2}\right)^2 + \tau^2}$$

$$\tau_{max} = \pm\sqrt{\left(\frac{\sigma}{2}\right)^2 + \tau^2}$$

Substituting for σ and τ yields

$$\sigma_1, \sigma_2 = \frac{16{,}035.3}{2} \pm \sqrt{\left(\frac{16{,}035.3}{2}\right)^2 + 866^2}$$

$$= 8{,}017.7 \pm 8064.3$$
$$\sigma_1 = 16{,}082 \text{ psi}$$
$$\sigma_2 = -46.6 \text{ psi}$$
$$\tau_{max} = \pm 8064.3 \text{psi}$$

The maximum shear stress is applied to determine the likelihood of failure or safety.

$$\text{Allowable} = \tau_{allowable} = 0.6 \text{ Sy}$$

Where Sy denotes the yield strength.
The yield strength of stainless steel Type 304 is 23.7 ksi.

Substituting into equation (32)
Allowable Stress = 0.6 x 23.7 = 14.22 ksi

$$\tau_{max} = 8.06 \text{ ksi} \leq 14.22 \text{ ksi}$$

Therefore, the factor of safety is given by

$$FS = \frac{14.22}{8.06} = 1.76 \text{ (this is for lifting 3W)}$$

2.12.3.2. Tie-Down Analysis

The purpose and scope of this analysis is to demonstrate the structural integrity of the tie-down rib. The Model 2000 Transport Package is shipped normally by truck. Figure 2.12.3-12 shows the overall plan for tying the package to the vehicle. Eight wire ropes or chains tie the package to the vehicle: four connect to the upper tie-down ribs of the overpack, and the other four connect to the overpack base tie-down ribs. In addition, the base of the package is wedged to the truck bed to prevent sliding. Evaluation of the tie-down loading on the tie-down rib adjacent area consisted of the following:

1) Identification of the maximum tie-down member tension force due to loading.
2) Evaluation of the effect of the above force on the tie-down rib.

Classical hand calculation is used to identify the maximum tie-down member tension forces due to the combined loads. The results of this analysis were added to establish the maximum load. Table 2.12.3-3 gives a summary of each rope tie-down tension load for each force component and the total force. The maximum tie-down wire tension force is estimated to be 148.62 kips. This maximum load is then applied to the tie-down rib to determine the structural integrity of the tie-down rib by analyzing the following modes of failure:

- Shear tear-out of tie-down rib hole
- Bearing of shackle pin on ear
- Yielding of weld joints and parent metal

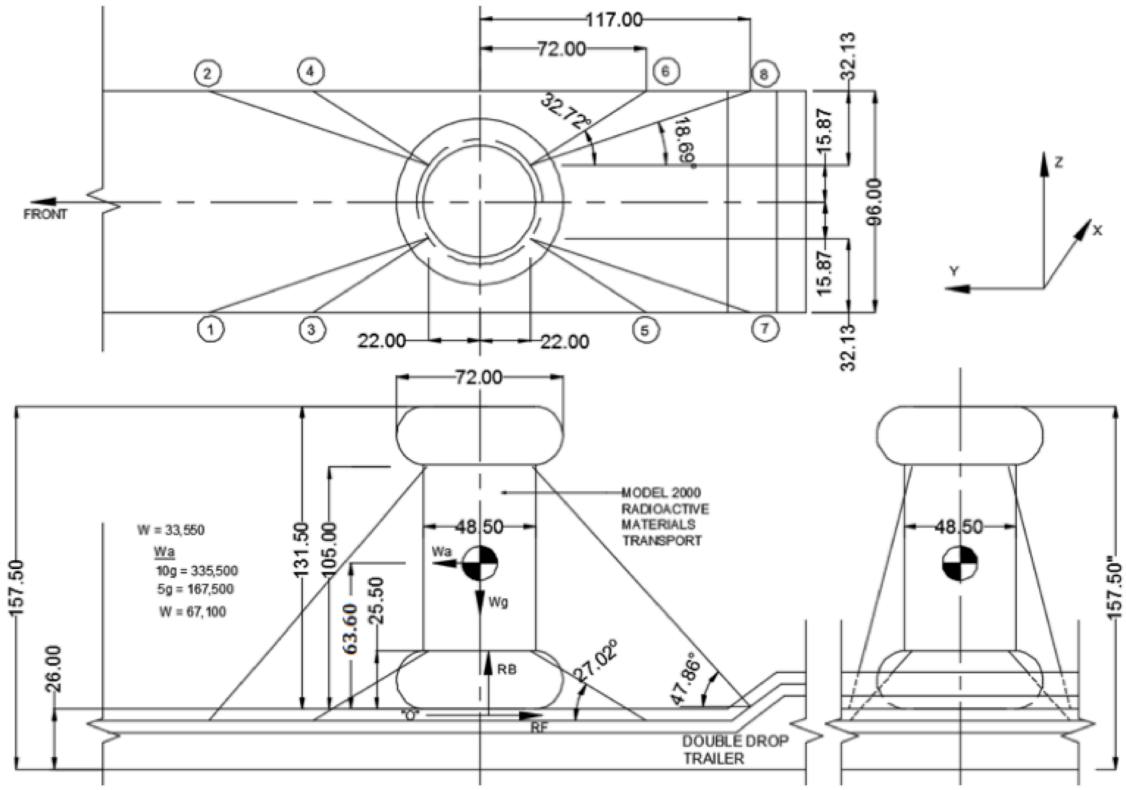

Figure 2.12.3-12. Tie-Down of Transport Package to Vehicle

- TIE-DOWN MEMBER TENSION FORCES

The package (wt. = 33,550 lb) is subject to accelerations of 10g longitudinal, 5g transverse, and 2g vertical (up) Per IAEA's "Package stowage and retention" regulations. These accelerations result in the following forces acting on the C.G. of the cask:

F_{long} = 33,550(10) = 335, 500 lbf

F_{trans} = 33,550(5) = 167, 100 lbf

F_{vert} = 33,550(2) = 67,100 lbf

In this calculation, each load is independently applied to the package and the tensile load on members for each case is calculated. The tensile loads are then added to calculate the maximum tension load on members.

10g Longitudinal

Because the base of the package is chocked, the 10g acceleration will cause it to rotate about point "o" counterclockwise (-x direction). This rotation will cause Ropes 1, 2, 3 and 4 to go slack and tension Ropes 5, 6, 7 and 8. From Figure 2.12.3-13.

F7 = F8

F5 = F6

The component forces for these ropes are:

$$F5y = F6y = F6 \cos 23.2° \cos 32.7° = 0.774\ F6$$
$$F5z = F6z = F6 \sin 23.2° = 0.394\ F6$$
$$F7y = F8y = F8 \cos 46.3° \cos 18.69° = 0.654\ F8$$
$$F7z = F8z = F8 \sin 46.3° = 0.723\ F8$$

The reaction forces from chocking and friction (R_F) and bearing on the package base (R_B) are:

$$RF = F5y + F6y + F7y + F8y - Wa$$
$$RB = F5z + F6z + F7z + F8z + Wg \quad \text{(assuming } F_1 = F_2 = F_3 = F_4 = 0\text{)}$$

The center of gravity is 63.60 inches.

$$\Sigma Mox = 0 = - Wa\ 63.60 + Wg\ 24.25 - RB\ 24.25 + (F5y + F6y)25.5 + (F7y + F8y)$$
$$105.0 + (F5z + F6z + F7z + F8z)\ 46.25$$

$$\Sigma Mox = - Wa\ 63.60 + Wg24.25 - (F5z + F6z + F7z + F8z + Wg)24.25 + \ldots$$
$$\ldots(F5y + F6y)25.5 + (F7y + F8y)105.0 + (F5z + F6z + F7z + F8z)46.25$$
$$= - Wa\ 63.60 - [2x0.394F6 + 2x0.723F8]24.25 + 2x0.774F6(25.5) + \ldots$$
$$\ldots 2x0.654F8\ (105.0) + [2x0.394F6 + 2x0.723F8]46.25$$
$$= -Wa\ 63.60 - 19.1F6 - 35.1F8 + 39.5F6 + 137.3F8 + 36.4F6 + 66.9F8$$
$$= -Wa\ 63.60 + (-19.1 + 39.5 + 36.4)\ F6 + (-35.1 + 137.3 + 66.9)\ F8$$
$$= - (63.60)\ Wa + (56.8)\ F6 + (169.1)\ F8$$
$$\Rightarrow 2.134\ (10^7) = (56.8)F6 + (169.1)\ F8$$

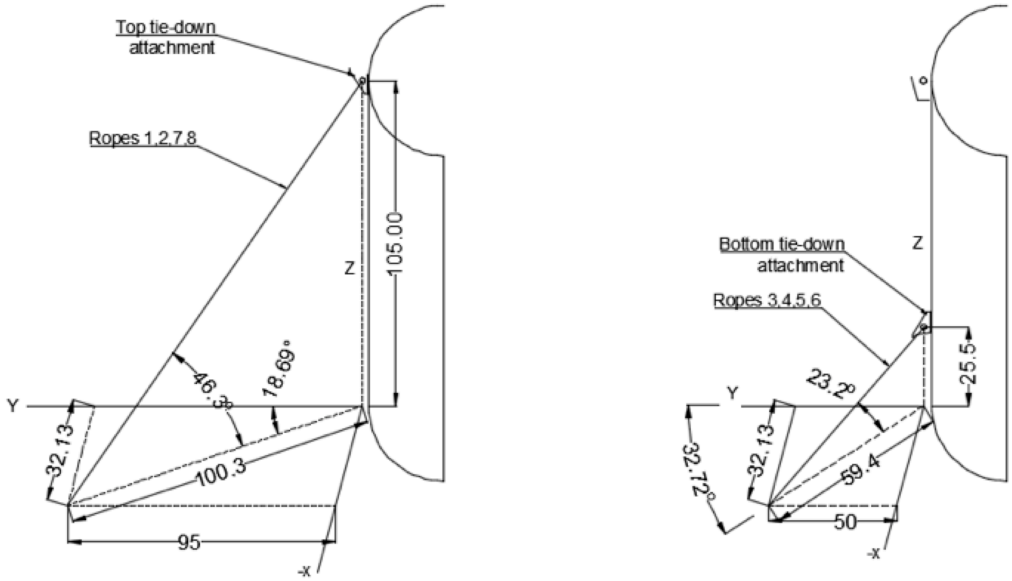

Figure 2.12.3-13. Tie-Down Wire Ropes

This cannot be solved for F6 and F8 so an additional equation relating F6 and F8 is required. By making certain assumptions, this equation can be obtained from consideration of the force and deflection (or extension) characteristics of the different length wire ropes. Figure 2.12.3-14 shows the extension of the ropes at small angle rotation. Assuming the ropes initially have no tension, the ratio of loads due to stretching of the ropes is:

$$\frac{F_7}{F_5} = \frac{\frac{\delta_7 EA}{L_7}}{\frac{\delta_5 EA}{L_5}}$$

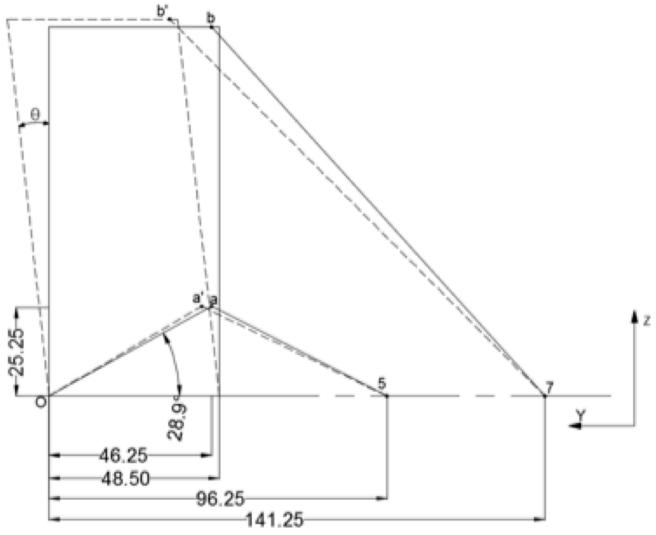

Figure 2.12.3-14. Wire Rope Extension at Small Angle (θ) Rotation

Because both ropes are of the same size and material,

$$\frac{F_7}{F_5} = \frac{\delta_7 L_5}{\delta_5 L_7}$$

For a rotation of θ° about point "O", line 5 would be extended as follows

$$\delta_5 Z\ L_5 f - L_5 i$$

$L_5 f$ is the final length of rope 5 as shown in Figure 2.12.3-15.

$$L_5 i = \sqrt{59.4^2 + 25.5^2} = 64.6 \text{ in}$$

$$\overline{oa'} = \overline{oa} = \sqrt{46.25^2 + 25.5^2} = 52.8 \text{ in}$$

Change in "a" in y direction is:

$$\overline{aa'_y} = 52.8[\cos 28.9° - \cos(28.9 + \theta)]$$

Change in "a" in z direction is:

$$\overline{aa'_z}$$

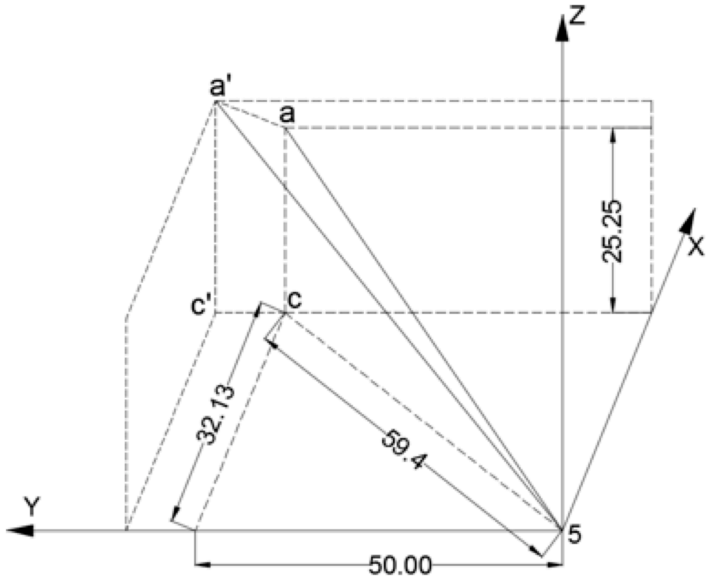

Figure 2.12.3-15. Final Length of Rope 5

$$L_5 f = \sqrt{\begin{matrix}(25.5 + 52.8[\sin(28.9° + \theta) - \sin 28.9°])^2 + \cdots \\ (32.13^2 + (50.0 + 52.8[\cos 28.9° - \cos(28.9° + \theta)])^2)\end{matrix}}$$

To evaluate the effect of small rotations, L_{5f} will be evaluated for θ = 0.1°, θ = 1° and θ = 10°.

$$L_5f_{.1^\circ} = \sqrt{\begin{matrix}(25.5 + 52.8[\sin(29.0)^\circ - \sin 28.9^\circ])^2 + \cdots \\ 32.13^2 + (50.0 + 52.8[\cos 28.9^\circ - \cos(29.0^\circ)])^2\end{matrix}}$$

$$= \sqrt{654.4 + 3{,}536.8} = 64.7 \text{ in}$$

$$L_5f_{1^\circ} = \sqrt{\begin{matrix}(25.5 + 52.8[\sin(29.9^\circ) - \sin 28.9^o])^2 + \cdots \\ 32.13^2 + (50.0 + 52.8[\cos 28.9^\circ - \cos(29.9^\circ)])^2\end{matrix}}$$

$$= \sqrt{691.8 + 3{,}577.8} = 65.3 \text{ in}$$

$$L_5f_{10^\circ} = \sqrt{\begin{matrix}(25.5 + 52.8[\sin(38.9^\circ) - \sin 28.9^\circ])^2 + \cdots \\ 32.13^2 + (50.0 + 52.8[\cos 28.9^\circ - \cos(38.9^\circ)])^2\end{matrix}}$$

$$= \sqrt{1{,}098.2 + 4{,}072.0} = 71.9 \text{ in}$$

A similar evaluation for line 7 yields:

$$L_7i = \sqrt{100.3^2 + 105^2} = 145.2 \text{ in}$$

$$\overline{ob} = \overline{ob'} = \sqrt{46.25^2 + 105^2} = 114.7 \text{ in}$$

Change in "b" in y direction is:

$$\overline{bb'_y} = 114.7[\cos 66.2^\circ - \cos(66.2 + \theta)]$$

Change in "b" in z direction is:

$$\overline{bb'_y} = 114.7\,[\sin(66.2 + \theta) - \sin 66.2]$$

$$L_7f = \sqrt{\begin{matrix}(105 + 114.7[\sin(66.2 + \theta) - \sin 66.2\,])^2 + \cdots \\ 32.13^2 + (95 + 114.7[cos66.2 - \cos(66.2 + \theta)])^2\end{matrix}}$$

Evaluation at θ = 0.1°, θ = 1° and θ = 10°gives:

$$L_7f_{.1^\circ} = \sqrt{\begin{matrix}(105 + 114.7[\sin 66.3 - \sin 66.2\,])^2 + \cdots \\ 32.13^2 + (95 + 114.7[cos66.2 - \cos 66.3])^2\end{matrix}}$$

$$= \sqrt{11041.9 + 10{,}092.2} = 145.4 \text{ in}$$

$$L_7f_{1^\circ} = \sqrt{11{,}191.9 + 10{,}410.1} = 147.0 \text{ in}$$

$$L_7f_{10^\circ} = \sqrt{12{,}419.6 + 14{,}011.7} = 162.6 \text{ in}$$

Calculation of the ratio $\frac{L_f}{L_i}$ for each rope at each rotation value yields:

	Lf/Li	
θ	**Rope 5**	**Rope 7**
0.1°	1.002	1.001
1°	1.011	1.012
10°	1.113	1.120

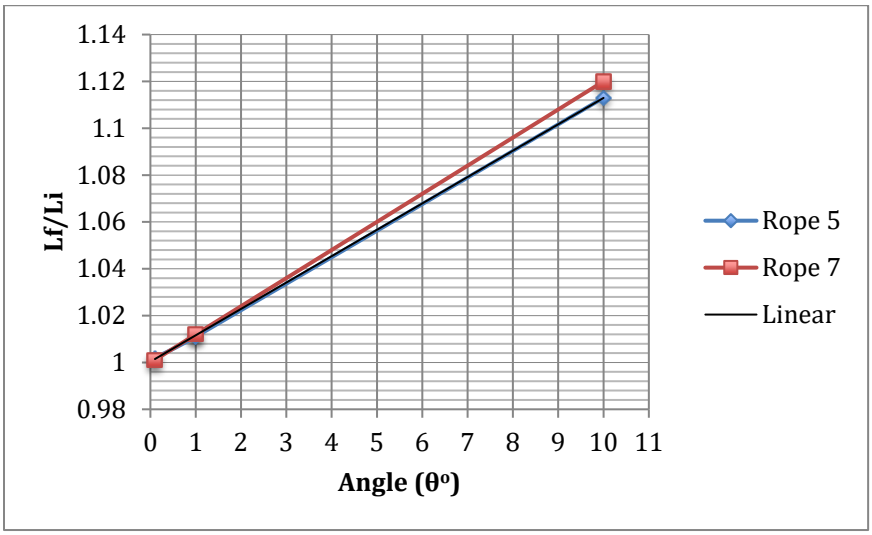

Figure 2.12.3-16. Final to Initial Rope Length Ratio per Small Angle Rotation

The fact that the ratios are the same for each rope and liner indicates that their derivation is correct. Their similarity and linearity would be expected from rigid body rotation.

Back to the relation between F_6 and F_8 (or F_5 and F_7), the ratio of loads due to stretching are for $\delta = 0.1°$:

$$\frac{F_7}{F_5} = \frac{\delta_7 L_5}{\delta_5 L_7}$$

$$\frac{F_7}{F_5} = \frac{0.2 * 64.6}{0.1 * 145.2} = 0.8898\ldots^{**}$$

$L_5 = 64.6$

$L_7 = 145.2$

$\delta_5 = L_5 f - L_5 i$

$= 64.7 - 64.6 = 0.1$

$\delta_7 = 145.4 - 145.2 = 0.2$

For $\theta = 10°$

$$\frac{F_7}{F_5} = \frac{17.4}{7.3} = 1.061$$

Because the ropes cannot stretch 7.3 or 17.4 inches, this just shows that the ratio of forces in the ropes is fairly close at the two extremes. For the purpose of analysis, the value of 0.8898 will be used as this represents a more realistic elongation of the ropes.

$$F_7 = F_8 = 0.8898\ F_5 = 0.8898\ F_6$$

F_6 56.8 + (0.8898 F_6)x169.1 = 2.134 (10^7)

F_5 = F_6 = 102,960.00
F_7 = F_8 = 0.8898 F_6 = 91,614.00
RF = F5y + F6y + F7y + F8y – Wa
= 0.774F5 + 0.774F6 + 0.654F7 +0.654F8 – 335,500 = -56,287 lb

5g Transverse

This time the 5g acceleration will cause the package to rotate at a point 90° clockwise from point "o". This will cause ropes 2, 4, 6 and 8 to go slack, and tension ropes 1, 3, 5 and 7. From symmetry the following assumptions can be made with reference to 2.12.3-11.

F_1 = F_7
F_3 = F_5

The component forces for these ropes are:

F_3x = F_5x = F_5 cos 23.2° sin 32.7° = 0.497 F_3
F_3z = F_5z = F_5 sin 23.2° = 0.394 F_3
F_1x = F_7x = F_7 cos 46.3° sin 18.69° = 0.221 F_1
F_1z = F_7z = F_7 sin 46.3° = 0.723 F_1

The reaction forces from chocking and friction (RF) and bearing on the package base (RB) are:

RF = $F_5x + F_3x + F_7x + F_1x$ – Wa
RB = $F_5z + F_3z + F_7z + F_1z$ + Wg

RB is calculated assuming $F_2 = F_4 = F_6 = F_8 = 0$

ΣMox = 0 = - Wa 63.60 + Wg 24.25 – RB 24.25 + ($F_5x + F_3x$)25.5 + ($F_7x + F_1x$)

105.0 + ($F_5z + F_3z + F_7z + F_1z$) 40.12

ΣMox = - Wa 63.60 + Wg 24.25 - ($F_5z + F_3z + F_7z + F_1z$ + Wg)24.25 + …

… ($F_5x + F_3x$)25.5 + ($F_7x + F_1x$)105.0 + ($F_5z + F_3z + F_7z + F_1z$)40.12

= - Wa 63.60 - [2 x 0.394F_3 + 2 x 0.723F_1]24.25 + 2 x 0.497F_3(25.5) + …

… 2 x 0.221F_1 (105.0) + [2 x 0.394F_3 + 2 x 0.723F_1]40.12

= -Wa 63.60 – 19.1F_3 – 35.1F_1 + 25.3F_3 + 46.41F_1 + 31.6F_3 + 58F_1

= -Wa 63.60 + (-19.1 + 25.3 + 31.6) F_3 + (-35.1 + 46.41 +58) F_1

= - (63.60) Wa + (37.8)F_3 + (69.31)F_1

=> 1.063 (10^7) = (37.8)F_3 + (69.3)F_1*

From equation** F_5 and F_7 are related as:

F_7 = 0.8898F_5
= 0.8898F_3 = F_1
=> 1.063 (10^7) = (37.8)F_3 + (69.3)(0.8898F_3)*
F_3 = 106,874

F_5 = 106,874
F_1 = 95,096
F_7 = 95,096

From above: RF = $F_5x + F_3x + F_7x + F_1x – Wa$
= 0.497F5 + 0.497F3 + 0.221F7 +0.221F1 – 167,100 = -18,835 lb

2g Vertical

During the 2g vertical load all 8 members are expected to experience tension, and all vertical components of the members will react. From symmetry, the following assumptions can be made with reference to Figure 2.12.3-13.

Assumption from symmetry: For the 2g vertical load, all ropes at the bottom (3,4,5,6) experience equal load and all ropes on top (1,2,7,8) experience equal load.

$F_5z = F_4z = F_3z = F_6z = \text{Sin}(23.2)F_3 = 0.394\ F_3$
$F_7z = F_2z = F_1z = F_8z = \text{Sin}(46.3)F_1 = 0.723\ F_1$
Where Fz is the vertical component of the forces on the ropes.

$\Sigma Fz = 0 = (F_5z + F_4z + F_3z + F_6z) + (F_7z + F_2z + F_1z + F_8z) + Wg – Wa = 0$
$= 4\ F_5z + 4\ F_7z + Wg – Wa = 0$
$= 4 \times 0.394\ F_3 + 4 \times 0.723\ F_1 + Wg – 2Wg = 0$
$= 1.576F_3 + 2.892F_1 - Wg = 0$
$= 1.576F_3 + 2.892F_1 = 33,500$

From above, $F_1 = 0.8898F_3$.

Hence $\Rightarrow \frac{1.576}{0.8898} F_1 + 2.892F_1 = 33,500$

$\Rightarrow 1.771F_1 + 2.892F_1 = 33,500$
$= 4.663F_1 = 33,500$

⇨ $F_1 = 7183.93 = F_2 = F_7 = F_8$
⇨ $F_3 = 8073.65 = F_4 = F_5 = F_6$

Table 2.12.3-4. Tie-Down Ropes Tension Forces

Rope No.	10W Long. (lb)	5W Transv. (lb)	2W Vert.(lb)	Total (lbf)
1	---	95,096	7,184	95,367
2	---	---	7,184	7,184
3	---	106,874	8,074	107,179
4	---	---	8,074	8,074
5	102,960	106,874	8,074	**148,620^{max}**
6	102,960	---	8,074	103,276
7	91,614	95,096	7,184	132,242
8	91,614	---	7,184	91,895
Friction	56,287	18,835	---	---

As documented in Table 2.12.3-4, the maximum cable tension force is 148.62 kip. This load value is used in subsequent tie-down analysis of the rib.

- TIE-DOWN RIB ANALYSIS

The tie-down ribs are triangular plate two inches thick supported at the short side by a 5 inch x 6.5 inch pad that is 0.5 inch thick. This plate is rolled to confirm with the toroidal shell contour. The vertical edge of the tie-down rib is welded to a stiffening ring. The tie-down rib, pad and stiffening ring are fabricated from ASTM A240, Type [[ ]] material. The toroidal shell material is ASTM A403, Type 304 stainless steel; and the overpack outer shell, where the stiffening ring attaches, is fabricated from ASTM A240, SS304.

The maximum temperature, 249°F, of the overpack bottom toroidal shell, where the tie-down ribs will be attached, is used as a reference.

Several modes of failure are investigated for the components of the tie-down rib system. These modes of failure are:

- Shear tearout of tie-down rib hole
- Bearing of shackle pin on ear
- Yielding of weld joints and parent metal

- SHEAR TEAROUT OF TIE-DOWN RIB HOLE

Figure 2.12.3-17 shows a sketch of the tie-down rib with the rope tension force line of action and lines of failure in shear.

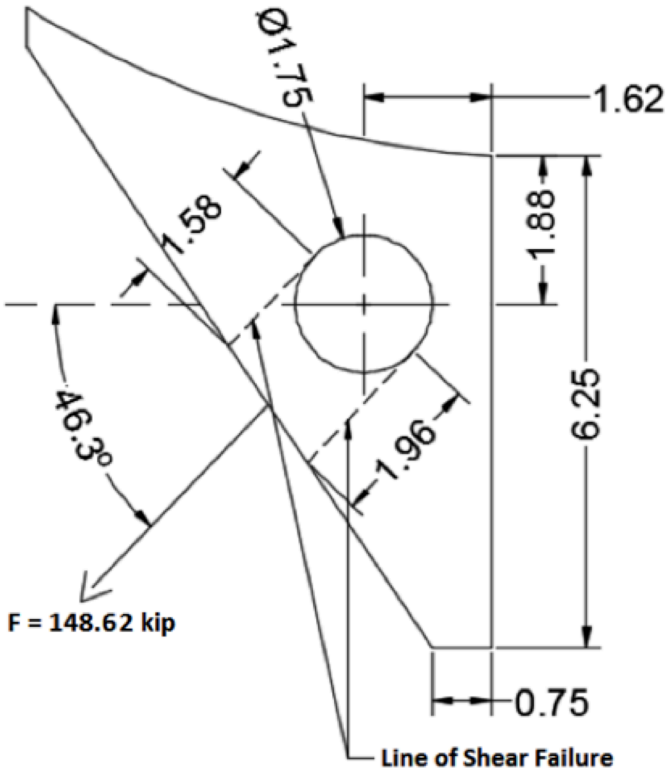

Figure 2.12.3-17. Tie-Down Rib Hole Loading

$$\tau = \frac{F}{A}$$

where A = 2 x (1.58 + 1.96) = 7.08 in²

$$\tau = \frac{148.62}{7.08} = 20.99 \text{ ksi} < 27.12 \text{ ksi}$$

- BEARING OF SHACKLE PIN ON EAR

The bearing stress is computed assuming that the force is uniformly distributed over the projected contact area of the pin's 1.75-inch diameter. This gives for the stress:

$$\sigma = \frac{F}{A} = \frac{148.62}{2.0*1.75} = 42.3 \text{ ksi}$$

$$\sigma = 42.5 \text{ ksi} < 45.2 \text{ ksi}$$

- YIELDING OF WELD JOINTS AND PARENT METAL

Figure 2.12.3-18 shows the approximate weld pattern for the top tie-down rib.

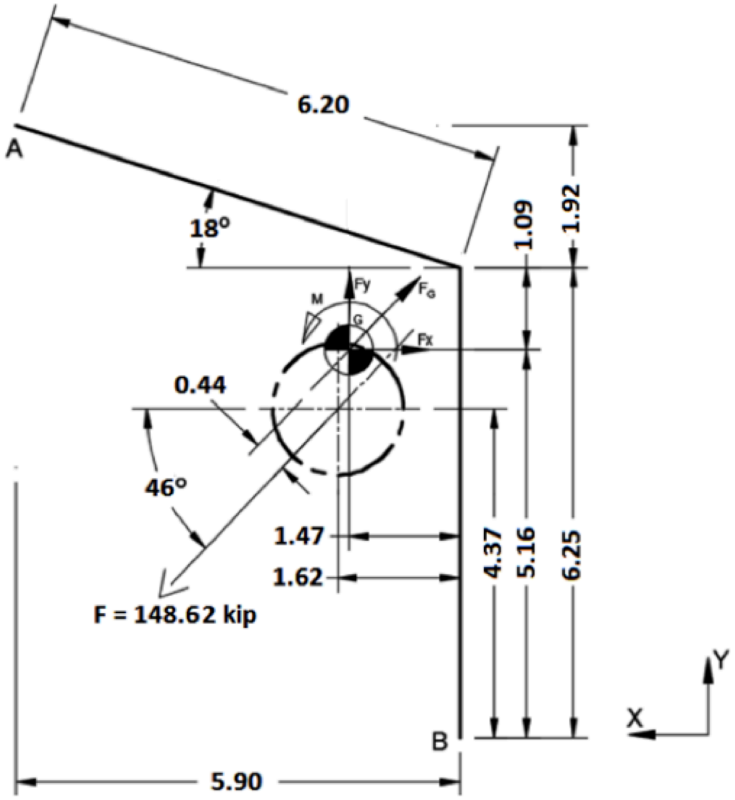

Figure 2.12.3-18. Weld Pattern of Top Tie Down Rib

Using the line load method (actual weld is ½ inch fillet 2 sides):

$$L = 6.2 + 6.25 = 12.45 \text{ inches}$$

$$\bar{X} = \frac{\sum \bar{X}_i L_i)}{\sum L_i} = \frac{6.2 \text{ x } \left(\frac{6.2 \cos(18°)}{2}\right)}{12.45} = \frac{6.2 \text{ x } 2.95}{12.45} = 1.47 \text{ in}$$

$$\bar{Y} = \frac{\sum \bar{Y}_i L_i}{\sum L_i} = \frac{6.25 \text{ x } (6.25/2) + 6.2 \text{ x } \left(6.25 + \left(\frac{6.2 \sin(18°)}{2}\right)\right)}{12.45} = 5.16 \text{ in}$$

$$I_X = \Sigma(I_o + Ad^2)$$

$$= \frac{6.25^3}{12} + 6.25\ (5.16 - (6.25/2))^2 + \frac{6.2^3 sin^2 18°}{12} + \ldots$$

$$\ldots\ 6.2(6.25 + \left(\frac{6.2 \sin(18°)}{2}\right) - 5.16)^2$$

$$= 74.13 \text{ in}^4/\text{in}$$

$$I_Y = \frac{6.2^3 cos^2(18°)}{12} + 6.2(2.95 - 1.47)^2 + 6.25\ (1.47)^2$$

$$= 45 \text{ in}^4/\text{in}$$

$\therefore I_Z = I_X + I_Y = 119.14\ in^4/in$

There are two welds:

$\therefore I_Z = 119.14 \times 2 = 238.28\ in^4/in.$
$\therefore M_Z = F \times r = 148.62 \times 0.44 = 65.39\ k\text{-}in.$

$F_X = F\cos\theta = 148.62 \cos 46° = 103.24\ kip$

$F_Y = F\sin\theta = 148.62\sin 46° = 106.91\ kip$

$\therefore$ @ Point A:

$$P_X = \frac{F_X}{L} + \frac{M_{ZY}}{I} = \frac{103.24}{2(12.45)} + \frac{(65.39)(6.25+1.92-5.16)}{(238.28)} = 4.97\ k/in$$

$$P_Y = \frac{F_Y}{L} + \frac{M_{ZX}}{I} = \frac{106.91}{(24.9)} + \frac{(65.39)(6.2\cos(18)-1.47)}{(238.28)} = 5.51\ k/in$$

$P_Z = 0$

Total line load:

$$P_T = \sqrt{P_X^2 + P_Y^2 + P_Z^2} = 7.42\ k/in.$$

Shear stress in the effective throat area of the weld is:

$$S_V = \frac{7.42}{0.707t} = \frac{7.42}{0.707*0.5} = 20.99\ ksi < 27.12\ ksi\ (allowable\ base\ metal)$$

Shear stress on the weld leg

$$S_t = \frac{7.42}{0.5} = 14.84\ ksi$$

$\therefore$ @ Point B:

$$P_X = \frac{103.24}{24.9} + \frac{(65.39)(5.16)}{(238.28)} = 5.56\ kip$$

$$P_Y = \frac{106.9}{(24.9)} + \frac{(65.39)(1.47)}{(238.28)} = 4.7\ k/in$$

$$P_T = \sqrt{(5.56^2 + 4.7^2 + 0)} = 7.28\ k/in$$

$$S_v = \frac{7.28}{0.3535} = 20.59\ ksi < 27.12\ ksi$$

Shear stress on leg of weld:

$$S_t = \frac{7.28}{0.5} = 14.56\ ksi < 27.12\ ksi$$

The following analysis checks weld failure mode of weld attaching tie-down rib and gusset to overpack, refer to Figure 2.12.3-19.

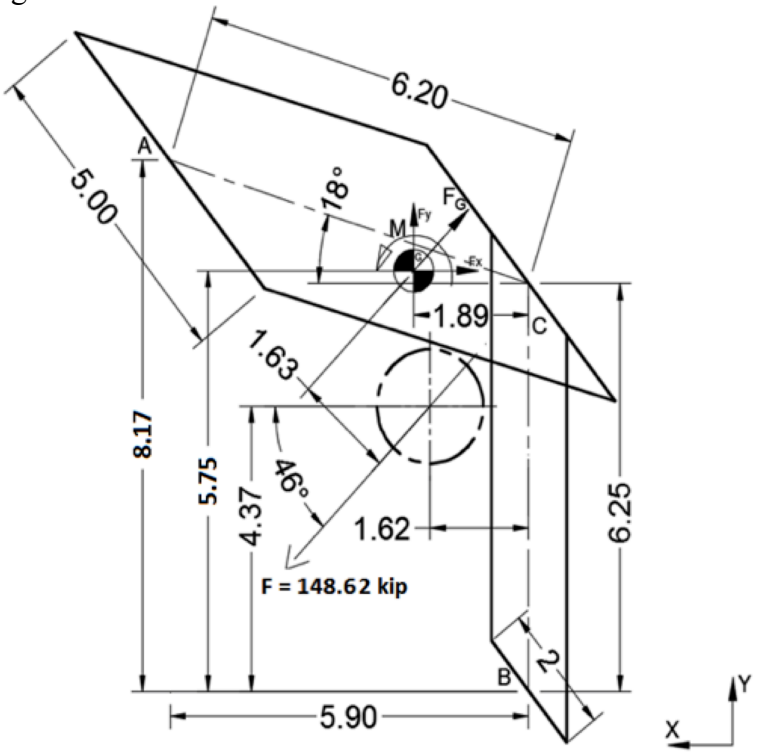

Figure 2.12.3-19. Weld Geometry of Tie-Down Rib and Gusset to Overpack

$$L = 5 + (6.2)x2 + 5 + 6.25 \times 2 = 34.9 \text{ inches}$$

$$\bar{X} = \frac{\sum \bar{X}_i L_i)}{\sum L_i} = \frac{5*6.2\cos(18)+12.4*\left(\frac{6.2\cos(18)}{2}\right)}{34.9} = 1.89 \text{ in}$$

$$\bar{Y} = \frac{\sum \bar{Y}_i L_i)}{\sum L_i} = \frac{5*(6.25+6.2\sin(18))+12.4*\left(6.25+\left(\frac{6.2\sin(18)}{2}\right)\right)+5*(6.25)+12.5*\left(\frac{6.25}{2}\right)}{34.9} = 5.75 \text{ in}$$

$$I_Z = (5)[(6.2\cos(18) - 1.89)^2 + (6.2\sin(18)+6.25-5.75)^2]$$
$$+ (12.4)[(\frac{6.2\cos(18)}{2} - 1.89)^2 + (6.25 + \frac{6.2\sin(18)}{2} - 5.75)^2]$$
$$+ (5)((6.25-5.75)^2+1.89^2) + (12.5)[1.89^2 + (\frac{6.25}{2} + (6.25-5.75))^2] + \frac{6.2^3}{12} + \frac{6.25^3}{12}$$
$$= 339.77 \text{ in}^3$$

$$MZ = 148.62 \text{ X } 1.15 = 170.91 \text{ k-in.}$$

∴ @ Point A:

$$P_X = \frac{103.24}{34.9} + \frac{(170.89)(8.17-5.75)}{339.77} = 4.18 \frac{k}{in}$$

$$P_Y = \frac{106.91}{34.9} + \frac{(170.55)(5.9-1.89)}{339.77} = 5.08\ \frac{k}{in}$$

$$P_Z = 0$$

∴ Total line load:

$$P_T = \sqrt{4.18^2 + 5.08^2} = 6.58\ \frac{k}{in}$$

Shear stress in the effective throat area of the weld is:

$$S_V = \frac{6.58}{0.707t} = \frac{6.58}{0.707*0.5} = 18.60 \text{ ksi} < 27.12 \text{ ksi (allowable base metal)}$$

For a ½ inch fillet, shear stress in the weld leg is:

$$S_V = \frac{6.58}{(0.5)} = 13.15 \text{ ksi} < 27.12 \text{ ksi}$$

∴ @ Point B:

$$P_X = \frac{103.24}{34.9} + \frac{(170.91)(5.75)}{339.77} = 5.85\ \frac{k}{in}$$

$$P_Y = \frac{106.91}{34.9} + \frac{(170.91)(1.89)}{339.77} = 4.02\ \frac{k}{in}$$

$$P_Z = 0$$

∴ Total line load:

$$P_T = \sqrt{5.83^2 + 4.00^2} = 7.09\ \frac{k}{in}$$

Shear stress in the effective throat area of the weld is:

$$S_V = \frac{7.09}{0.707t} = 20.07 \text{ ksi} < 27.12 \text{ ksi}$$

For a ½ inch fillet, maximum shear stress on the weld is:

$$S_v = \frac{7.09}{(0.5)} = 14.19 \text{ ksi} < 27.12 \text{ ksi}$$

The lower allowable stress for welds made to the A240 material is not a problem because of the direction of the applied load. The weld takes the load in tension. At Point C:

$$P_X = \frac{103.24}{34.9} + \frac{170.91\ (-0.5)}{339.77} = 2.71\ \frac{k}{in}$$

$$P_Y = \frac{106.9}{34.9} + \frac{170.91\ (1.89)}{339.77} = 4.01\ \frac{k}{in}$$

Forces acting in tension against the A240 are:

$$P_T = P_X \sin\theta + P_Y \cos\theta$$

$$= 2.71 \text{ x } \sin 18° + 4.01 \text{ x } \cos 18° = 4.65\ \frac{k}{in}$$

$$S_t = \frac{4.65}{0.5} = 9.31 \text{ ksi} < 23.7 \text{ ksi}$$

- EXCESSIVE LOAD FAILURE

The tie-down system must be designed such that its failure under excessive load would not impair the ability of the package to meet the requirements of 10 CFR 71. The tie-down system is attached to the overpack structure; the cask (containment vessel) resides within the overpack without attachment to its inner surface. Therefore, failure of the tie-down will not affect the performance of the cask. The results are presented in Table 2.12.3-5.

Table 2.12.3-5. Tie-Down System Stress Analysis Results

Condition	Stress Level (ksi)	Allowable based on Yield Strength (ksi)	MS (y)	Allowable based on Ultimate Strength (ksi)	MS (U)
Shear tear-out of hole	20.99	0.6*45.2 = 27.12	0.29	36.95	0.76
Bearing of shackle pin	42.46	45.2	0.06	96.80	1.28
Yielding of weld joints	20.99	0.6*45.2 = 27.12	0.29	36.95	0.76

The tie-down rib and pin materials are type [[ ]] stainless steel.

The margins of safety (MS (y)) with respect to yield is calculated as follows:

$$\text{MS (yield)} = \frac{\text{Allowable based on yield strength}}{Stress\ level} - 1$$

The margins of safety with respect to ultimate failure are:

Shear Strength:

$$\frac{\sigma_{ult}}{2(1+\mu)} = \frac{96.8}{2(1.31)} = 36.95 \text{ ksi}$$

Shear tear-out of tie-down rib hole

$$\text{MS} = \frac{36.95}{20.99} - 1 = 0.76$$

Bearing of shackle pin

$$\text{MS} = \frac{96.8}{42.46} - 1 = 1.28$$

Yielding of weld joints

$$\text{MS} = \frac{36.95}{20.99} - 1 = 0.76$$

2.12.4. Cask Closure Bolt Evaluation

2.12.4.1. Cask Lid Bolt Load Calculation

This section documents the cask lid bolt load calculations.

Cask Bolt Preload

The torque/preload relationship is defined as follows:

$$T = K \times D \times P_i \qquad \text{Reference 2-14, Page 19}$$

Solving for P_i yields:

$$P_i = T/(K \times D)$$

where

K	=	Torque friction coefficient
	=	0.15 (Reference 2-30)
D	=	Nominal bolt diameter (in)
	=	1.25 in
T	=	720±30 lb-in

The maximum cask bolt preload is:

$P_{i\,Max}$ = 750 x 12/(0.15 x 1.25) = 48.00 kips

Cask Bolt Applied Load: Non-Prying

The bolt non-prying load is defined as the sum of the non-prying tensile bolt force due to temperature, non-prying tensile bolt force due to pressure, axial load for gasket seating, and axial load for gasket operation for this calculation. The non-prying tensile bolt force due to temperature and non-prying tensile bolt force due to pressure can be easily calculated utilizing the parameters and formulas specified in NUREG-6007 (Reference 2-15). The axial load for gasket varies depending on the gasket material used and gasket width, which is the focus of the following evaluation.

Gasket Load

The formulas for the axial loads for gasket seating and gasket operation are given in Equation (1) and Equation (2), respectively (Reference 2-15, Table 4.2, page 13).

$$F_a = \frac{\pi D_{lg}\, b\, y}{N_b} \qquad (1)$$

where

D_{lg}	=	Closure lid diameter at the location of the gasket load Reaction (in)
	=	29.25 in
b	=	Effective gasket surface seating width (in)
y	=	Minimum design seating stress (psi)
N_b	=	Total number of closure bolts
	=	15

$$F_a = \frac{2\pi D_{lg}\, b\, m\,(P_{li} - P_{lo})}{N_b} \qquad (2)$$

m	=	Gasket factor for operating conditions
P_{li}	=	Pressure inside the closure lid (psi)
	=	30 psi
P_{lo}	=	Pressure outside the closure lid (psi)
	=	15 psi

Equations (1) and (2) use two experimentally determined constants, which are the gasket factor, m, and the minimum design seating stress, y. The gasket factor is taken into consideration for the axial load for gasket operation and is defined as the ratio of the required minimum gasket pressure to the pressure contained by the gasketed joint. Additionally, the seating stress is applied for the axial load for gasket seating and is defined as the minimum design seating stress of the gasket. Both of these constants are determined per Table E-1210-1 of the ASME Boiler and Pressure Vessel Code (B&PVC) Section III Division 1 Appendices (Reference 2-18, page 222).

Further, equation (1) and equation (2) both utilize the parameter b, which is the effective gasket or joint contact surface seating width. The effective gasket seating width is determined by first calculating the basic gasket seating width (b_o) per Table E-1210-2 of the ASME B&PVC Section III Division 1 Appendices (Reference 2-18). From Table E-1210-2, face sketch is used for the evaluation due to the fact that this sketch is the closest to the actual geometry as Figure B-1 depicts. It can be seen that b_o is a function of the variable w for face sketch, which is based upon the contact width between the flange facing and the gasket. Following, the effective gasket seating width is determined based off of the following criteria (Reference 2-18, page 223):

$$b = b_o \text{ , when } b_o \leq \tfrac{1}{4} \text{ in}$$

$$b = C_b\sqrt{b_o} \text{ , when } b_o > \tfrac{1}{4} \text{ in}$$

where

C_b = effective width factor
= 0.5 for U.S Customary calculations
= 2.5 for SI calculations

Once the effective gasket seating width is determined, both axial loads for gasket seating and gasket operation can be calculated by use of Equation (1) and Equation (2). For the calculations of this document, the parameters presented above are determined for soft aluminum. Furthermore, the seal detail drawing shown in Figure 2.12.4-1 is used to establish the contact width between the flange facing and the gasket (w) and is shown to be 0.872 inches (0.218 inches × 4).

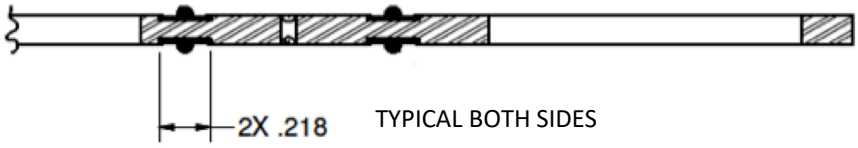

Figure 2.12.4-1. Seal with Contact Width Dimension

The gasket factor, minimum design seating stress, basic gasket seating width (b_o), and effective gasket width (b) are tabulated in Table 2.12.4-1 for the aluminum gasket material.

Table 2.12.4-1. Input Parameters

Material	Gasket Factor, *m*	*Gasket Seating Stress, y* (psi)	Basic Gasket Seating Width, b_o (in)	Effective Gasket Seating Width, b (in)
Aluminum	4.00	8800	.109	.109

The calculation for the basic gasket seating width (b_o) and effective gasket seating width (b) is determined by use of face sketch per Table E-1210-2. Therefore, the effective gasket width is:

$$b_o = \frac{w}{8} = \frac{.872\ in}{8} = .109\ \text{in}$$

Because b_o is less than ¼ in, b_o is equal to b.

With all parameters calculated, the axial loads due to gasket seating and gasket operation can be calculated.

The sections below provide a detailed analysis of the forces and moments that are subjected to the bolted joint of the Model 2000 cask during normal and accident conditions.

2.12.4.2. Lid Bolt Evaluation

2.12.4.2.1. Required Length of Engagement

For this analysis, a 1¼-7 UNC-2A external thread with a 1¼-7 UNC-2B internal thread is considered at an operating temperature of 150°F. The external thread material is ASTM A-540, Grade B22, Class 3 and the internal thread material is ASME SA-182, F304. Table 2.12.4-2 lists the required parameters needed for the analysis.

Table 2.12.4-2. Lid Bolt Evaluation Input Parameters

Parameter	Variable	Input	Units
Tensile Strength of External Thread at 150°F	S_{u1}	145*	ksi
Tensile Strength of Internal Thread at 150°F	S_{u2}	73	ksi
Minimum Pitch Diameter (External Thread)	$E_{s,min}$	1.1476	in
Minimum Major Diameter (External Thread)	$D_{s,min}$	1.2314	in
Maximum Pitch Diameter (Internal thread 2B)	$E_{n,max}$	1.1668	in
Maximum Major Diameter (Internal thread 2B)	$K_{n,max}$	1.123	in
Threads Per Inch	n	7	in
Bolt Pre-Load	P	82.8	kip

References:
Reference 2-30 Minimum Pitch Diameter: Table 3, Page 1827
Reference 2-30 Minimum Major Diameter: Table 3, Page 1827
Reference 2-30 Maximum Pitch Diameter (2B): Table 3, Page 1827
Reference 2-30 Maximum Minor Diameter (2B): Table 3, Page 1827

Based on these given inputs, it must be determined if the bolt will fail before the threads of either the internal or external fixtures or vice versa. To do this, the required length of engagement must be calculated and checked against the actual geometry. The length of engagement (L_e) is calculated as follows (Reference 2-30, Page 1536),

$$L_e = \frac{2A_t}{\pi(K_{n,max})(½+.57735n[E_{s,min} - K_{n,max}])}$$

Where,

A_t = Screw thread tensile stress area

and A_t is given by the equation,

$$A_t = \pi\left[\frac{E_{s,min}}{2} - \frac{0.16238}{n}\right]^2$$

The length of engagement (L_e) is for mating external and internal threads of the same strength. If the materials of the internal and external threads do not have the same strength, the relative strength (J) must be calculated to determine if the internal thread could strip before the bolt breaks. The relative strength is calculated as follows,

$$J = \frac{A_s \times S_{ut}\ of\ external\ thread\ material}{A_n \times S_{ut}\ of\ internal\ thread\ material}$$

where

A_s = Shear area of external threads

A_n = Shear area of internal threads

Also, the shear area of the external and internal threads are given by,

$$A_s = \pi\, n\, L_e\, K_{n,max}\left[\frac{1}{2n} + .57735(E_{s,min} - K_{n,max})\right]$$

and,

$$A_n = \pi\, n\, L_e\, D_{s,\,min}\left[\frac{1}{2n} + .57735(D_{s,min} - E_{n,max})\right]$$

where

n = number of threads per inch

If the relative strength is calculated to be less than or equal to 1, then the length of engagement (L_e) is sufficient to prevent stripping of the internal thread. If the relative strength is calculated to be greater than 1, then the required length of engagement is calculated by taking the product of the J factor and the length of engagement as given is:

$$Q = JL_e$$

where

Q = Required length of engagement

Once the required length of engagement is calculated, this value is checked against the actual geometry to determine if the internal threads will strip before the bolt breaks or vice versa. Table 2.12.4-3 presents the results.

Table 2.12.4-3. Calculation of Required Length of Engagement at 150°F

Parameter	Variable	Result	Units
Tensile stress area of bolt	A_t	0.952	in^2
Effective length	L_e	0.901	in
Shear area of internal threads	A_n	2.652	in^2
Shear area of external threads	A_s	1.905	in^2
Relative strength of external/internal threads	J	1.427	--
Required length of engagement if J > 1	Q	1.285	in

Looking at the actual geometry, the engagement = 3.00 inches (lid bolt length) – 1.625 inches (flange + seal) = 1.375 inches. At 150°F, the required length of engagement is less than the engagement of the geometry. Therefore, a thread engagement of 1.375 inches will ensure that the threads of either the internal or external fixture will not strip before the bolt fails for a Class 2A bolt in 2B threads.

2.12.4.2.2. Applied Load Analysis

The maximum load on the bolt to break the threaded portion is determined by taking the product of the ultimate tensile strength of the external thread and the bolt thread tensile stress area (Reference 2-30).

$$P_{max} = S_{u1}A_t$$

$$= (145\ ksi)(.952\ in^2)$$

$$P_{max} = 138\ kip$$

Now that the maximum load has been calculated, the minimum thread engagement, L_e, based on the applied pre-load is:

$$P = \sigma A_n$$

$$= \text{bolt pre-load}$$

$$= 82.8\ kip$$

$$= \text{Tensile strength of internal thread}$$

A_n = Internal thread shear area (Class 2A + 2B)

From Reference 2-30:

$$P = \sigma \times \pi \times n \times L_e \times D_{s,min} \times [1/2n + .57735(D_{s,min} - E_{n,max})]$$

Solving for the effective length:

$$L_e = P / (\sigma \times \pi \times n \times D_{s,min} \times [1/2n + .57735(D_{s,min} - E_{n,max})])$$

Solving, the minimum thread engagement is 0.3852 inches at an operating temperature of 150°F. accordingly, calculating the product of the effective length and the number of threads per inch, the minimum thread engagement to prevent internal 2B thread stripping is approximately three threads.

2.12.4.2.3. Bolt Stress Analysis

The cask lid of the Model 2000 cask is fastened to the cask flange by way of 15 uniformly spaced ASTM A540, Grade B-22, Class 3 socket head screws. Table 2.12.4-4 provides the input parameters that are to be used in the analysis at an operating temperature of 500°F.

Table 2.12.4-4. Model 2000 Stress Analysis Design Input Parameter

Parameter	Variable	Input	Units
Number of Bolts	N_b	15	--
Lid Diameter at Bolt Circle	D_{lb}	32.25	in
Lid Diameter at Gasket	D_{lg}	29.25	in
Nominal Bolt Diameter	D_b	1.25	in
Lid Diameter at Inner Edge	D_{li}	28	in
Lid Diameter at Outer Edge	D_{lo}	34.75	in
Equivalent Thickness of Lid	t_l	7.89	in
Thickness of Lid Flange	t_{lf}	1.5	in
Thickness of Cask Wall	t_c	6	in
Bolt Length Between the Top and Bottom of Closure Lid at Bolt Circle	l_b	1.5	in
Bolt Engagement Length	BEL	1.625	in
Bolt Moment of Inertia/Cir	XIB	0.018	in^3
Young's Modulus For Lid	E_l	25900000	psi
Young's Modulus For Cask	E_C	25900000	psi
Young's Modulus For Bolt	E_b	27400000*	psi
Poisson's Ratio For Lid	N_{ul}	0.31	--
Poisson's Ration For Cask	N_{uc}	0.31	--
Lid Thermal Expansion Coefficient	a_l	9.70E-06	1/°F
Bolt Thermal Expansion Coefficient	a_b	7.30E-06*	1/°F
Weight of Cask Contents	W_C	5450	lb
Weight of Cask Lid	W_l	1900	lb
Dynamic Load Factor	DLF	1	--
Preload Torque	Q_{NOM}	720	lb-ft
Preload Torque Tolerance	Q_{TOL}	30	lb-ft
Maximum Preload Torque	Q_{MAX}	9000	lb-in
Minimum Preload Torque	Q_{MIN}	8280	lb-in
Nut Factor For Preload Torque	K_q	0.15	--
Gasket Seating Width	G_b	0.109	in
Gasket Seating Stress	G_y	8800	psi
Gasket Factor	G_m	4	--
Wall Thermal Expansion Coefficient	a_c	9.70E-06	1/°F
Basic Allowable Stress Limit	S_m	7.71E+04	psi
Minimum Yield Strength	S_y	115700	psi
Minimum Ultimate Strength	S_u	145000	psi
Pressure Inside Closure Lid	P_{li}	30	psi

Parameter	Variable	Input	Units
Pressure Outside the Closure Lid	P_{lo}	15	psi
Pressure Inside the Cask Wall	P_{ci}	30	psi
Pressure Outside the Cask Wall	P_{co}	15	psi
Temperature Change of the Closure Lid	T_l	117.5	°F
Temperature Change of the Closure Bolt	T_b	111.9	°F
Temperature Change of the Cask Wall	T_c	118.0	°F
Temperature Change of Inner Surface of Closure Lid	T_{li}	116.8	°F
Temperature Change for Outer Surface of Closure Lid	T_{lo}	118.1	°F
Maximum rigid body impact acceleration (g)	a_i	25**	--
Impact angle between the cask axis and the target surface	xi	90°	--
Maximum axial vibration acceleration (g) at the cask support	ava	2	--
Maximum transverse vibration acceleration (g) at the cask support	avt	5	--
Vibration transmissibility of acceleration between the cask support and the closure lid	VTR	1	--

References:
Reference 2-31 Gasket Seating Width: Table E-1210-2
Reference 2-31 Gasket Seating Stress: Table E-1210-1
Reference 2-31 Gasket Factor: Table E-1210-1
Reference 2-15 Basic Allowable Stress Limit: Table 6.1, Page 28
Reference 2-1 Maximum Axial Vibration Acceleration (g) at the cask support
Reference 2-1 Maximum Transverse Vibration Acceleration (g) at the cask support
Reference 2-15 Vibration transmissibility of acceleration between the cask support and the closure lid
Notes:
* Grade B21 bolt properties used because temperature dependent values could not be found for Grade B22.
** Section 2.12.1, Figure 2.12.1.11-30 presents the justification for the reduced impact acceleration during the HAC end drop.

NUREG/CR-6007 (Reference 2-15) is used to accurately verify whether or not the closure bolts can effectively hold up to the various loads in both normal conditions of transport and hypothetical accident conditions. This includes forces and moments due to pressure, temperature, vibration, impact, preload, gasket, puncture, and prying. Also, NUREG/CR-6007 gives procedures for combining loads and stress limits that must be met. Loads include the axial force (F_a), shear force (F_s), fixed-edge closure-lid force (F_f), fixed edge closure lid moment (M_f), and also torsional moments (M_t) that are created by the torque wrench in the preload and gasket seating operations. All of which are elaborated on in the following sections.

2.12.4.2.4. Forces/Moments Generated By Preload

Found in Table 4.1 in NUREG/CR-6007, are the bolts loads due to use of a torque wrench. The non-prying axial bolt force per bolt is given by the equation,

$$F_a = Q / (K_q \times D_b)$$

The torsional bolt force per bolt is defined by the formula,

$$M_t = 0.5\ Q$$

2.12.4.2.5. Forces/Moments Generated By Gasket Loads

Per Table 4.2 in NUREG/CR-6007, are the formulas for calculating the forces and moments generated by gasket loads by utilization of a torque wrench. The axial force produced by the gasket seating operation is evaluated by use of the following equation,

$$F_a = \frac{\pi \times D_{lg} \times G_b \times G_y}{N_b}$$

and the torsional bolt moment due to the seating operation is,

$$M_t = \frac{0.5 \times \pi \times K_q \times D_b \times D_{lg} \times G_b \times G_y}{N_b}$$

Also, The non-prying tensile bolt force per bolt produced by the operating gasket seating is determined by,

$$F_a = \frac{2 \times \pi \times D_{lg} \times G_b \times G_m (P_{li} - P_{lo})}{N_b}$$

2.12.4.2.6. Forces/Moments Generated By Pressure Loads

Table 4.3 in NUREG/CR-6007 is applied to determine the moments and forces that are generated due to the pressure difference between the inside and outside of the cask. The associated equation for the axial force due to pressure loads is,

$$F_a = \frac{\pi \times D_{lg}^2 \times (P_{li} - P_{lo})}{4 \times N_b}$$

where

P_{li} = Pressure inside the closure lid
= 30 psi
P_{lo} = Pressure outside the closure lid
= 15 psi

The shear bolt force per bolt is then,

$$F_s = \frac{\pi \times E_t \times t_t \times (P_{li} - P_{lo}) \times D_{lb}^2}{2 \times N_b \times E_c \times t_c \times (1 - N_{ul})}$$

where

P_{ci} = Pressure inside the cask wall
= 30 psi
P_{co} = Pressure outside the cask wall
= 15 psi

The fixed-edge closure-lid force generated by internal pressure is,

$$F_f = \frac{D_{lb}(P_{li} - P_{lo})}{4}$$

and the fixed-edge moment is,

$$M_f = \frac{D_{lb}^2(P_{li} - P_{lo})}{32}$$

2.12.4.2.7. Forces/Moments Generated By Temperature Loads

Table 4.4 of NUREG/CR-6007 gives the formulas for bolt forces/moments generated by thermal expansion difference between the closure lid, bolt, and wall. The axial force due to a temperature difference between the closure bolt and lid is:

$$F_a = ¼ \times \pi \times D_b^2 \times E_b \times (\alpha_l \times T_l - \alpha_b \times T_b)$$

where

T_l = Temperature change of the closure lid
= 117.5°F

T_b = Temperature change of the closure bolt
= 111.9°F

The shear force acting on each bolt is given by,

$$F_s = \frac{\pi \times E_l \times t_l \times D_{lb} \times (a_l \times T_l - a_c \times T_c)}{N_B \times (1 - N_{ul})}$$

where,

T_c = Temperature change of the cask wall
= 118°F

Fixed-edge force and fixed-edge moment due to temperature difference between the inner and outer surface of the closure lid is determined by use of the following equations.

F_f = 0 lb/bolt

$$M_f = \frac{E_l \times a_l \times t_l^2 \times (T_{lo} - T_{li})}{12 \times (1 - N_{ul})}$$

where,

T_{lo} = Temperature change of the outer surface of the closure lid
= 118.1°F

T_{li} = Temperature change of the inner surface of the closure lid
= 116.8°F

2.12.4.2.8. Forces/Moments Generated By Impact Loads

For this evaluation, the loads created by impact are analyzed for a cask with a protected closure lid and are found via Table 4.5 in NUREG/CR-6007. As follows, the non-prying tensile bolt force per bolt due to impact is:

$$F_a = \frac{1.34 \times \sin(xi) \times DLF \times a_i \times (W_l - W_c)}{N_b}$$

Further, the shear bolt force per bolt is evaluated using,

$$F_s = \frac{\cos(xi) \times a_i \times W_l}{N_b}$$

Accordingly, the fixed-edge force and fixed-edge moment are defined by:

$$F_f = \frac{1.34 \times \sin(xi) \times DLF \times a_i \times (W_l - W_c)}{\pi \times D_{lb}}$$

and,

$$M_f = \frac{1.34 \times \sin(xi) \times DLF \times a_i \times (W_l - W_c)}{8\pi}$$

2.12.4.2.9. Forces/Moments Generated By Vibration Loads

Looking at Table 4.8 in NUREG/CR-6007, the loads that are generated due to vibration are outlined. The tensile bolt force per bolt due to vibration is:

$$F_a = \frac{VTR \times ava \times W_l}{N_b}$$

The shear bolt force per bolt is calculated by use of the equation,

$$F_s = \frac{VTR \times avt \times W_l}{N_b}$$

The fixed-edge force and fixed edge moment are:

$$F_f = \frac{VTR \times ava \times W_l}{\pi \times D_{lb}}$$

and,

$$M_f = \frac{VTR \times ava \times W_l}{8\pi}$$

2.12.4.2.10. Prying Action Forces Generated by Applied Loads

Table 2.1 of NUREG/CR-6007 lays out the analysis to evaluate the axial bolt force per bolt caused by prying action of the lid is:

$$F_{ap} = \left(\frac{\pi D_{lb}}{N_b}\right)\left[\frac{\frac{2 \times M_f}{D_{lo} - D_{lb}} - C1(B - F_f) - C2(B - P)}{C1 + C2}\right]$$

where

$C1 = 1$

$$C2 = \left(\frac{8}{3(D_{lo} - D_{lb})^2}\right)\left(\frac{E_l \times t_l^3}{1 - N_{ul}} + \frac{(D_{lo} - D_{li})E_{lf} \times t_{lf}^3}{D_{lb}}\right)\left(\frac{L_b}{N_b D_b^2 E_b}\right)$$

L_b = Bolt length between the top and bottom surfaces of the closure lid at the bolt circle

= = 1.5 in

B = F_f if $F_f > P$, otherwise B = P

It should be noted that the fixed-edge force and fixed-edge moment are inputs from Table 4.2, 4.3 and 4.8 for NCT and Table 4.2, 4.3 and 4.5 for HAC.

2.12.4.2.11. Bending Bolt Moment Generated by Applied Loads

Located in Table 2.2 of NUREG/CR-6007 is the formula for calculating the bending bolt moment per bolt caused by the rotation or bending of the closure lid and is:

$$M_{bb} = \left(\frac{\pi D_{lb}}{N_b}\right)\left(\frac{K_b}{K_b + K_l}\right) M_f$$

where

$$K_b = \left(\frac{N_b}{L_b}\right)\left(\frac{E_b}{D_{lb}}\right)\left(\frac{D_b^4}{64}\right)$$

$$K_l = \frac{E_l t_l^3}{3\left[\left(1-N_{ul}^2\right)+\left(1-N_{ul}\right)^2\left(\frac{D_{lb}}{D_{lo}}\right)\right]D_{lb}}$$

Once again, it should be noted that the fixed-edge force and fixed-edge moment are inputs from Table 4.2, 4.3 and 4.8 for NCT and Table 4.2, 4.3 and 4.5 for HAC.

2.12.4.2.12. Calculation of Total Loads and Bolt Stresses

In order to accurately combine tensile bolt forces, Table 4.9 of NUREG/CR-6007 is applied. To calculate the total non-prying axial load, the axial bolt force from Tables 4.3-4.8 is summed. The same process is used to determine the total fixed-edge force and fixed-edge moment. Further, the bolt stresses can be formulated from Table 5.1 of NUREG/CR-6007. Calculating the average bolt direct stress caused by the tensile bolt force is:

$$S_{ba} = 1.2732\ F_a\ /\ D^2$$

and the average bolt shear stress is formulated as,

$$S_{bs} = 1.2732\ F_s\ /\ D^2$$

The maximum bending stress and maximum shear stress are represented as,

$$S_{bb} = 10.186\ M_{bb}\ /\ D^3$$

$$S_{bt} = 5.093\ M_t\ /\ D^3$$

Where F_a, F_s, M_{bb}, and M_t all represent total values of the tensile bolt force, shear bolt force, bending bolt moment, and torsional bolt moment respectively.

2.12.4.2.13. Limits on Bolt Stresses

Table 6.1 of NUREG/CR-6007 gives the acceptance criteria for normal conditions of transport. The acceptance criteria state that the average stress must be less than the allowable stress in tension. For shear, the average stress must be less than 60 percent of the allowable stress. In addition, the sum of the squares of the stress ratio for average tensile stress and stress ratio for average shear stress must be less than one. Further, the maximum stress intensity must be less than 1.35 times the allowable stress for bolts having a minimum tensile strength greater than 100 ksi and 1.5 times for bolts having a minimum tensile strength less than 100 ksi.

Looking at Table 6.3 for HAC, the average stress in tension must be less than the smaller of $0.7S_u$ or S_y at temperature. The average stress in shear must be less than the smaller of $0.42S_u$ or $0.6S_y$ at temperature. Furthermore, the sum of the squares of the stress ratio for average tensile stress and stress ratio for average shear stress must be less than one.

2.12.4.2.14. Analytical Results

Forces and Moments

The forces and moments that the Model 2000 Transport Package closure lid, wall, and bolt are subjected to during normal conditions of transport and hypothetical accident conditions are shown in Table 2.12.4-5 and Table 2.12.4-6, respectively.

Table 2.12.4-5. Forces/Moments Results (NCT)

Load Condition	Forces/Moments	Variable	Magnitude	Units
PRESSURE	Non-Prying Tensile Bolt Force	F_a	671.96	lb
	Shear Bolt Force Per Bolt	F_s	3113.55	lb
	Fixed-Edge Closure-Lid Force	F_f	120.94	lb
	Fixed-Edge Closure-Lid Moment	M_f	487.53	lb-in
TEMPERATURE	Non-Prying Tensile Bolt Force	F_a	10856.79	lb
	Shear Bolt Force Per Bolt	F_s	-9701.92	lb
	Fixed-Edge Closure-Lid Force	F_f	0	lb
	Fixed-Edge Closure-Lid Moment	M_f	2455.49	lb-in
VIBRATION	Non-Prying Tensile Bolt Force	F_a	253.33	lb
	Shear Bolt Force Per Bolt	F_s	633.33	lb
	Fixed-Edge Closure-Lid Force	F_f	37.51	lb
	Fixed-Edge Closure-Lid Moment	M_f	151.2	lb-in
PRELOAD	Non-Prying Tensile Bolt Force Per Bolt	F_a	48000	lb
	Torsional Bolt Moment Per Bolt	M_t	4500	lb-in
GASKET	Axial Load For Gasket Seating	F_a	5876.16	lb
	Axial Load For Gasket Operation	F_a	80.13	lb
	Torque Due to Gasket	M_t	550.89	lb-in
PRYING	Axial Load Due to Prying	F_a	-2339.42	lb
	Bending Moment Due to Prying	M_{bb}	9.99	lb-in

Table 2.12.4-6. Forces/Moments Results (HAC)

Load Condition	Forces/Moments	Variable	Magnitude	Units
PRESSURE	Non-Prying Tensile Bolt Force	F_a	671.96	lb
	Shear Bolt Force Per Bolt	F_s	3113.55	lb
	Fixed-Edge Closure-Lid Force	F_f	120.94	lb
	Fixed-Edge Closure-Lid Moment	M_f	487.53	lb-in
TEMPERATURE	Non-Prying Tensile Bolt Force	F_a	10856.79	lb
	Shear Bolt Force Per Bolt	F_s	-9701.92	lb
	Fixed-Edge Closure-Lid Force	F_f	0	lb
	Fixed-Edge Closure-Lid Moment	M_f	2455.49	lb-in
IMPACT	Non-Prying Tensile Bolt Force	F_a	16415.00	lb
	Shear Bolt Force Per Bolt	F_s	0	lb
	Fixed-Edge Closure-Lid Force	F_f	2430.26	lb
	Fixed-Edge Closure-Lid Moment	M_f	9796.98	lb-in
PRELOAD	Non-Prying Tensile Bolt Force Per Bolt	F_a	48000	lb
	Torsional Bolt Moment Per Bolt	M_t	4500	lb-in
GASKET	Axial Load For Gasket Seating	F_a	5876.16	lb
	Axial Load For Gasket Operation	F_a	80.13	lb
	Torque Due to Gasket	M_t	550.89	lb-in
PRYING	Axial Load Due to Prying	F_a	-2149.02	lb
	Bending Moment Due to Prying	M_{bb}	41.13	lb-in

2.12.4.2.15. Total Loads and Bolt Stresses Results

Now that all of the forces and moments have been calculated for both NCT and HAC, the loads can be combined appropriately to determine the total loads. Additionally, the bolt stresses can be calculated from the total loads. The results are displayed below for NCT and HAC in Table 2.12.4-7 and Table 2.12.4-8 respectively.

Table 2.12.4-7. Total Loads/Bolt Stresses (NCT)

Total Loads/ Bolt Stresses	Variable	Magnitude	Units
Total Bolt Axial Load	F_a	63318.83	lb
Total Bolt Shear Load	F_s	-5995.04	lb
Total Bolt Bending Moment	M_b	3094.22	lb-in
Total Bolt Torsional Moment	M_t	4500	lb-in
Average Bolt Direct Stress	S_{ba}	65335.10	psi
Average Bolt Shear Stress	S_{bs}	-6144.66	psi
Maximum Bending Stress	S_{bb}	22994.83	psi
Maximum Shear Stress	S_{bi}	16720.98	psi
Maximum Stress Intensity	S_{bt}	90827.37	psi

Table 2.12.4-8. Total Loads/Bolt Stresses (HAC)

Total Loads/ Bolt Stresses	Variable	Magnitude	Units
Total Bolt Axial Load	F_a	79670.89	lb
Total Bolt Shear Load	F_s	-6588.37	lb
Total Bolt Bending Moment	M_b	12781.13	lb-in
Total Bolt Torsional Moment	M_t	4500	lb-in
Average Bolt Direct Stress	S_{ba}	82207.87	psi
Average Bolt Shear Stress	S_{bs}	-6798.17	psi
Maximum Bending Stress	S_{bb}	94983.60	psi
Total Bolt Shear Stress	S_{bt}	16720.98	psi

2.12.4.2.16. Limits on Bolt Stresses Results

Accordingly, the code evaluation is conducted using the information given in the previous subsection and the appropriate tables from NUREG/CR-6007 for both NCT and HAC. Per Table 6.1 of NUREG/CR-6007, the limits for NCT are evaluated as,

$$S_{ba} < S_u$$
$$65335.10 \text{ psi} < 77{,}130 \text{ psi}$$

and,

$$S_{bs} < 0.6S_u$$
$$-6144.66 \text{ psi} < 46278 \text{ psi}$$

also,

$$R_t^2 + R_s^2 < 1$$
$$(0.8474)^2 + (-0.1328)^2 < 1$$

where,

R_t = Stress ratio for average tensile stress
R_s = Stress ratio for average shear stress

Per Table 6.3 of NUREG/CR-6007, the limits for HAC are evaluated as,

$$S_{ba} < 0.7S_u$$
$$82207.87 \text{ psi} < 101500 \text{ psi}$$

and,

$$S_{bs} < 0.42S_u$$
$$-6798.17 \text{ psi} < 60900 \text{ psi}$$

also,

$$R_t^2 + R_s^2 < 1$$
$$(0.8099)^2 + (-0.1116)^2 < 1$$

2.12.4.2.17. Fatigue Analysis

The fatigue analysis considers vibration and operating stresses, which come from the NCT bolt stress. Included in the operating stress are the pressure, preload, gasket load, and temperature stresses. Therefore, the loads are:

$$S_{Operating} = 67487.62 \text{ psi}$$

$$S_{Vibration} = 261.40 \text{ psi}$$

Using ASME Code, Section III, NB-3232.3 (Reference 2-32, page 91), the alternating stresses can be found by the equation below,

$$S_{a\text{-}Operating} = RF \times S_{Operating} \left(\frac{E_{dc}}{E_a}\right)^U$$

$$S_{a\text{-}Vibration} = RF \times S_{Vibration} \left(\frac{E_{dc}}{E_a}\right)^U$$

where

RF = Fatigue Strength Reduction Factor (Reference 2-32)

E_{dc} = Modulus of Elasticity on Design Fatigue Curve (Reference 2-18, Figure I-9.4, page 12)

E_a = Modulus of Elasticity used in the Analysis

U = Cumulative Usage Factor

U = 1 (Reference 2-32)

Applying ASME Section III, Figure I-9.4, the fatigue limit for maximum nominal stress ≤ 2.7 S_m for the loads of this analysis are,

$$N_{a\text{-}Operating} = 466 \text{ Cycles}$$

$$N_{a\text{-}Vibration} = 10^{11} \text{ Cycles}$$

The above values are accurately calculated by interpolating the tabular data given in ASME Section III, Table I-9.0 (Reference 2-18, page 2). Assuming 10^7 cycles for vibration load and 190 transports:

$$N_{Operating} = 190 \text{ Cycles}$$

The accumulative usage is then,

$$R = \left(\frac{N_{Operating}}{N_{a-Operating}}\right) + \left(\frac{N_{Vibration}}{N_{a-Vibration}}\right)$$

Shown in Table 2.12.4-9 are the results from the analysis.

Table 2.12.4-9. Fatigue Analysis Results

Parameter	Variable	Value	Units
Vibration Stress	$S_{vibration}$	261.40	psi
Operating Stress	$S_{operating}$	67487.62	psi
Fatigue Strength Reduction Factor	RF	4	--
Cumulative Usage Factor	U	1	--
E given on design curve	E_{dc}	30000000	psi
E used in analysis	E_a	27400000	psi
Ratio of Modulus of Elasticity	E_{ratio}	1.09	--
Alternating Stress due to Vibration	$S_{a\text{-}Vibration}$	572.41	psi
Alternating Stress due to Operating	$S_{a\text{-}Operating}$	147783.10	psi
Number of Alt. Cycles due to Vibration	$N_{a\text{-}Vibration}$	1E+11	--
Number of Alt. Cycles due to Operating	$N_{a\text{-}Operating}$	466	--
Number of Cycles for Vibration Load	$N_{Vibration}$	1.00E+07	--
Number of Cycles for Operating Load	$N_{Operating}$	190	--
Accumulative Usage	R	0.4078	--

Because the accumulative usage is less than one, it is acceptable to have up to 190 transports before all bolts are replaced. After 190 transports, all bolts must be replaced.

2.12.5. Model 2000 Scale Model Drop Test Report

Model 2000 Drop Test Report No. 87-08-01 is provided in the following pages.